People's democratic republic of Algeria ministry of higher education
and scientific research
University of Echahid Cheikh Larbi Tebessi -Tebessa
Faculty of exact sciences and natural and life science
Department of matter sciences

THESIS of MASTER
Specialty: **Physics of materials**

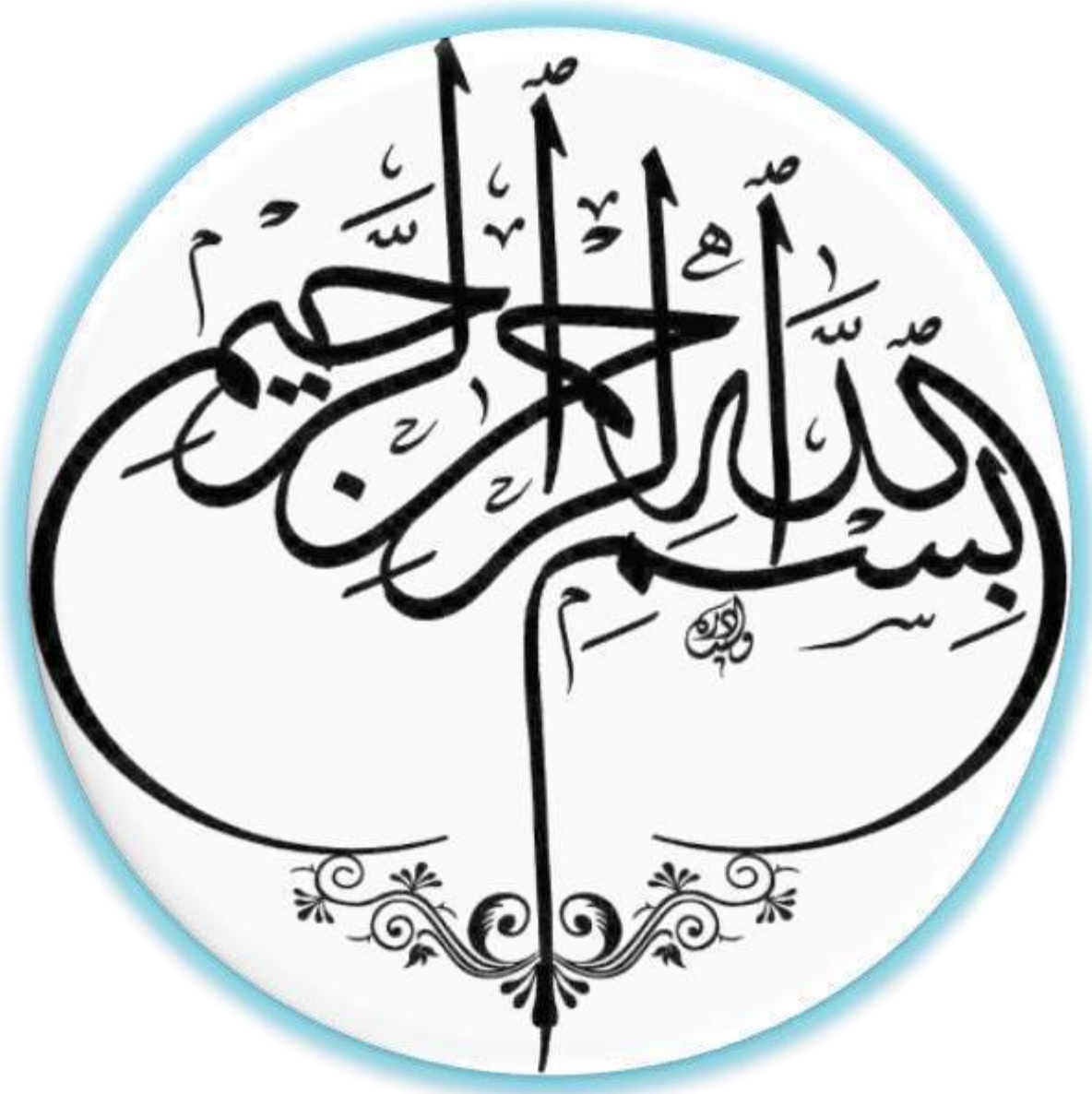
Effect of Zn, Mn, Cu and Fe doping on optical properties of SnO_2 thin films deposited by spray pyrolysis technique

Presented by : BOUKHALFA Riadh

Members of the discussion committee:

Dr. HANINI Faouzi	President	university of Tebessa
Dr.BOUKHALFA Radhia	Supervisor	university of Tebessa
Dr. HERISSI Labidi	Examiner	university of Tebessa

Discussion date
10/06/2025


بسم الله الرحمن الرحيم

Acknowledgment

In the name of Allah, the Almighty, to whom I am eternally indebted. Praise be to Allah that I am typing these final words as the last step in completing this thesis.

To my aunt, **Dr Radhia BOUKHALFA:** thank you for your steady guidance and support as both my supervisor and my aunt. Your insight and belief in this work were invaluable and burned brighter than any doubt. It was a true privilege to be mentored by you. I am sincerely grateful to you.

It is a great honor to have my work assessed by my professors, **Dr. Faouzi HANINI** and **Dr. Labidi HERISSI**. I was your student once, I am your student now, and I always will be.

Dedication

I am deeply grateful to **Allah**, whose help enabled me to reach this stage and express these words to **my mother** and **father** for whom I have done this, and for whom I will do everything in the future, by Allah's will. I pray that this makes you proud, even if just a little. I am determined to keep striving to make you proud until my last breath and beyond, by Allah's will.

I also dedicate this to the people I cherish most: **Alla, Nabil, Wassim**, and my **little sister**. Your ability to make the toughest moments feel lighter and more bearable meant the world to me.

I would like to dedicate this work to my professors **Pr. Faycal CHEMAM, Dr. Abdelkader HAFDALLAH, Dr. Mourad KHECHBA, Dr. Faouzi HANINI, Dr. Labidi HERESSI** and most especially my dear professor **Dr. Radhia BOUKHALFA** who have supported me greatly over the years, particularly when I needed it most. This work is a humble way of showing that your help was not in vain.

I would like to express my sincere gratitude to **MOKHER Souria**, the official sponsor of the experimental part of this work.

Lastly, I would like to thank the entire Physics Department for making this easier for me

List of tables

List of tables

Table No.	Title	Page
I.1	Some types of transparent carrier oxides	4
I.2	Properties of transparent conducting oxides	6
I.3	Band gap energy of some transparent carrier oxides	7
I.4	Electrical Properties of transparent conducting oxides	8
I.5	General properties of tin dioxide	11
II.1	Zinc acetate masses for doping concentrations	37
II.2	Deposition conditions (concentration, temperature, etc.)	38

List of figures

List of figures

Figure No.	Title	Page
I.1	Transmission spectrum illustration	6
I.2	Unit cell of tin dioxide (rutile-type structure)	12
I.3	Band structure of pure SnO_2	13
I.4	Schematic diagram showing the direct and indirect transport of semiconductors	14
I.5	Schematic diagram showing the structure of SnO_2 energy gap	15
I.6	CO sensor based on SnO_2 thin films	16
I.7	Response of a tin dioxide-based chemical sensor to ethanol at 450°C	16
I.8	Si-TCO electrode	17
I.9	Charge-discharge curves	17
II.1	DC sputtering voltage configuration (2–5 kV). Labels: (A) Target (cathode), (B) Substrate, (C) Plasma generation region	23
II.2	Ar^+ ion bombardment mechanism. Argon ions striking the target, ejecting atoms that deposit on the substrate	23
II.3	Schematic of thermal evaporation setup	24
II.4	Electron beam evaporation setup	25
II.5	PLD system representation	26
II.6	Spin-coating stages: (1) solution deposition, (2) rotational spreading, (3) solvent evaporation	27
II.7	Dip-coating stages: (a) immersion, (b) withdrawal, (c) evaporation	27
II.8	Basic 2-electrode electrodeposition setup	28
II.9	Schematic of the spray pyrolysis setup process (air atomizing nozzle, precursor solution, and heated substrate)	29
II.10	Schematic diagram showing the stages of growth: (a) positioning of atoms (b) formation of islands (c)	31

	coalescence (d) growth	
II.11	shows the experimental installation of the used thermal chemical spraying system	33
II.12	Microscope slides used as substrates for deposition	34
II.13	Substrate Cleaning Steps	35
II.14	Precision weighing of zinc acetate dehydrate (10% doping: 0.353g).	36
II.15	Homogenization of SnO_2: Zn solution via magnetic stirring (500 rpm, 25°C)	36
II.16	Appearance of spray solutions after magnetic stirring (a) undoped SnO_2,(b)X-doped SnO_2, which X=Mn, Cu, Fe	37
II.17	Prepared samples	39
II.18	JASCO V-730 spectrophotometer used for measurements	40
II.19	Schematic diagram of the working principle of the UV-VIS spectrometer	40
II.20	Absorption coefficient (α) as a function of photon energy (hν) for Undoped SnO_2 thin films	42
II.21	The direct band gap (Eg = 3.72 eV) for Undoped SnO_2 thin films was determined by extrapolating the linear	43
II.22	Urbach extremity plot (ln(α) vs. hν) for SnO_2 thin films. The Urbach energy (Eu = 0.26 eV) was calculated from the slope of the linear region.	44
III.1	Optical transmittance spectra of SnO_2 at different percentage of Zn	47
III.2	Variation of Average Optical Transmittance of Zinc doped SnO_2 as function of concentration	49
III.3	Variation of thickness of Zinc doped SnO_2 as function of concentration	49
III.4	typical variation of $(\alpha h\nu)^2$ as function of zinc concentration	50
III.5	Optical band gap energy of SnO_2 thin film at different Zinc concentration	51

III.6	Urbach energy of SnO_2 thin film Vs Zinc concentration	52
III.7	the inverse relationship Eg and EU of SnO_2 thin films versus Zn doping concentration	53
III.8	Optical transmittance spectra of undoped SnO_2, SnO_2:Zn, SnO_2:Mn, SnO_2:Cu and SnO_2:Fe	54
III.9	thickness of undoped SnO_2, SnO_2:Zn, SnO_2:Mn, SnO_2:Cu and SnO_2: Fe	55
III.10	band gap of undoped SnO2, Zn, Mn, Cu, Fe- doped SnO_2 thin films	56
III.11	band gap Vs Urbach energy of undoped SnO_2, Zn, Mn, Cu, Fe- doped SnO_2 thin films	57



List of symbols



List of symbols

Symbol	Signification	Most common units
n_i	Intrinsic carrier concentration	cm^{-3}
n	Electron concentration	cm^{-3}
p	Hole concentration	cm^{-3}
λ	Wavelength	nm
E_g	Energy of the optical band gap	eV
$h\nu$	Photon energy	eV
E_u	Urback energy	eV
E_{ion}	First ionization level	meV
σ	Electrical conductivity	S/m
ρ	Resistivity	Ω.m
R_s	Surface resistance	Ω/square
μ	Mobility	$cm^2/(V.s)$
T_{opt}	Optical transmittance	%
α	Absorption coefficient	cm^{-1}
α_0	Pre-exponential absorption factor	cm^{-1}
λ_{gap}	Band gap wavelength	nm
λ_p	Plasma wavelength	nm
C	Speed of light	m/s
π	Mathematical constant	NONE
ω_p	Plasma frequency	rad/s
I_0	Incident light intensity	W/m^2
I_T	Transmitted light intensity	W/m^2
d_{film}	Thickness	cm
q	Carrier charge	C
τ	Relaxation time between two collisions	sec
v	Carrier velocity	m/s

l	Mean free path	m
m^*	Effective mass	Kg
T	Temperature	°C
T_s	Substrate temperature	°C
M	Molar mass	g/mol
C_{sol}	Solution concentration	mol/L
V	Volume	L
m	Mass	g
ρ_{mass}	Mass density	g/cm^3
k	Wave vector	m^{-1}
C_{th}	Theoretical capacity	mAh/g
r_{ion}	Ionic radius	Å
a	Lattice parameter	nm
b	Lattice parameter	nm
c	Lattice parameter	nm
U	Voltage	V
P	Pressure	mbar
ν	Frequency	kHz
d	Distance	cm
rpm	Revolutions per minute	sec



List of Abbreviation



List of abbreviation

SnO	Tin oxide
SnO_2	Tin dioxide
Sn_3O_4	Mixed-valence tin oxide
Sn	Tin
ZnO	Zinc oxide
In_2O_3	Indium oxide
Zn	Zinc
Mn	Manganese
Cu	Copper
Fe	Iron
Sb	Antimony
F	Fluorine
Co	Cobalt
Ar	Argon
N	Nitrogen
Ga	Gallium
SiO_2	Silicon dioxide
TCO	Transparent Conducting Oxides
AZO	Aluminum doped ZnO
FTO	Fluorine doped SnO_2
ITO	Tin-doped indium oxide
TiO_2	Titanium dioxide
NiO	Nickel oxide
PdO	Palladium oxide

Ag_2O	Silver oxide
La_2O_3	Lanthanum oxide
Ta_2O_5	Tantalum oxide
AVT	Average visible transmission
FOM	Figure of merit
AHP	Analytic hierarchy process
PCE	Power conversion efficiency
TeO_2	Tellurium dioxide
PbO_2	Plumbic oxide
VB	Valence band
CB	Conduction band
CH_4	Methane
H_2	Hydrogen
CO	Carbon monoxide
H_2S	Hydrogen sulfide
Pd	Palladium
a-Si:H	hydrogenated amorphous silicon
LIBs	lithium-ion batteries
Li_2O	Lithium oxide
Li_xSn	Lithium-tin alloy
Li_2SnO_3	Lithium stannate
$LiMn_2O_4$	Lithium manganese oxide
LiO_2	Lithium superoxide
$\ddot{V}_o$	Doubly charged oxygen vacancy
Zn_2SnO_4	Zinc tin oxide
PVD	Physical vapor deposition
PLD	Pulsed laser deposition

DC	Direct current
Sol-gel	Solution-gelation
CdS	Cadmium sulfide
$SnCl_2 \cdot 2H_2O$	Tin(II) chloride dihydrate
$C_4H_6O_4Zn \cdot 2H_2O$	Zinc acetate dihydrate
$Mn(C_2H_3O_2)_2 \cdot 4H_2O$	Manganese(II) acetate tetrahydrate
$CuO_4S \cdot 5H_2O$	Copper(II) sulfate pentahydrate
$Fe(NO_3)_3 \cdot 9H_2O$	Iron (III) nitrate nonahydrate
UV-VIS	Ultraviolet–visible spectroscopy
Near-IR	Near-Infrared



Table of contents



Table of Contents

List of tables i
List of figures ii
List of symbols v
List of abbreviation vii
Table of contents x
General Introduction 1

Chapter I :Bibliographic studies of free Tin dioxide and doped Tin dioxide thin films 3

I.1 Introduction 4
I.2. Definition and Concept of transparent conducting oxides 4
I.3.Classification of transparent conducting oxides 4
I.3.1.n type and P type TCO 4
I.3.2. Simple and complex oxides 5
I.3.3. Undoped and doped oxides 5
I.4. Properties of Transparent Conducting Oxides 5
I.4.1. Optical Properties 6
I.4.1.1. Transmittance 7
I.4.1.2.Energy gap 7
I7.4.1.3.Absorption coefficient 7
I.4.1.4.Dormancy coefficient 7
I.4.2. Electrical Properties 8
I.4.2.Superficial resistance 8
I.4.3. Electrical mobility 8
I.5. TCOs Doping definition 9
I.5.1.Doping types 9
I.5.2.Importance of TCOs Doping 9
I.6. Criteria for Selecting TCOs and Merit Factor Evaluation 10
I.7. Tin Oxide (SnO2) 10
I.6. Criteria for Selecting TCOs and Merit Factor Evaluation 11
I.7. Tin Oxide (SnO2 11
I.7.1.Different Phases of tin oxides 11

1.7.2. General properties of SnO2 11
I.7.3.Physical properties of tin oxide 12
I.7.3.1 Structural properties (Crystal structure) 12
I.7.3.2. Electronic Properties of SnO_2 12
I.7.3.3. Electrical Properties of SnO_2 13
I.7.3.4. Optical Properties of Tin Dioxide SnO_2 13
I.7.3.4.1. SnO2 energy gap 14
I.7.4.Factors Affecting Optical Properties 15
I.7.5. Applications of SnO_2 Thin Films 15
I.7.5.1.Gas Sensors 15
I.7.5.2. Transparent Electrodes (Photovoltaic) 17
I.7.5.3. Lithium-Ion Batteries 17
I.7.5.4. Other Applications 18
I.8. Doping in SnO2 18
I.8.1 Definition and Purpose of SnO2 Doping 19
I.8.2.n-Type and P-Type SnO2 Doping 19
I.8.3. Doping Mechanisms in SnO2 19
I.8.4. Common Dopants for SnO_2 (Zn, Cu, Mn, and Fe) 19
I.8.4.1. Zn-Doped SnO_2 Thin Films 20
I.8.4.2. Fe-Doped SnO_2 Thin Films 20
I.8.4.3. Cu-Doped SnO_2 Thin Films 20
I.8.4.4. Mn-Doped SnO_2 Thin Films 20
I.9. Summary 20

Chapter II :Sample preparation method and characterization technique **21**

II.1. Introduction 22
II.2. Thin Films 22
II.2.1 General Concept and Advantages 22
II.2.3 Thin Film Deposition Mechanism 22
II.3. Deposition Techniques Overview 23
II.3.1.Physical Deposition Methods (PVD) 23
II.3.1.1.Sputtering 23
II.3.1.2. Thermal Evaporation Process 24
II.3.1.3. Electron Beam Evaporation 25

II.3.1.4. Pulsed Laser Deposition (PLD) 26
II.3.2.Chemical Deposition Methods 27
II.3.2.1.Sol-Gel Method 27
II.3.2.2.Electrodeposition Process 29
II.3.2.3.Spray Pyrolysis technique 29
II.3.2.3.1.Process Overview 29
II.3.2.3.2.Atomization Methods 30
II.3.2.3.3.Advantages and disadvantages 30
II.3.2.3.4. Factors Affecting Chemical Spraying with Pyrolysis 30
II.4. Thin Film Growth Mechanisms 31
II.4.1. Nucleation phase 31
II.4.2. Docking phase 31
II.4.3. The growth phase 31
II.5. Growth forms 31
II.6. Experimental aspect 32
II.6.1.Description of the experimental apparatus 32
II.6.2. Effect of substrate temperature on Droplets 33
II.6.3. Different stages of sample preparation 33
II.6.3.1. Substrate choice 34
II.6.3.2. Substrate Preparation (Cleaning and Pre-treatment) 34
II.6.3.3. Preparation of Deposition Solutions 35
II.6.3.4. Thin film deposition process 38
II.6.3.5. Trial Work Conditions 38
II.7. UV-Visible Spectroscopy Characterization 39
II.8. Optical parameter Studied 40
II.8.1.Absorption Coefficients 40
II.8.2. Extinction Coefficients 41
II.8.3. Optical Band Gap (Eg) 41
II.8.4. Urbach Energy (Eu) 42
II.9. Conclusion 43

Chapter III: Results and discussion 44

III.1. Introduction 45
III.2.1. Transmittance 45

III.2.First section: Effect of Zn concentration on optical Properties of SnO2 thin films 45
III.2.2. band gap energy 48
III.2.3. Urbach energy 50
III.3.Second section: Effect of doping type on optical Properties of SnO2 thin films 51
III.3.1.effect of Zn-, Mn-, Cu-, Fe- doping on the optical transmittance of SnO2 thin films 51
III.3.2.Effect of Zn-, Mn-, Cu-, Fe- doping on the thickness of SnO2 thin films 53
III.3.3.Effect of Zn-, Mn-, Cu-, Fe- doping on the band gap of SnO2 thin films 54
III.3.4.Effect of Zn-, Mn-, Cu-, Fe- doping on the Urbach energy of SnO2 thin films 55
III.4.Influence of Methanol Solvent 56
III.5.Implications for UV Detection and TCO Applications 56
III.6.Conclusion 57
General Conclusion 58
References 60
Abstract 72
Résumé 73
ملخص 74



General Introduction



General Introduction

The science of transparent conducting oxides was initiated in 1907 by Badeker, who made the first cadmium metal film, and in 1937, tin oxide was deposited as a thin film to provide a quantum leap in the science of transparent conducting oxides and their deposition as thin films to improve their physical and optical properties. tin oxide (SnO_2), zinc oxide (ZnO) , indium oxide (In_2O_3), and cadmium oxide (CdO) have received much attention in recent years due to their unique properties and applications in displays, solar cells, smart windows, photodiodes, and other photovoltaic devices **[1,2,3].**

The vast amount of existing studies and research in the field of using transparent carrier oxides as thin films of different types of raw materials and their specifications created the urgent need for the emergence of preparation techniques that suit their characteristics and field of applications, so the preparation techniques also witnessed great developments over the years, and many techniques appeared that were not customary, such as the pyrolysis spraying method **[4, 5].**

Among all these methods, thermal spray pyrolysis is widely used to prepare Tin oxide thin films as it is simple and less expensive to prepare compared to other methods. The impregnation process can also be easily controlled and films with good purity can be obtained. In addition to the above, it is desirable from an economic point of view because it uses less expensive commercial chemicals and is carried out under atmospheric pressure conditions, i.e. without the need for different pressures **[6].**

In recent years, the effect of many impurities and their concentration on the physical properties of tin oxide has been studied, recent research on tin oxide thin films has shown that the addition of varying proportions of Sb and F improves the crystallinity of tin oxide films, increases their transparency and improves their electrical conductivity **[7].**

The work presented in this paper belongs to this field of research that in this work, we studied the effect of doping with different types of transition materials on the optical properties of tin oxide (SnO_2). We prepared all samples by the thermal chemical spray method at 450°C and at atmospheric pressure, and because the doping process depends on the type and concentration of the dopant, we prepared two groups of samples:

The first group: Zinc was chosen as the impregnating material in different concentrations, namely 2%, 4%, 6% and 8%.

The second group: we chose different types of transition materials with the same concentration to dope the tin oxide, namely: Zinc (Zn), Manganese (Mn), Copper (Cu) and Iron (Fe).

The reason for studying the two groups of samples is the aim of this work, which is to find out the effect of doping process on the optical properties of tin oxide.

The optical properties of the samples were deduced from the transmittance curves extracted from UV-visible light spectra in the range [300nm-1100nm].

We can summarize the idea of the work in stages arranged in three chapters as follows:

The first chapter: In this chapter, we will present a theoretical study of the most important information and general concepts about transparent carrier oxides and their main features, we will highlight tin oxide and its various properties, the process and types of doping and its importance for tin oxide, then we will look at the characteristics and properties of the materials used as impregnators (zinc, manganese, copper, iron).

Chapter Two: We will focus on an introductory study of physical and chemical deposition methods, thin-film deposition mechanism and growth patterns, and then address the applied aspect of this work, from sample preparation to the technique of studying their optical properties.

Chapter Three: It will summarize and discuss the results obtained and draw some important conclusions about what the process of doping tin oxide thin films with different dopants. The third chapter will be divided into two parts. The first part will study the results obtained from the zinc- doped tin oxide at different concentrations to see the effect of concentration, and the second part will study the effect of different types of dopants on the optical properties.

Chapter I:
Bibliographic studies of undoped Tin dioxide and doped Tin dioxide thin films

I.1 Introduction

In this chapter, general concepts about transparent conductive oxides and their applications will be presented. Devoting the largest part to studying undoped and doped tin dioxide, mentioning its properties and various applications, then giving an overview of how to dope it with different materials.

I.2. Definition and Concept of transparent conducting oxides

Transparent Conducting Oxides (TCOs) are a class of materials composed of metal oxides, represented by the general formula $MxOy$, where M is the metal and O represents oxygen. These materials exhibit a wide band gap (Eg>3.1eV), ensuring high transparency in the visible spectrum (400 nm < λ< 800 nm), along with good electrical conductivity, typically around 10^3 $\Omega^{-1}\cdot cm^{-1}$**[8]**. This unique combination of optical transparency and electrical conductivity makes TCOs essential in various technological applications, including optoelectronic devices, solar cells, and display technologies. Among the most studied TCOs are SnO_2, ZnO, and In_2O_3, often doped with elements such as indium, cadmium, tin, zinc, or gallium to enhance their electrical properties **[9]**.

I.3.Classification of transparent conducting oxides

I.3.1.n type and P type TCO

TCOs are categorized into two types': n and P as shown in Table (I.1):

- **Type n:** This category is characterized by the fact that the majority of charge transporters are electrons, and oxides of this type are the most common and widely used in scientific applications due to their high efficiency and the ease with which they can be obtained **[10]**.
- **Type P**: On the other hand, holes are the majority charge transporters in this type. Despite the limited availability of transparent conductive oxides of this type, scientific research has recently intensified with the aim of developing materials of this type due to their wide prospects in the fields of modern technology **[11].**

Table I.1: Some types of transparent conductive oxides [12]

TCO of P type	TCO of n type
NiO	ZnO
CuO	SnO_2
PdO	TiO_2
Ag_2O	Ln_2O_3
La_2O_3	TaO_5

I.3.2. Simple and complex oxides

Metal oxides can be classified into main categories:

- **Simple conductor oxides :** consist of a one metal in the oxide such us: SnO_2, TiO_2, ZnO, NiO,……**[13]**
- **Mixed oxides:** containing two or more components such us: $BaTiO_3$, $CdIn_2O_4$,… **[14]** ,that have slightly or very different properties corresponding simple oxides**.**

I.3.3. Undoped and doped oxides

- **Undoped TCOs:** Transparent Conducting Oxides (TCOs) are often characterized as degenerate n-type semiconductors. In their undoped form, their electrical conductivity mainly arises from structural imperfections, particularly oxygen vacancies that are naturally formed during film deposition. These vacancies act as ionized donors by introducing energy levels slightly below the conduction band, thereby enhancing free carrier concentration. For instance, in tin dioxide (SnO_2), the first ionization level appears approximately 30 meV beneath the conduction band edge. In addition to oxygen deficiencies, excess metal atoms occupying interstitial sites can also contribute to electrical conduction in intrinsic (undoped) TCOs.

Undoped TCOs are formed when no grafted atom is present and the relationship is fulfilled: $n_i=n=p$, where n_i is the self-concentration

- **Doped TCOs**: The electrical performance of TCOs can be significantly personalized through intentional doping. This involves introducing external atoms that create extrinsic defects, modifying the material's electronic band structure. In the case of n-type doping, donor elements like antimony (Sb) in SnO_2 introduce shallow energy states just below the conduction band, making it easier for electrons to be thermally excited, thus increasing conductivity. On the other hand, p-type doping remains a major challenge due to the formation of deep acceptor states above the valence band. These deeper levels make whole generation inefficient and limit overall conductivity. Achieving stable and effective p-type TCOs often requires complex synthesis conditions and precise control over deposition parameters.[15]

I.4. Properties of Transparent Conducting Oxides

Transparent conductive oxides have excellent electrical and optical properties, making them a focus of interest for researchers to develop. This is due to their high transparency to light and their good efficiency in electrical transport, in addition to the deposition techniques used in terms of the most suitable electrical and optical properties within the values shown in Table (I-2).

Table I-2: Properties of transparent conducting oxides

properties	TCO	Ref
Optical band gap Eg (eV)	(3.01-4,6)	11
Resistance ρ(Ω. cm)	(1,47-11.1) × 10−3	40
Surface resistance RS(Ω)	21-138	40
Mobility μ($cm2. V. s$)	29.57-35.95	29
Carrier Density (cm−3)	(0.04-0.75) × 1019	40
Transmittance T(%)	60-88	11
properties	TCO	Ref

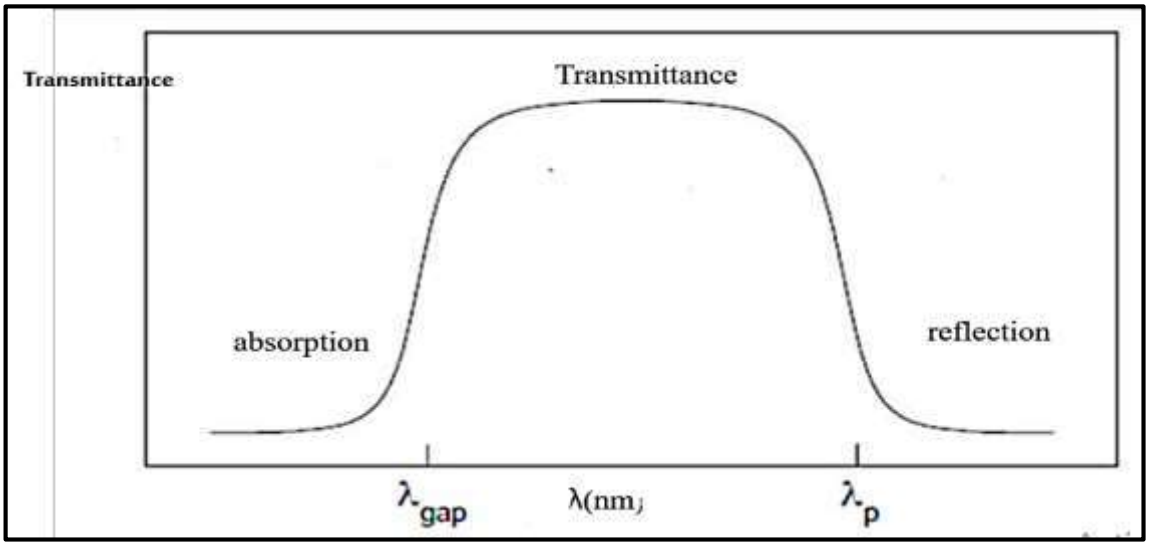
I.4.1. Optical Properties

TCOs are defined by their high optical transmission in the visible spectrum (typically >80%), governed by two critical wavelengths (see figure1.I):

- Band gap absorption edge (λ_{gap}): Photons with energy ≥ E_g are absorbed via band-to-band transitions.
- Plasma wavelength (λ_p): In the near-IR, free-electron plasma oscillations (Drude model) dominate, causing reflection. The plasma wavelength is given by**[16,17]**:

$$\lambda_p = (2\pi c)/\omega_p \quad \text{..... (I.1)}$$

Where c is the speed of light and ω_p is the plasma frequency (see Equation I.4).



FigureI.1. Transmission spectrum illustration

I.4.1.1. Transmittance

Is the ratio between the initial intensity of the radiation incident I_0 on the material and the intensity of the radiation passing through it I_T (see equation (I.2)) **[18]**:

$$T(\%) = \frac{I_T}{I_0}.100 =. \quad \text{.....(I.2)}$$

The transmittance spectrum is highly dependent on the distribution of energy levels, which is determined by the chemical composition and crystal structure of the material, in addition to being affected by other factors such as the thickness of the sample and the level of doping **[19].**

I.4.1.2.Energy gap

TCO is characterized by a wide energy interval (energy gap) that changes from 3 eV to 4,2 eV **[20]** where the width of this gap varies depending on the technique used in the deposition, experimental conditions and the type of compound used and Table (I-3) shows the energy interval for some oxides:

Table (I-4): Energetic separation of some transparent conductive oxides

Transparent Conductive Oxides	Energy Interval (E_g)
SnO_2	(3,6-4,3)eV
ZnO	(3,2 -3,3)eV
TiO_2	(3-3,2)eV
NiO	(3,6-4)eV

I.4.1.3.Absorption coefficient

It is expressed by the symbolα, and is calculated based on the Ber-lumbert relation that shows the relationship between the transmitted light flux and the absorption coefficient and is given by the relation (I.3) **[21]**

$$\alpha(cm^{-1}) = \frac{1}{d}\ln(\frac{100}{T(\%)}) = \quad \text{.....(I.3)}$$

α: absorption coefficient (cmm^{-1}), T : Transmittance and d: Thickness (cm)

I.4.1.4.Dormancy coefficient

This coefficient expresses the amount of energy absorbed by the electrons of the material from the energy of the incident radiation photons and is related to the absorption coefficient α and is given by the relationship (I.4) **[22]:**

$$K = \frac{\alpha\lambda}{4\pi} = \quad \text{.....(I.4)}$$

λ : The wavelength of the incident rays

I.4.2. Electrical Properties [23]

Since 1970, interest in the study of the electrical properties of transparent conductive oxides began these oxides are classified according to their electrical properties as semiconductors with a relatively large energetic separation: Electrical conductivity, surface resistance, and electro kinetics.

- The conductivity (σ)(relation I.5) of TCOs depends on carrier density (n_v), mobility (μ), and electron charge (q **)[16]**

$$\sigma = 1/\rho = qn_v\mu \quad \text{(I.5)}$$

q: The charge of the charge carriers

ρ: Electrical resistivity, which is the reciprocal of conductivity, expresses the resistance of a material to the flow of electric current through it and has the unit (cm.Ω) , while: (ρ) < 10^{-3} (Ω·cm)

σ For device applications, TCOs must achieve average visible transmission (AVT) > 80%

Table (I-3) shows the electrical properties of some transparent conductive oxides:

Table I-3: Electrical Properties of transparent conducting oxides

TCO	Deposition method	ρ (Ω.Cm)	μ (Vs/Cm²)	T(%)	σ (10^{-3} Ω^{-1})	Ref
ITO	Spray	$8.0x10^{-4}$	12.4	85	2.15	[24]
SnO_2	Spray	$4.3x10^{-3}$	-	97	1.45	[24]
ZnO:Al	Spray	$8.0x10^{-2}$	-	<80	-	[24]

I.4.2.Superficial resistance

Transparent conductive Oxides (TCO) are prepared in the form of thin layers, so that the superficial resistance ρ is an important electrical characteristic for understanding the nature of the surface in TCO, which is the ratio between the electrical resistance ρ and the thickness of the thin layer d denoted by (Rs) and its unit (Ω) expressed by the relationship (I.6)**[16]:**

$$R_S = \frac{\rho}{d} \quad \text{(I.6)}$$

I.4.3. Electrical mobility

Electrical mobility depends on the diffusion of charge carriers within the crystal lattice of the material, where a high concentration of these carriers leads to a decrease in mobility as a result of increased collisions, which in turn leads to a decrease in electrical conductivity. The mobility is an essential factor to ensure good

conductivity, symbolized by the symbol μ and its unit (s^{-1}. $V^{-1}.cm$) given by the relationship (I.7)**[11]**:

$$\mu = \frac{q\tau}{m^*} = \frac{ql}{v.m^*} \text{.....(I.7)}$$

q: Electron charge, τ: Relaxation time between two collisions, m^*: Effective mass of the electron, l: Mean free path, v: Thermal velocity of the electron

I.5. TCOs Doping definition

Doping transparent conductive layers (TCOs) is an essential process for improving their electrical such as carrier concentration and electrical conductivity and optical properties. So Doping is the addition of impurities to modify the conductivity and transparency of TCOs.

The doping can be substitution, vacation, or implantation interstitial **[25]**; its causes new electron acceptor and donor levels to appear in the band structure of the doped material. These levels appear in the gap between the conduction band and the valance band. There are two type of doping **[26]:**

Doping introduces impurities that alter the electronic properties of the TCO, either by increasing the number of free electrons (n-type) or by creating holes (p-type) that act as positive charge carriers

I.5.1.Doping types

- **n-type doping:** Introducing elements with more valence electrons than the TCO's host material**[27].** These dopants donate electrons to the conduction band, increasing the concentration of free electrons and making the material conductive. Such us Fluorine doping of SnO_2 (FTO), aluminum doping of ZnO **[28].** and gallium doping of ZnO.
- **P-type doping**: Introducing elements with fewer valence electrons than the TCO's host material. These dopants create "holes" in the valence band, which act as positive charge carriers, allowing the material to conduct. For Examples: Copper doping of SnO_2 (p-type SnO_2) **[29].**.

I.5.2.Importance of TCOs Doping

- **Enhanced Conductivity:** Doping significantly increases the electrical conductivity of TCOs, making them suitable for applications requiring high electrical current flow**[19].**.
- **Tunable Properties:** By carefully choosing dopants and their concentration, the electrical and optical properties of TCOs can be tailored for specific applications **[30].**

- **pn Junctions:** Doping with both n-type and p-type materials allows for the creation of pn junctions, which are crucial components in many optoelectronic devices

I.6. Criteria for Selecting TCOs and Merit Factor Evaluation [31].

When selecting transparent conductive oxides (TCOs) and evaluating their performance, several factors and figure of merit approaches are considered. Key criteria include: Optical transmission, electrical conductivity, cost, and the ability to integrate with other device components. Figure of merit (FOM) calculations, like Haacke's FOM, help quantify the trade-off between optical transmission and electrical conductivity, aiding in the selection of TCOs **[32]**.

- **Optical Transmission:** High optical transmission across the desired wavelength range is crucial, especially for applications like solar cells where light needs to reach the active layer.
- **Electrical Conductivity:** TCOs must exhibit good electrical conductivity to facilitate charge transport.
- **Cost:** Cost-effectiveness is a significant factor, especially for large-scale applications.
- **Integration:** The ability of the TCO to be deposited and integrated with other device components (e.g., active layer, electrodes) is important.
- **Stability:** TCOs should be stable over time and under various environmental conditions.
- **Process ability:** The ease with which the TCO can be deposited and fabricated into desired shapes and structures is crucial. Merit Factor Evaluation:
- **Haacke's Figure of Merit (FOM):** This widely used FOM assesses the performance of TCOs by considering both optical transmission and electrical conductivity. It often uses the average optical transmission around 500 nm, a region near the solar spectrum maximum **[32]**.
- **AHP (Analytic Hierarchy Process):** This criteria method can be used to assign weights to different criteria (e.g., FOM, PCE, cost) and then calculate a combined score to assess the overall performance of different TCO materials **[33].**

I.7. Tin Dioxide (SnO_2)

Tin dioxide, also known as stannic oxide or tin dioxide, is an inorganic compound with the chemical formula SnO_2. It's a white or off-white crystalline solid or powder with various applications **[34]**.

SnO_2 tin dioxide is one of the most exciting and unique semiconductors due to its low electrical resistance, high optical transmittance in the visible spectrum, infrared reflectivity and chemical stability in acidic and basic environments **[35]**, Its resistance to melting up to a temperature of C°1620**[36]**, as well as its low cost,

allows it to be used in many applications such as optoelectronics, solar cells, as a gas detector, and as an anode material in a lithium battery **[35]**.

I.7.1.Different Phases of tin oxides

When tin dioxide (SnO_2) thin films are deposited at temperatures below 350 °C, they remain in an amorphous state. Crystallization only initiates once this temperature threshold is reached. Films obtained through various synthesis techniques are often non-stoichiometric and can temporarily exhibit metastable forms such as SnO and Sn_3O_4.

The SnO phase tends to appear at around 400 °C during deposition, but disappears by 500 °C. It undergoes decomposition into Sn and SnO_2 when annealed at approximately 450 °C. To obtain films with good SnO_2 stoichiometry, annealing at 500 °C is thus essential. As for the Sn_3O_4 phase, it emerges after a brief heat treatment at 600 °C and gradually converts into SnO_2 if the treatment is extended to one hour at the same temperature **[15].**

1.7.2. General properties of SnO_2

Tin dioxide have many properties, the table I-4 **[37]** show their general properties

Table I-4: general properties of tin dioxide

SnO_2	Chemical formula
Rutile structure.	Crystal structure
crystalline solid or powder	Appearance
150,69g/mol	Molar mass
White or off-white	Color
6.95 g/cm³.	Density
E_g=3.6 eV	Energy gap
1500-1630C°	Melting Point
2330°C	Boiling point:

I.7.3.Physical properties of tin dioxide

I.7.3.1 Structural properties (Crystal structure)

Tin dioxide (SnO_2) has a single stable state at atmospheric pressure and is known as Cassitérite. It is characterized by a Rutile-type tetragonal hinge structure belonging to the space group P4/mnm and its basic unit contains six atoms: Two atoms of tin and four atoms of oxygen **[38]**. Each (Sn^{4+}) ion is positioned at the center of a regular octagon, surrounded by six oxygen ions (O_2(-)), while each oxygen ion is surrounded by three tin ions (Sn), arranged on the vertices of an isosceles triangle**[39,38]**. Several metal oxides, such as TiO_2, TeO_2, and PbO_2, share this structure **[38]**. Figure I.2 shows the basic structure of tin dioxide, where the tin atoms form a hexagonal arrangement, with oxygen as the nearest neighbor, the lattice parameters are a = b = 0.475 nm, c = 0.318 nm **[39].**

I.7.3.2. Electronic Properties of SnO_2

SnO_2 exhibits **[17]**:

- Direct band gap (3.6 eV) with valence band (VB) from O-2p orbitals ($1s^2\ 2s^2\ 2p^4$)
- Conduction band (CB) from Sn-5s/5p orbitals ($4d^{10}5s^25p^2$)
- Strong Sn-5s character (90%) at CB minimum, figure I.3 show the Band structure of undoped SnO_2

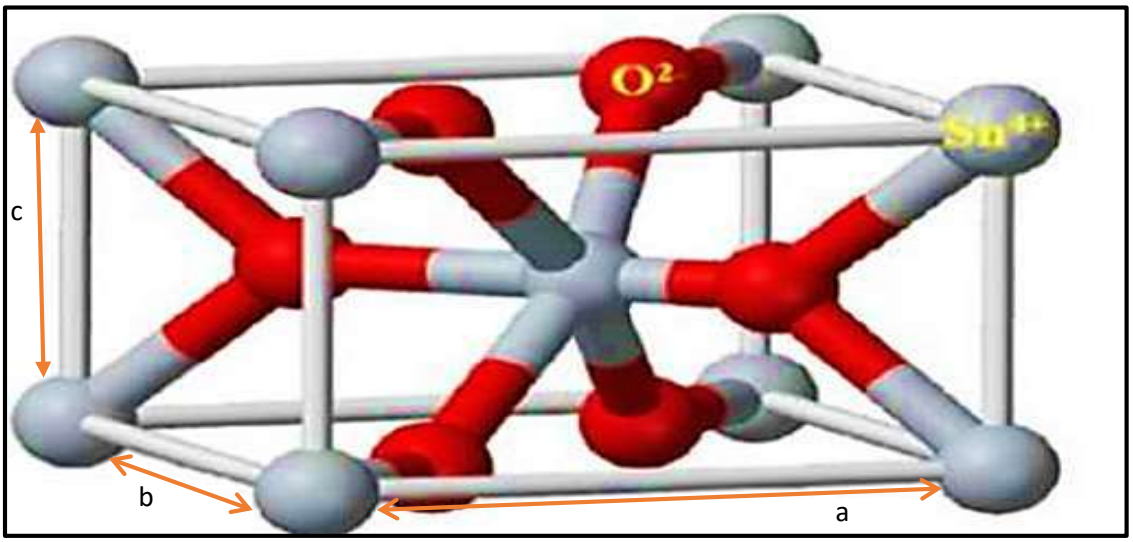


Fig I.2. Unit cell of tin dioxide (rutile-type structure) [40].

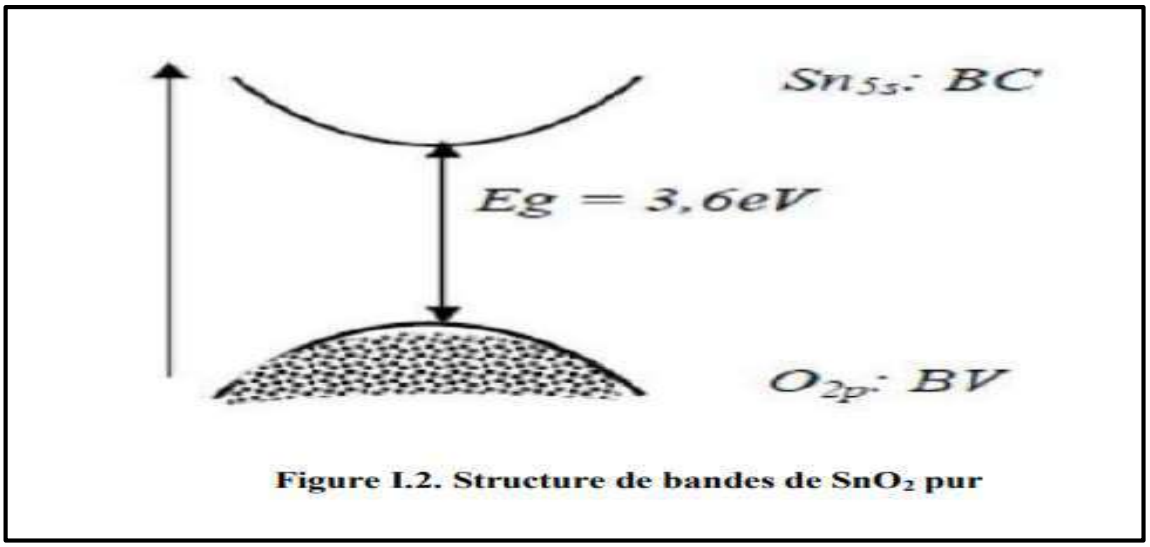


Figure I.2. Structure de bandes de SnO_2 pur

Figure I.3. Band structure of undoped SnO_2 [17]

I.7.3.3. Electrical Properties of SnO_2

Tin dioxide in its undoped state is a single-crystal semiconductor material with an energy gap width of (3.5-4.2eV) at room temperature, SnO_2 is a self-insulating material. However, its electrical properties can be significantly improved when deposited as a thin film at 480°C, where it becomes a non-stoichiometric material, giving it better conductivity properties **[41]**.

SnO_2 is a wide-band gap (3.6 eV) n-type semiconductor that behaves as an insulator in its stoichiometric state but achieves significant conductivity through doping **[29].** Two primary mechanisms govern this transition **[40]**:

1. Intrinsic doping via oxygen vacancies, releasing free electrons into the conduction band **[4].**
2. Extrinsic doping by substituting Sn^{4+} with group III/V elements (e.g., Sb, F) or O^{2-} with group VI elements **[4].**

I.7.3.4. Optical Properties of Tin Dioxide SnO_2

Optical behavior of tin dioxide (SnO_2) is determined by how electromagnetic waves interact with electrons in semiconductors. When these waves strike the material, they can be entirely absorbed if their energy is sufficient to excite electrons from the valence band to the conduction band. Consequently, the material's transparency in the visible spectrum is dictated by its band gap; if the band gap energy is equal to or lower than the incident photon energy, the material will appear opaque**[42].**

For a material to exhibit strong transparency in the visible spectrum, its band gap must exceed the energy corresponding to wavelengths between 400nm and 800 nm. Generally, materials with a band gap of at least 3.1 eV demonstrate good optical transmission in this range.

In the case of nanostructured SnO_2, the band gap varies between 3.5 eV and 4.2 eV. Meanwhile, thin films of SnO_2 typically have a band gap close to 3.8 eV, making them highly transparent to visible light.

I.7.3.4.1. SnO_2 energy gap

Tin dioxide films have a direct energy cut-off between 3.5eV and 4.2eV, which varies depending on the deposition method used**[37]**. The concept of an energy separator, whether direct or indirect (also known as a forbidden band), is determined by the positions of the maximum values of the valence band and the minimum values of the transfer band. According to Figure I.4: These energies are displayed in terms of the wave vector (k). If the transfer and valence bands coincide with the same wave vector (k), the transfer of electrons is perpendicular, making it a direct energy separation. If the minimum values of the transfer band are shifted so that they do not coincide with the maximum values of the valence band, the transfer is indirect **[43]**. Figure I.5 shows the structure of its energy gap.

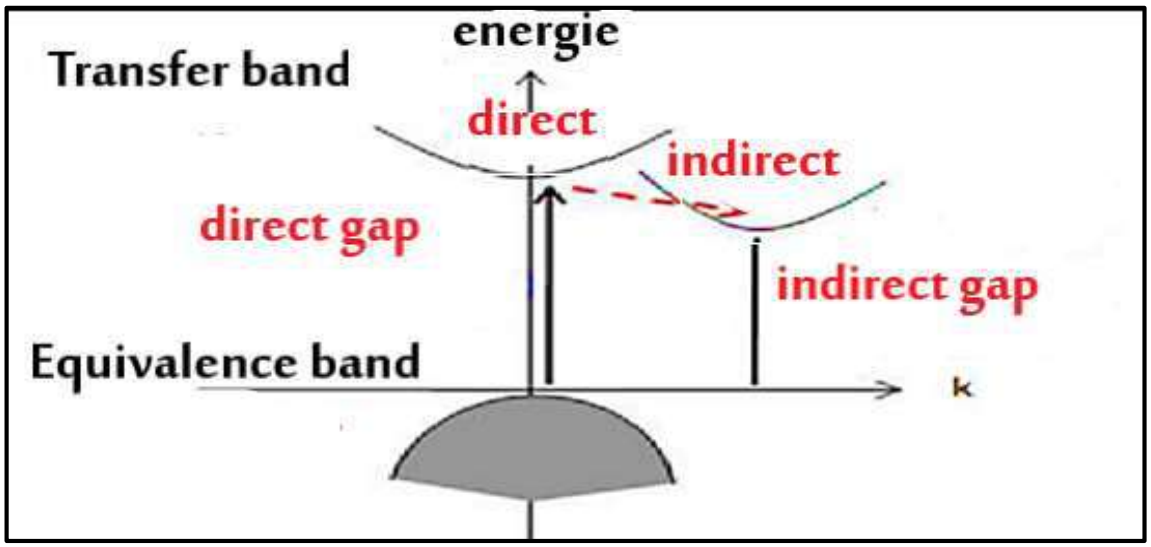


Figure I.4. Schematic diagram showing the direct and indirect transport of semiconductors [44].

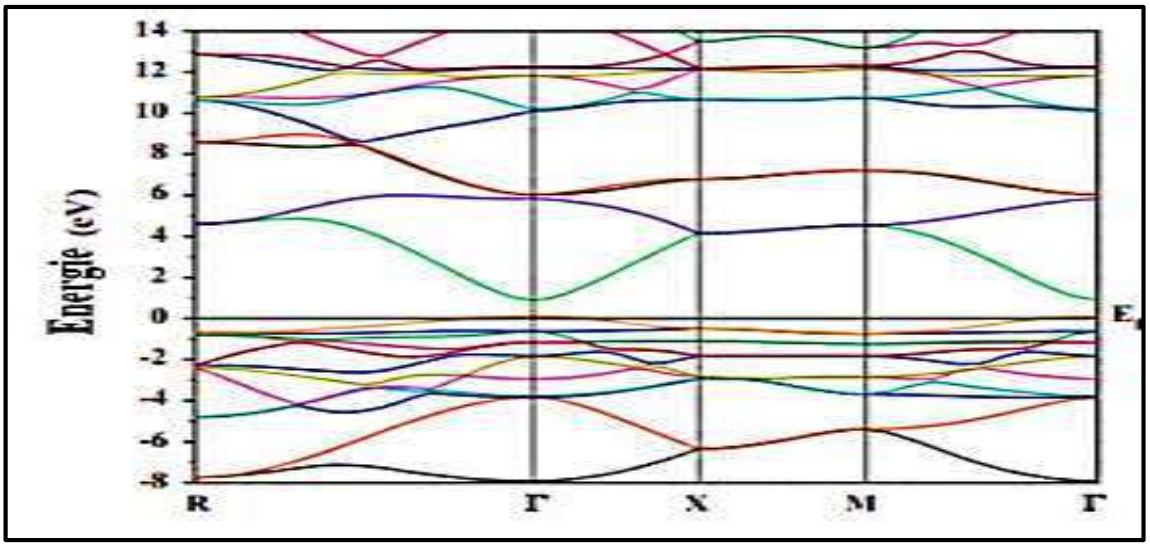


Figure I.5. Schematic diagram showing the structure of SnO_2 energy gap. [45]

I.7.4.Factors Affecting Optical Properties

- **Synthesis Method:** Different methods, like chemical vapor deposition, sputtering, or sol-gel, can affect the structural and optical properties of SnO_2 **[46]**.
- **Annealing Temperature:** Annealing can affect the optical properties, including transmittance, refractive index, and band gap **[47]**.
- **Thickness:** The thickness of SnO_2 thin films can influence its optical performance **[48]**.
- **Substrate:** The substrate on which SnO_2 is deposited can also affect its optical properties **[49]**.
- **Doping:** Doping SnO_2 can modify its optical properties **[50]**.

I.7.5. Applications of SnO_2 Thin Films

SnO_2 thin films enable diverse technological applications due to their unique combination of optical transparency and electrical conductivity.

I.7.5.1.Gas Sensors

SnO_2 is the most widely used material for semiconductor gas sensors due to its sensitivity to various gases (flammable (CH_4, H_2) and toxic gases (CO, H_2S)) **[51].** Figure I.6 indicate an example for CO captor based on SnO_2 thin films.The detection mechanism relies on conductivity changes when gases adsorb onto the SnO_2 surface. For example, CO reacts with pre-adsorbed oxygen ions (O^-), releasing electrons and increasing conductivity **[52].**

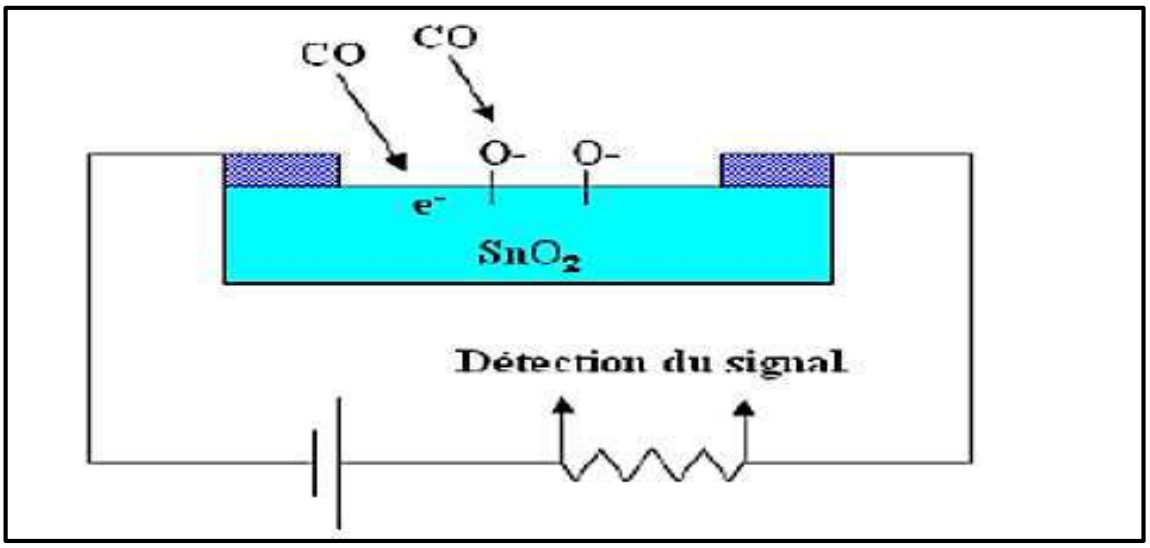


Figure I.6.CO sensor based on SnO_2 thin films [37]

Doping SnO_2 with metals (Pd, Pt, or Sb) enhances selectivity—e.g., Pd improves CO detection at 50°C **[51].** Sensor sensitivity is defined as the resistivity ratio before/after gas exposure (Figure 1.7) **[37].**
Taguchi's 1962 patent pioneered this technology, leading to commercial sensors like Figaro's domestic gas detectors **[51].**

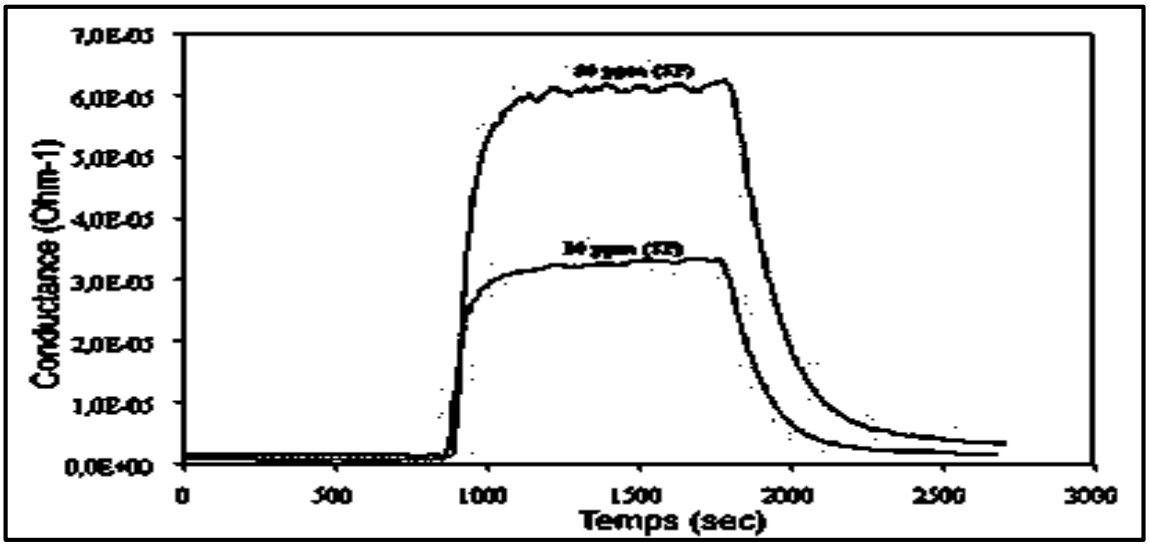


Figure 1.7. (Ethanol response): Insert after "resistivity ratio" to show real-world sensitivity [37].

I.7.5.2. Transparent Electrodes (Photovoltaic)

SnO_2 thin films serve as transparent conductive electrodes in solar cells due to their high optical transmission (>85%) and electrical conductivity (when doped with F or Sb) **[53, 54].** In amorphous silicon (a-Si:H) solar cells, SnO_2 acts as a front contact layer, collecting electrons generated by photon absorption in the silicon layer (Figure 1. 8) **[53].**

Its wide bandgap (3.6 eV) minimizes UV absorption, while surface roughness scatters light to enhance trapping in the a-Si:H layer **[54].** Undoped SnO_2 deposited by spray pyrolysis also functions as an anti-reflective coating (3% reflectivity at 600–1000 nm) **[54].**

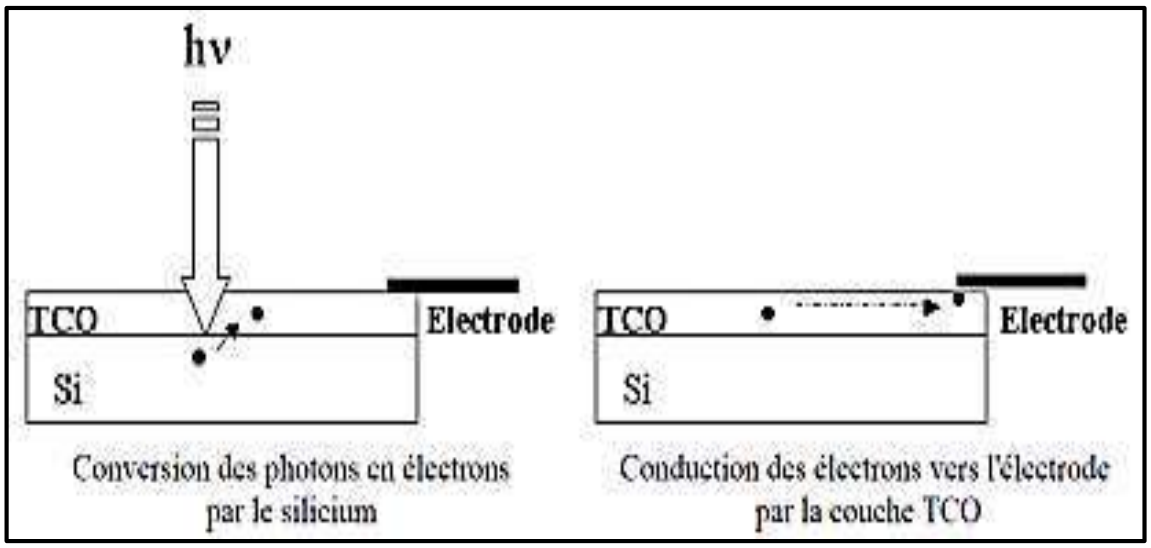


Figure 1.8. (Si-TCO electrode): Place after "front contact layer" to illustrate electron collection [37].

I.7.5.3. Lithium-Ion Batteries

SnO_2 is a promising anode material for lithium-ion batteries (LIBs), offering higher theoretical capacity (790 mAh/g) than graphite (372 mAh/g) **[52, 51].** During charging, Li^+ insertion converts SnO_2 to Sn and Li_2O, followed by alloying ($Sn + Li^+ \rightarrow Li_xSn$). However, volume expansion (~300%) causes degradation. Composite anodes (e.g., $Li_2SnO_3/LiMn_2O_4$ or Sn/LiO_2 multilayers) improve cyclability (Figure 1.9**) [52, 45].**

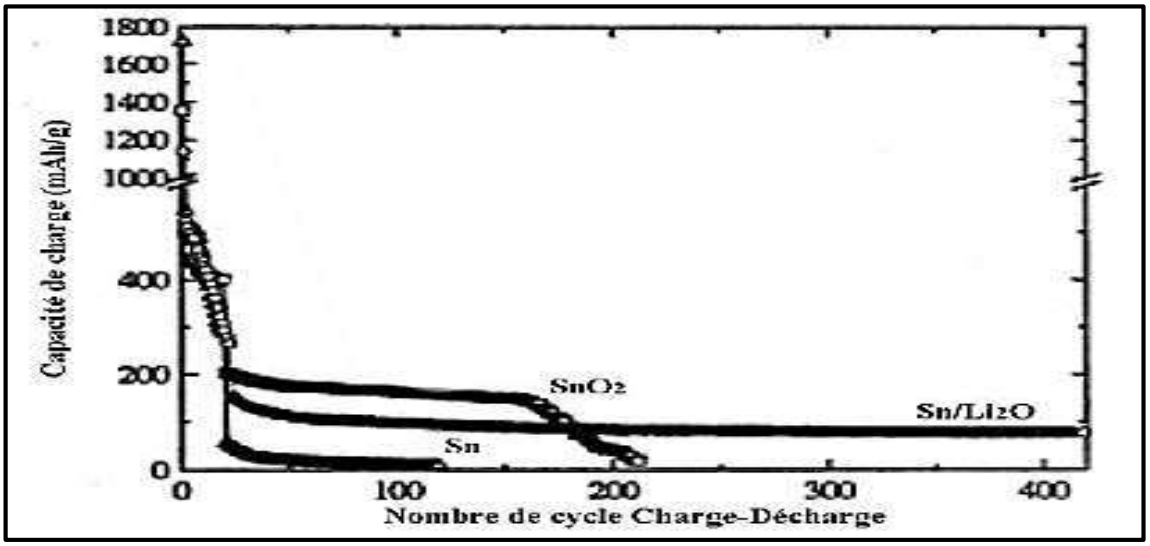


Figure 1.9. Charge-discharge curves [37]

I.7.5.4. Other Applications

SnO_2 is used as a TCO in other various devices like solar cells, light-emitting diodes, and touchscreens.

- **Electrode Material:** SnO_2 is used as an electrode material in solar cells and other optoelectronic devices **[32].**
- **Transparent Electromagnetic Shielding:** SnO_2 can be used for transparent electromagnetic shielding **[55]**.
- **Heat Mirrors:** SnO_2 can act as a heat mirror due to its high reflectance in the near-infrared region **[20].**
- Photo catalysis: SnO_2 degrades organic pollutants (e.g., phenols) under UV light by generating hydroxyl radicals **[51, 54].** Mixed Sb-Sn oxides catalyze propylene oxidation to acrylic acid **[51].**
- Low-Emissivity Coatings: Fluorine-doped SnO_2 (FTO) layers (300–400 nm thick) reflect infrared radiation while maintaining visible **transparency [52].**

I.8. Doping in SnO_2

The primary doping mechanisms in TCOs include substitution doping, where donor or acceptor atoms replace host atoms in the crystal lattice; interstitial doping, where dopants occupy empty spaces within the lattice; and vacancy doping, where native defects such as oxygen vacancies serve as intrinsic sources of conductivity **[58], [59].** For example, in SnO_2, oxygen vacancies and interstitial atoms contribute to conduction even in the undoped state, while dopants like Sb alter the electronic structure to shift the balance of charge carriers **[59], [61].**

I.8.1 Definition and Purpose of SnO_2 Doping

Doping is the process of intentionally introducing a small amount of impurities into a semiconductor or a transparent conducting oxide (TCO) to alter its physical properties—most commonly its electrical conductivity. In an undoped SnO_2, the number of electrons in the conduction band equals the number of holes in the valence band, maintaining equilibrium **[29].** Doping disturbs this balance to favor either electrons or holes as the majority carriers. In SnO_2, doping serves a similar purpose by increasing the number of charge carriers, enhancing their electrical performance **[59].** The success of doping depends on factors such as the dopant's solubility and its integration into the host lattice, which can occur via substitution, vacancy, or interstitial mechanisms **[58], [59].**

I.8.2.n-Type and P-Type SnO_2 Doping

In n-type doping, donor elements with extra valence electrons introduce shallow energy levels just below the conduction band, contributing free electrons that increase conductivity **[60], [29], [59].** This can occur via substitution doping, oxygen vacancies, or interstitial implantation **[5], [59].** In materials like SnO_2 and ZnO, n-type doping is dominant due to their natural tendency toward electron conduction. Common dopants include antimony (Sb), fluorine (F), copper (Cu), iron (Fe), cobalt (Co), and nickel (Ni) **[29], [59], [61].**

P-type doping, on the other hand, uses acceptor impurities that create electron- deficient sites or "holes" by introducing energy levels near the valence band **[60], [29].** While elements like nitrogen (N), aluminum (Al), lithium (Li), and gallium (Ga) are explored for p-type doping in SiO_2, achieving stable and efficient hole conduction remains difficult due to self-compensation effects **[29], [61].**

I.8.3. Doping Mechanisms in SnO_2

The primary doping mechanisms in TCOs include substitution doping, where donor or acceptor atoms replace host atoms in the crystal lattice; interstitial doping, where dopants occupy empty spaces within the lattice; and vacancy doping, where native defects such as oxygen vacancies serve as intrinsic sources of conductivity **[58], [59].** For example, in SnO_2, oxygen vacancies and interstitial atoms contribute to conduction even in the undoped state, while dopants like Sb alter the electronic structure to shift the balance of charge carriers **[59], [61].**

I.8.4. Common Dopants for SnO_2 (Zn, Cu, Mn, and Fe)

Doping SnO_2 with various metallic elements can effectively tailor its structural, optical, and electrical properties for applications in optoelectronics and gas sensing.

I.8.4.1. Zn-Doped SnO_2 Thin Films

When Zn^{2+} ions (0.74 Å) substitute Sn^{4+} ions (0.69 Å) in the SnO_2 lattice **[62],** they introduce tensile strain and oxygen vacancies ($\ddot{V}_o$) to maintain charge neutrality, with each Zn^{2+} generating approximately one $\ddot{V}_o$ **[63].** At Zn levels below 5 at.%, the rutile structure remains stable, and the band gap narrows from 3.6 eV to ~3.4 eV due to defect tail states, while transmittance drops from ~85% to 75% **[63].** At higher doping, Zn_2SnO_4 secondary phases emerge, disrupting the lattice and scattering carriers, consistent with degenerate n- type semiconductor behavior **[63].**

I.8.4.2. Fe-Doped SnO_2 Thin Films

Fe doping alters the crystallization and morphology of SnO_2 films, increasing porosity and enhancing conductivity by narrowing the band gap **[64].** The presence of Fe improves gas sensor sensitivity due to more active sites and has been particularly effective at ~3% doping, where faster response times have been observed **[64], [65].**

I.8.4.3. Cu-Doped SnO_2 Thin Films

Cu doping significantly affects the optical and structural features of SnO_2 films. The band gap decreases from 3.75 eV (undoped) to 3.50 eV at 4% Cu **[68].** At this level, films show high visible transmittance and a smooth, uniform surface **[68].** However, higher concentrations lead to surface changes and reduced transmittance. Cu also enhances electrical conductivity and gas sensing performance, especially at 3%, where fast response and recovery times are achieved **[68], [69].**

I.8.4.4. Mn-Doped SnO_2 Thin Films

Mn doping improves the crystallinity and optical transparency of SnO_2 thin films **[16].** It also reduces the band gap, enhancing electrical conductivity and catalytic activity, particularly valuable for gas sensing applications **[66], [67].** Mn- doped films demonstrate improved sensitivity and faster response times **[66].**

I.9. Summary

In this chapter, a bibliography is provided on the conductive oxides, with an extensive study of undoped and doped tin dioxide in terms of its definition, various physical properties, and applications. We will discuss how to prepare it and how to study its optical properties in the second chapter.

Chapter II:
Sample preparation method and characterization technique

II.1. Introduction

In this chapter, the experimental method for sample preparation and the technique for investigating their optical properties is discussed, since the samples are thin films. Firstly, the definition of thin films and their chemical and physical deposition methods. Secondly, explain in detail the method which chosen for the experimental work from its working principle and everything related to it. Thirdly the technique of extracting the optical properties of the prepared samples are all discussed.

.

II.2. Thin Films

Thin films play a crucial role in modern materials science due to their unique dimensional constraints, which significantly alter their physical behavior compared to bulk materials. This section outlines the general concept, key advantages, and basic deposition principles of thin films relevant to this study.

II.2.1 General Concept and Advantages

A thin film refers to a material layer whose thickness has been significantly reduced—often to values measured in angstroms—forming a quasi-two-dimensional structure deposited on a solid substrate such as glass or silicon, this dimensional confinement alters many physical properties, distinguishing thin films from their bulk counterparts. In the bulk state, surface effects are negligible, but in thin films, the influence of boundary surfaces becomes predominant. As the film becomes thinner, this surface-dominated behavior becomes even more pronounced **[70], [71].**

Thin films exhibit anisotropic properties due to their directional dependence, which arises from both their geometry and the influence of the substrate on which they are deposited. Even when films of identical material and thickness are used, their physical properties can differ greatly depending on whether the substrate is amorphous (e.g., glass) or crystalline (e.g., silicon) **[70].** This underlines the critical role of the substrate in determining the structural and functional behavior of the film **[70], [71].**

The advantages of thin films include their economical use of materials and the simplicity of deposition technologies. They are employed across a broad spectrum of materials, including metals, polymers, alloys, and refractory compounds such as oxides, nitrides, and carbides **[70].**

II.2.3 Thin Film Deposition Mechanism

The deposition of a thin film involves transferring the material in a way that allows it to form a continuous layer on the substrate. This process generally requires the material particles to pass through a medium—liquid, solid, or gas—that delivers them to the substrate surface. Upon arrival, the particles either adhere to the surface

via van der Waals forces or undergo chemical reactions with it **[71].** Deposition methods fall into two main categories:

- **Carrier Gas Methods:** The material to be deposited is transported from its source to the substrate using a gas stream, resembling diffusion-based techniques in microelectronics **[70], [71].**
- **Low-Pressure/Vacuum Methods**: In this case, the deposition takes place under vacuum conditions, with the material driven toward the substrate by thermal or mechanical impulses. Techniques such as sputtering and thermal evaporation fall under this category **[70].**

Each method enables the fabrication of uniform and tailored thin films for diverse applications, with the technique selected depending on the nature of the material and the desired properties of the resulting layer **[70].**

II.3. Deposition Techniques Overview

II.3.1.Physical Deposition Methods (PVD)

The Physical Vapor Deposition (PVD) methodology encompasses a group of vacuum-based coating techniques in which material deposition proceeds through three fundamental phases **[70]**:

- **Vaporization:** Source materials are converted into atomic or molecular vapor—often as nanoparticle clusters—by means of thermal energy (evaporation), plasma bombardment (sputtering), or pulsed laser irradiation (ablation).
- **Transport:** The vaporized species travel through a low-pressure environment toward the target substrate surface.
- **Film Formation:** Upon reaching the substrate, the particles undergo nucleation and gradually form a thin film through surface adhesion and atomic rearrangement. PVD enables the fabrication of high-purity metallic, ceramic, and compound coatings with precise control over thickness, often at the sub-micron scale.

II.3.1.1.Sputtering

Sputtering is a physical deposition process in which atoms are ejected from a target material due to bombardment by high-energy particles. This process takes place in a vacuum chamber with a controlled gas atmosphere, typically using inert argon at a specific processing pressure. The target, acting as the cathode, is positioned facing the substrate. When a voltage is applied, electrons accelerate away from the target, colliding with gas molecules and generating a weakly ionized plasma (figureII.1). The resulting ions bombard the target, causing atoms to be ejected and subsequently deposited as a thin film on the substrate. Additionally, other plasma-induced processes, such as excitation, de-excitation, and dissociation, may influence the growth and properties of the deposited film(see figure II.2), so Positive argon

atoms in the plasma is accelerated towards the negative target where they dislodge group of atoms. Some of these atoms deposited on to the substrate to form the film**[72]**.

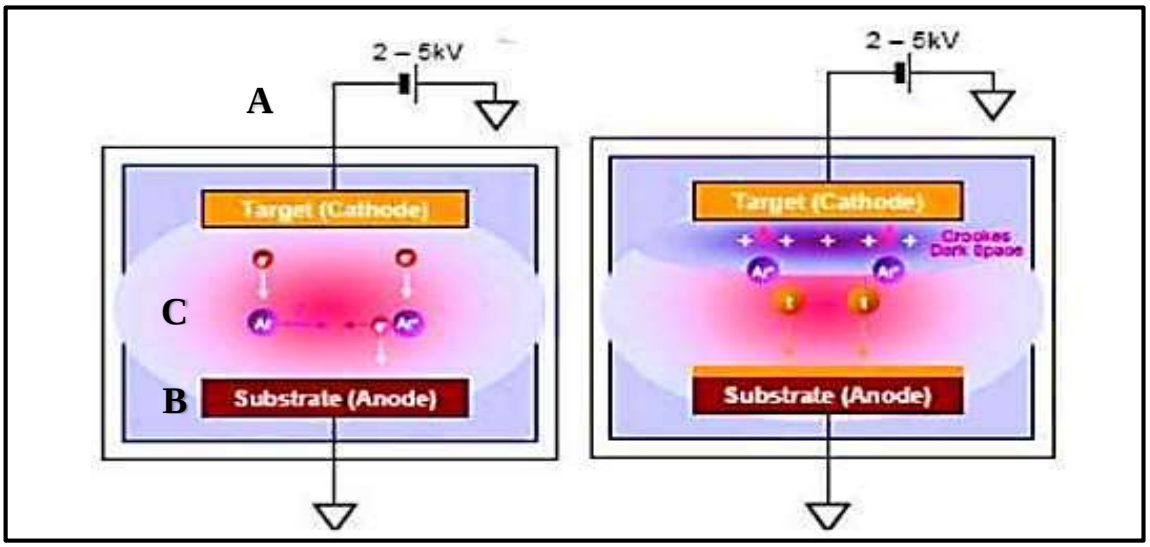


Figure II.1. DC sputtering voltage configuration (2–5 kV). Labels: (A) Target (cathode), (B) Substrate, (C) Plasma generation region [73].

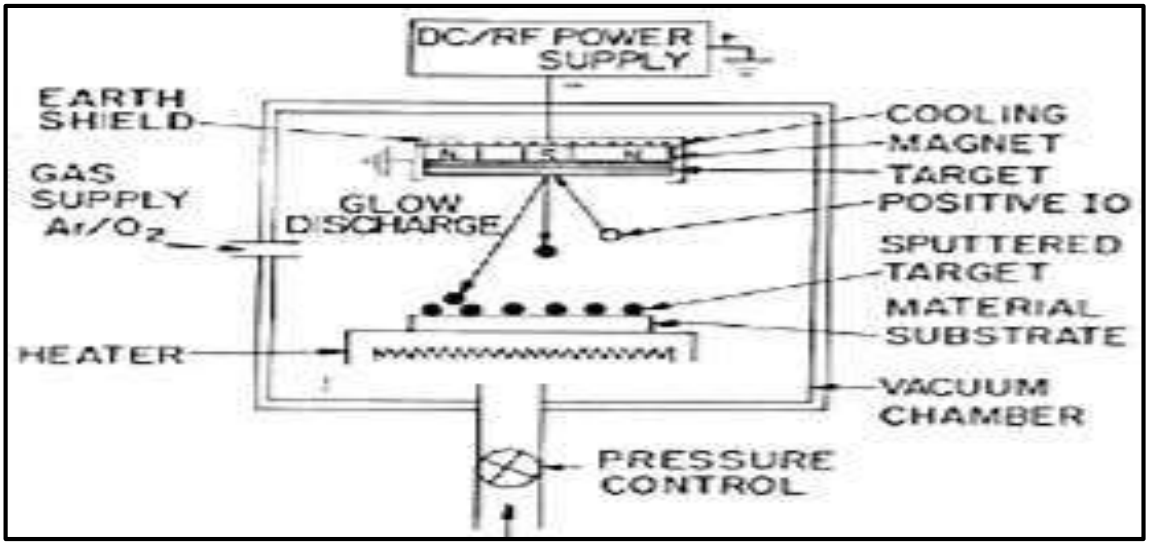


Figure II.2. Schematic view of sputtering process [74].

II.3.1.2. Thermal Evaporation Process

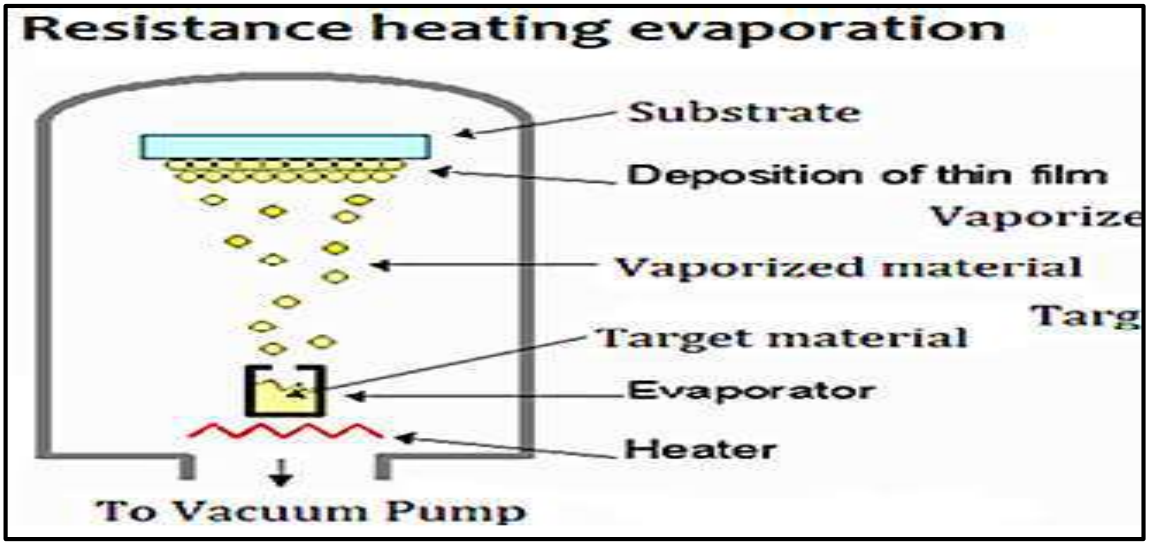
Thermal evaporation is a physical vapor deposition (PVD) technique where the source material is vaporized through Joule heating under high vacuum. The low pressure (~10^{-5} mbar) ensures linear particle trajectories, meaning only substrates directly facing the evaporation source are coated **[75]**.

A typical setup (FigureII.3) consists of a heated crucible (e.g., tungsten)

that vaporizes the target material, with particles condensing on the substrate under vacuum **[77].** However, this method requires high power for refractory materials and produces low-energy particles, which can result in weak film adhesion **[75].**

The experimental procedure involves **[76]**:

- Mounting substrates on a holder inside the chamber.
- Placing the source material (e.g., metal) in a tungsten crucible.
- Evacuating the chamber to ~1.5×10^{-5} mbar.
- Heating the crucible until evaporation, followed by cooling before venting

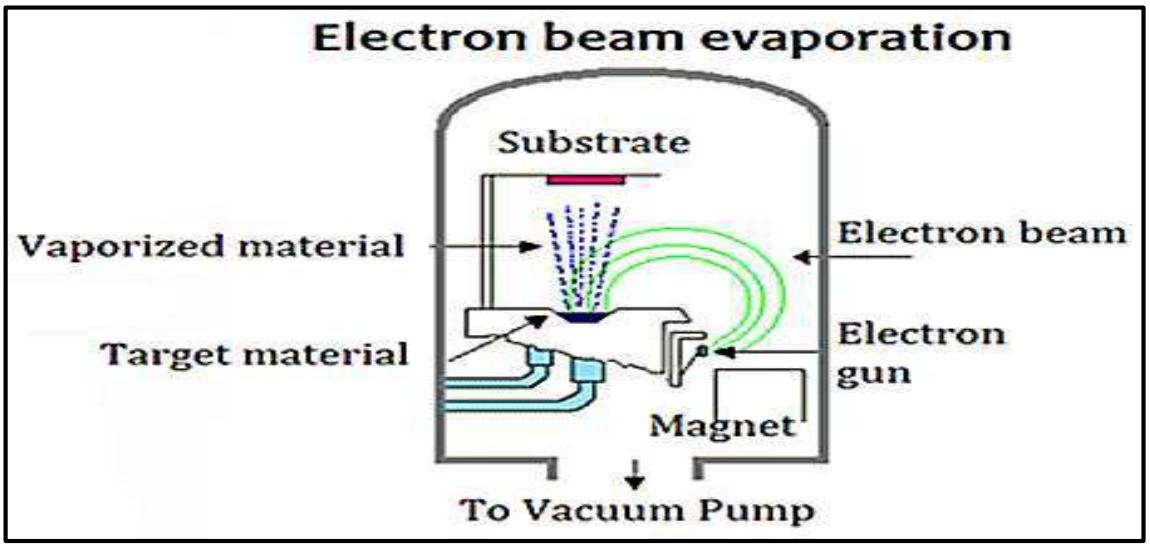


FigureII.3. Schematic of thermal evaporation setup [77].

II.3.1.3. Electron Beam Evaporation

In this technique, a high-energy electron beam, controlled by a magnetic field, is used to directly heat and evaporate the target material (Figure II.4).

Unlike thermal evaporation, where heat is transferred through a crucible, E-Beam Evaporation allows the material to reach its melting point almost instantly by focusing the electron beam directly onto it. This method enables the simultaneous evaporation of multiple materials while minimizing contamination, as the material does not come into contact with a container. The intense energy from the electron beam ensures efficient melting and vaporization, making this technique ideal for high-purity thin film deposition**.**[73].



FigureII.4.Electron beam evaporation setup [78].

II.3.1.4. Pulsed Laser Deposition (PLD)

A PLD system indicate in the figure.II.5: consists of a vacuum chamber with at least one window transparent to the laser wavelength. Inside, the target and substrate holder are positioned at a fixed distance, with the target surface facing the substrate .When the laser strikes the target, it ablates the material, producing a plasma that expands toward the substrate. The energetic species within this plasma deposit onto the substrate, leading to thin-film formation **[79]** PLD's advantages include fast deposition and compatibility with reactive gases like oxygen **[80].**

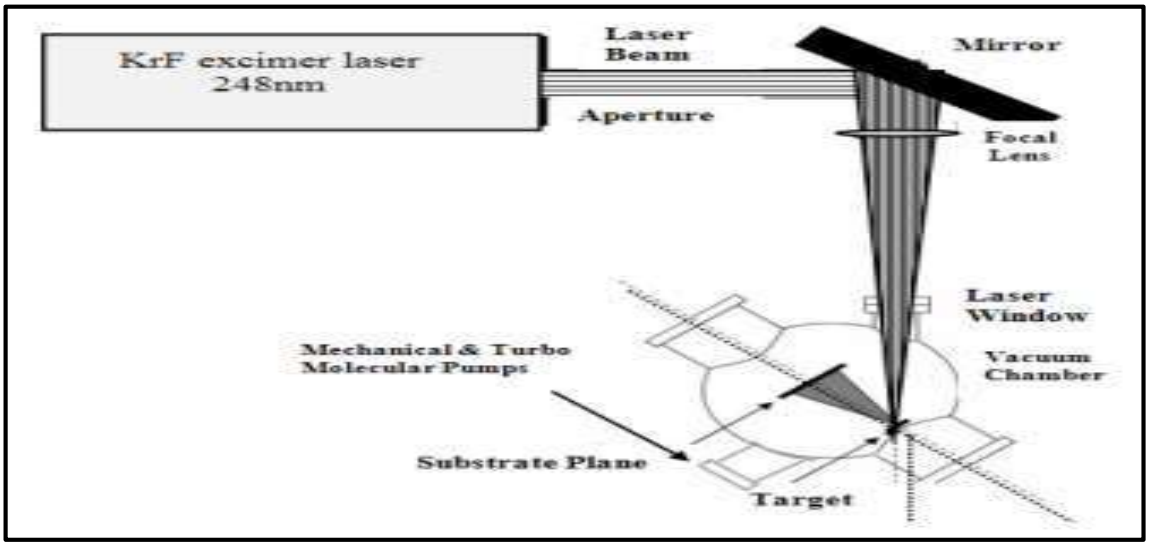


Figure II.5. PLD system representation [81].

By this method thin film quality depends on **[80]**:

- Laser parameters (wavelength, energy, pulse duration).
- Ambient gas pressure.
- Target-to-substrat distance.
- Substrat temperature

II.3.2.Chemical Deposition Methods

To achieve high-quality thin films at a lower cost, chemical deposition techniques have become widely adopted. These methods offer an economical alternative, requiring simpler equipment while still ensuring well-structured films. The effectiveness of chemical deposition depends on various factors, including solution composition **[82].** PH balance, and viscosity. Among the most commonly used techniques, sol-gel processing, electrodeposition, and spray pyrolysis stand out for their ability to produce high-quality films with minimal resource consumption **[80].**

II.3.2.1.Sol-Gel Method

The sol-gel method is a chemical process used to fabricate various materials, including glasses, gels, and ceramic powders. It involves preparing a liquid-based system containing dispersed solid nanoparticles (sol), which gradually evolves into a structured, interconnected solid network (gel). As the liquid component evaporates, a dense, glass-like material is left behind.

The sol-gel process consists of two primary reactions: hydrolysis and condensation. The hydrolysis reaction leads to the formation of the sol, while the condensation reaction results in the gelation process, forming a solid network. When applied to a substrate, this process enables the deposition of thin films with high purity at relatively low temperatures **[82].**

The sol-gel process can be carried out using different methods **[83]:**

- **Spin-coating** is a method for depositing thin films on flat surfaces. The process begins by applying a liquid solution to a stationary substrate. Once the substrate starts spinning at high speed (Figure II.6), the liquid spreads outward due to centrifugal force, forming a thin and even layer while the excess solution is ejected.

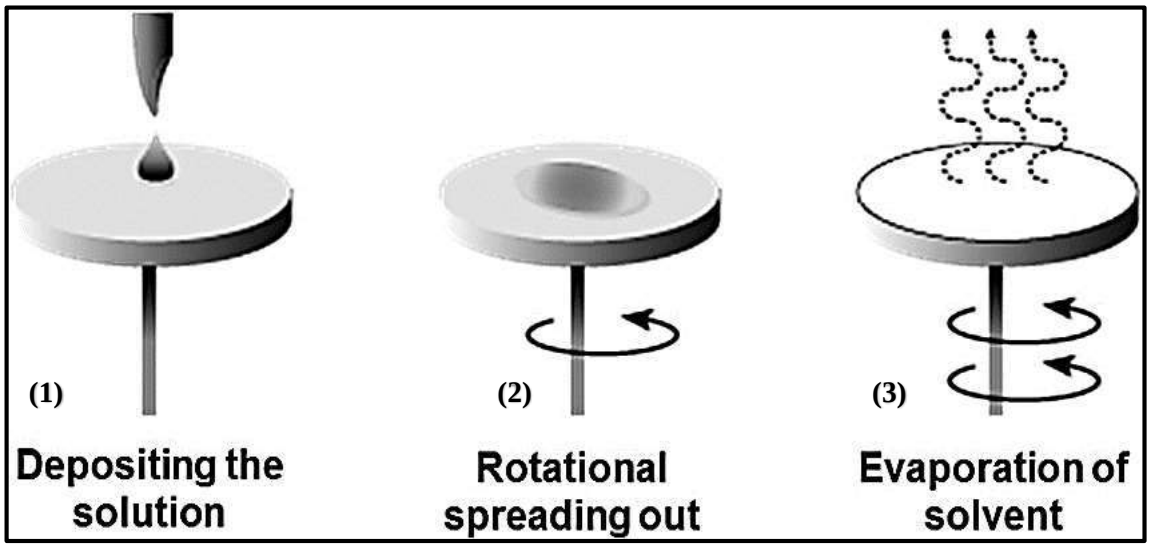


Figure II.6. Spin-coating stages: (1) solution deposition, (2) rotational spreading, (3) solvent evaporation[84].

• **Dip-coating** is a method used to deposit thin films by immersing a substrate into a solution and then gradually withdrawing it at a rate of few centimeters per minute (Figure II.7). As the substrate is lifted, a thin liquid layer adheres to its surface. Following solvent evaporation, the removal of excess liquid, and the polymerization process, a xerogel film is formed, retaining some residual solvent.

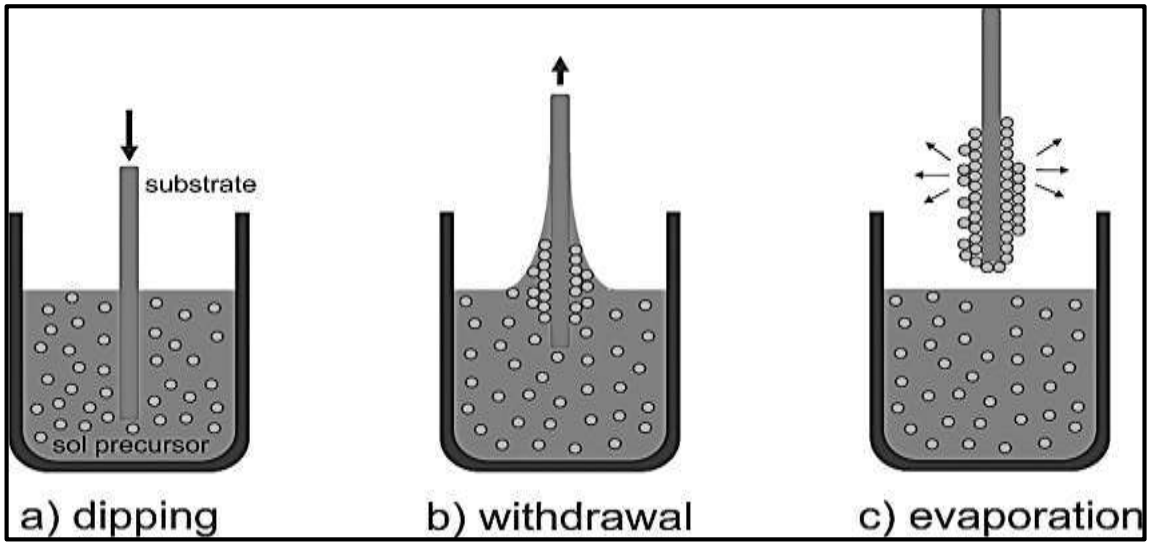


Figure II.7. Dip-coating stages: (a) immersion, (b) withdrawal, (c) evaporation [85].

II.3.2.2.Electrodeposition Process

Electrodeposition, also known as electrolytic deposition, is a technique used to coat a thin layer of a material onto a conductive substrate by applying an electric current (FigureII.8).

This process is based on electrolysis, where metal cations from an electrolyte are reduced and deposited onto the cathode. Electrodeposition is widely used to modify surface properties such as electrical conductivity, corrosion resistance, wear resistance, and aesthetics. The thickness and quality of the deposited layer depend on factors such as applied voltage, deposition time, and electrolyte composition **[86].**

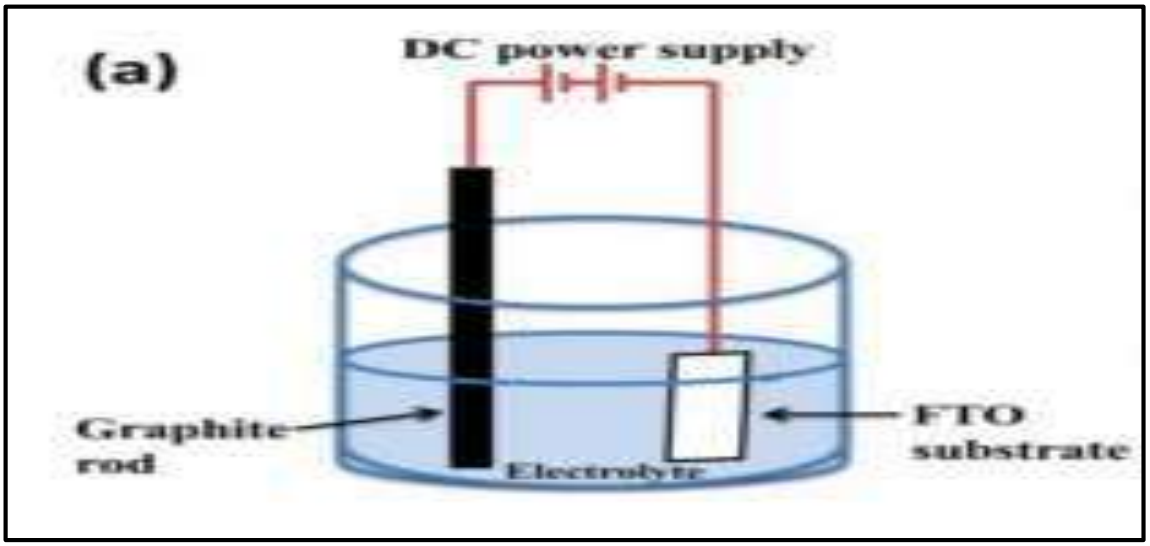


Figure II.8. Basic 2-electrode electrodeposition setup[87]

II.3.2.3.Spray Pyrolysis technique

Spray pyrolysis is a cost-effective and versatile deposition technique for thin films, with applications ranging from solar cells to transparent conductive oxides. First proposed by Chamberlin and Skarman in 1963 for CdS films, it has since been adapted for SnO_2, ZnO, and other functional materials **[88].** The method combines spray (atomization of a precursor solution into droplets) and pyrolysis (thermal decomposition on a heated substrate) **[89].**

II.3.2.3.1.Process Overview

The technique involves three key steps **[52]:**

- **Atomization**: The precursor solution (e.g., metal salts dissolved in water/alcohol) is broken into fine droplets.
- **Transport:** Droplets are carried by a carrier gas **[88]** to the substrate.
- **Pyrolysis:** On the heated substrate, droplets decompose, forming the desired compound **[89, 52].**

The pyrolysis sputtering system consists of a simple set of devices used to prepare thin films on different types of substrates as shown in Figure II.9:

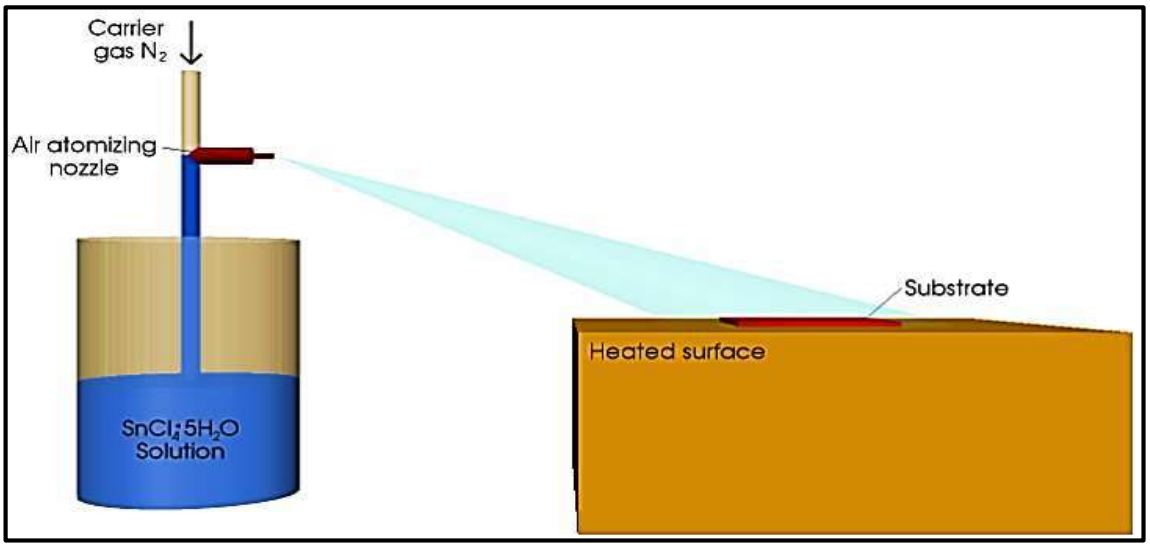


Figure II.9. Schematic of the spray pyrolysis setup process (air atomizing nozzle, precursor solution, and heated substrate) [90].

II.3.2.3.2.Atomization Methods

Two common approaches are used:

- **Pneumatic Spray:** Compressed gas (e.g., air) forces the solution through a nozzle, creating high-velocity droplets with non-uniform sizes **[91, 89].** This method was employed in our experiments (FIG II.9).
- **Ultrasonic Spray**: High-frequency waves (~40 kHz) produce finer, more uniform droplets at lower energy costs **[91], [52].** While pneumatic spray enables faster deposition, ultrasonic spray yields superior film homogeneity **[52]**.

II.3.2.3.3.Advantages and disadvantages

Spray pyrolysis excels in simplicity, low energy consumption, and adaptability for diverse materials **[91], [92].** It accommodates both dense and porous films **[93]** and operates in air or mild vacuum (50 Torr) **[91], [94].** The film properties (thickness, morphology) depend on precursor concentration, substrate temperature, and deposition time **[95], [52]**.

II.3.2.3.4. Factors Affecting Chemical Spraying with Pyrolysis

This technique depends on a range of factors including **[96].**

- The nature of the material used **[96]**.
- The deposition rate **[96].**

- Type of glass substrate **[97].**
- Substrate surface temperature **[98].**
- The distance between the substrate and the sprayer **[96].**
- Type of glass substrate **[32].**
- Spray droplet size **[32].**
- Pressure. **[99].**
- Distance of the substrate from the sprayer **[100].**
-

II.4. Thin Film Growth Mechanisms

In summary the thin film deposition process goes through three basic stages that form the basis of all its techniques **[70].**

- Preparation of materials suitable for deposition depending on the type of preparation method.
- Transfer of the deposited material from the source to the substrate.
- Condensation of the deposited material on the substrate either directly or by chemical reaction, which in turn is divided into three stages (Figure II.10) **[101]** :

II.4.1. Nucleation phase

At this stage, the deposited atoms begin to gather on the upper surface of the substrate, forming small clusters, as shown in Figure (II.10.a). As the atoms continue to precipitate and collide, these clusters gradually grow, and when they reach a certain size, they become thermodynamically stable and are called islands (Figure (II.10.b)).

II.4.2. Docking phase

This stage is characterized by the union and cohesion of the islands, so that they approach each other, leaving small gaps or spaces between them. One of the factors that accelerate this coalescence and increase the agglomeration of the islands ((Figure (II.10.c)) is the high temperature of the substrate.

II.4.3. The growth phase

This stage is the final step in the thin film formation process, where small islands come together to form a continuous layer. Over time, the size of these
Over time, these islands increase in size and come closer to each other until they unite to form a thin film covering the surface of the substrate, and the neighboring islands are separated by boundaries known as grain boundaries (Figure (II.10.d))

II.5. Growth forms

It has been experimentally established that there are three main forms of thin film growth: Frank-van der Merwe (layer-by-layer), Stranski-Krastanov (mixed), and Volmer-Weber (island).

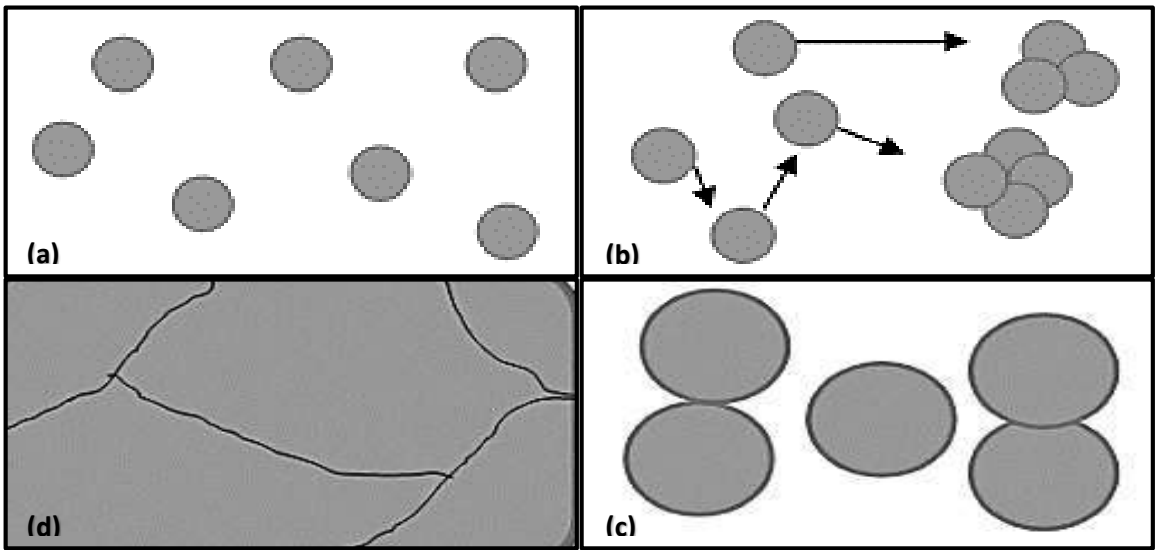


Figure II.10. Schematic diagram showing the stages of growth: (a) positioning of atoms (b) formation of islands (c) coalescence (d) growth.

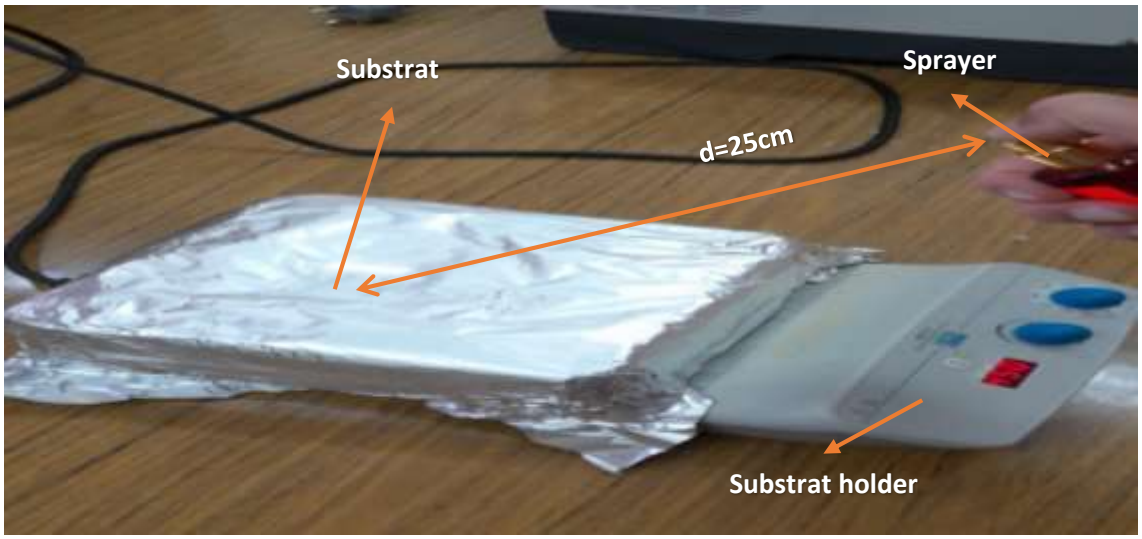
II.6. Experimental aspect

II.6.1.Description of the experimental apparatus

In this study, the spray pyrolysis we used to prepare undoped and doped SnO_2 thin films composed of very simple and inexpensive tools shown in Figure II.11, This method was chosen due to its efficiency in producing uniform coatings across large areas while offering a flexible setup that allows for precise control over critical parameters such as droplet size, solution concentration, and substrate temperature. the main elements of this device are:

- **Sprayer:** A glass vial with a volume of v=25 ml, whose role is to spray the solution in the form of small droplets towards the substrate surface at a distance d=25cm between the substrate and the sprayer.
- **The substrate:** We used glass slides.
- **Substrate holder:** A hotplate used to heat the substrate and its temperature is determined using a digital thermostat connected to a thermocouple.

The principle of film deposition is based on the reaction of tin electrolytes in solution with oxygen, which from the air to form a thin film of tin oxide



FigureII.11. shows the experimental installation of the used thermal chemical spraying system

II.6.2. Effect of substrate temperature on Droplets

The substrate temperature has a direct impact on the behavior of spray pyrolysis droplets. At temperatures below 200°C, the droplets retain a large amount of solvent, leading to incomplete reactions and resulting in powdery deposits. As these droplets dry quickly, internal stresses develop, which may cause cracking. In contrast, at temperatures above 350°C, the droplets tend to re-evaporate before spreading properly. This re-evaporation results in the formation of discrete particles on the substrate surface and causes the films to become porous with increased surface roughness.

Consequently, the number of particles on the surface rises as the deposition temperature increases, which affects the morphology and quality of the thin film **[102].**

A study investigating the effects of substrate temperature on SnO_2 thin films determined that a temperature of 450°C resulted in the optimal structural, optical, and electrical properties, providing a solid foundation for the deposition conditions in this research **[52].**

II.6.3. Different stages of sample preparation

The work on the deposition of pure and doped tin oxide films was carried out at the level of the pedagogical laboratory of physics at the University of Martyr Cheikh Larbi Tebessi in Tebessa.

Since thin films are prepared using the pyrolysis spray technique, cleaning the substrates and preparing the appropriate spray solution are essential steps that precede the sample preparation process

II.6.3.1. Substrate choice:

We used glass substrates (CAT, NO, 7101, Microscopy, SLIDES) with dimensions (25.4mmX76.2mmX1-1.2mm) shown in Figure II.12. Glass microscope slides are a standard substrate in thin-film deposition. For example, one study notes using "25.4 mm × 76.2 mm × 1.5 mm microscope glass slides" as the deposition substrate **[103].**

glass was chosen as a substrate due to its high transparency and low cost, it is efficiently used in thin film photo catalysis **[104],** we cover 25.4 mm of this glass slide to make a reference area, and the choice of these substrates for thin film deposition is due to the following reasons **:**

Convergence of the thermal expansion coefficient of the glass and oxides used, which promotes good adhesion and minimizes thermal stresses at the substrate interface **[105].**

High transparency is suitable for analyzing the optical properties of the prepared thin films in the visible domain (enabling direct UV-Vis characterization) **[106].**

Thermal stability: Glass retains rigidity up to its deformation point (514°C)**[107],** safely exceeding our deposition temperature (450°C).

Cost-effectiveness and availability **[106]:** Glass is widely used for SnO_2-based TCOs due to its compatibility with optoelectronic applications **[108].**



FigureII.12.Microscope slides used as substrates for deposition

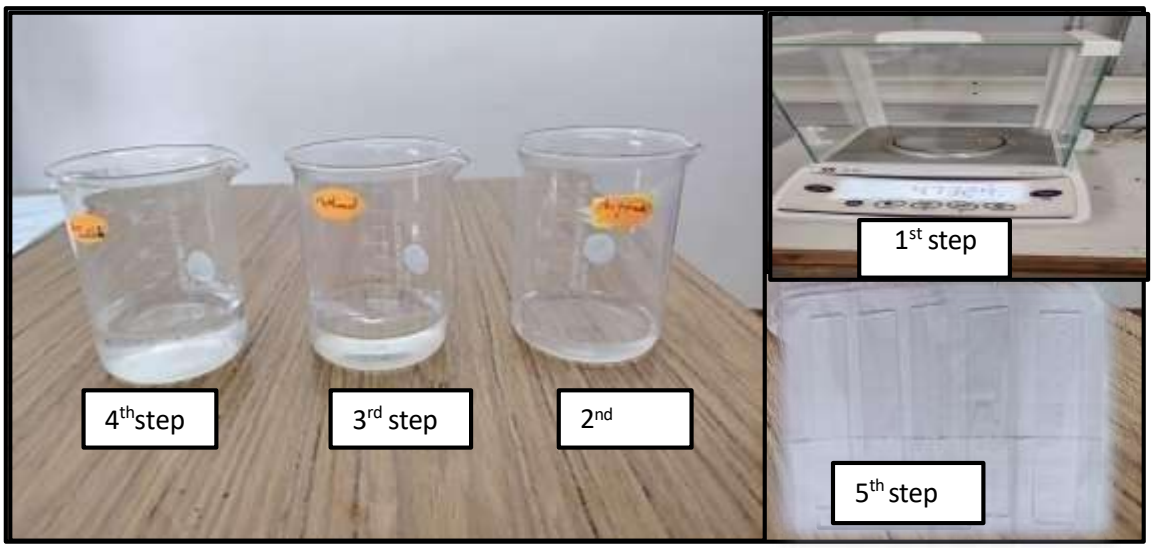
II.6.3.2. Substrate Preparation (Cleaning and Pre-treatment)

To confirm strong adhesion to the substrates and a relatively uniform thickness, it is essential to clean the substrates thoroughly to remove grease, dust and other impurities, making sure that the surfaces are free of defects. Cleaning is an essential step to ensure safety and quality results

We have adopted the following steps for cleaning the substrates such us showing in the figure II.13:

- Calculate the weight of each substrate and record it on its own clipboard.
- Place the substrate in acetone for 5 minutes to dissolve organic contaminants.
- Immersing the substrate in methanol for 5 minutes as a secondary solvent wash.
- Wash the substrate with distilled water for 5 minutes to remove polar residues.

Finally, the substrates were then manually dried using cellulose-based laboratory tissue, followed by air-drying at room temperature. Although this method poses a slight risk of microfiber transfer, visual inspection under ambient lighting confirmed the absence of macroscopic debris. A similar solvent-cleaning approach for SnO_2 films was reported by Benhaoua in **[40].**





FigureII.13. Substrate Cleaning Steps

II.6.3.3. Preparation of Deposition Solutions

- **The precursor solution for undoped SnO_2** was prepared by dissolving 2.00 g of $SnCl_2 \cdot 2H_2O$ (Sigma-Aldrich, reagent grade, 95% purity; CAS: 20018-2500) in methanol (Sigma-Aldrich, ≥99.8%, acetone-free; CAS: 67-56-1), yielding a 0.1 mole/L solution (total volume = 0.0886 L).
- **The precursor solution for Zn doped SnO_2:** The Sn mass was calculated as 1.0522 g using the molar mass of $SnCl_2 \cdot 2H_2O$ (M = 225.65 g/mole). For Zn doping, zinc acetate dehydrate ($C_4H_6O_4Zn \cdot 2H_2O$; Riedel-de Haën, 99–102% purity; CAS:

5970-45-6), was added at concentrations of 0%, 2%, 4%, 6%, 8%, and 10% relative to Sn mass (TableII-1). The precision weighing process for zinc acetate (10% doping: 0.353 g) is shown in Figure II.14.

Each solution was magnetically stirred at 500 rpm for 1.5 hours at 25°C (ambient temperature) to ensure homogeneity (see Figure II.15).



FigureII.14. Precision weighing of zinc acetate dehydrate (10% doping: 0.353g).



Figure II.15. Homogenization of SnO_2: Zn solution via magnetic stirring (500 rpm, 25°C).

Table II-1. Zinc acetate masses for doping concentrations

Doping Level (%)	Zinc Acetate Mass (g)
2	0.071
4	0.141
6	0.212
8	0.282

- For Mn, Cu, and Fe doping, individual precursor solutions were prepared using 0.27078 g of $SnCl_2 \cdot 2H_2O$ (corresponding to 0.142452 g of Sn). Each dopant was added at a 6% mass ratio relative to Sn, using the following compounds:
- **Mn-doped SnO_2:** 0.03811 g manganese(II) acetate tetrahydrate ($Mn(C_2H_3O_2)_2 \cdot 4H_2O$)
- **Cu-doped SnO_2:** 0.03358 g copper(II) sulfate pentahydrate ($CuSO_4 \cdot 5H_2O$)
- **Fe-doped SnO_2:** 0.06182 g iron (III) nitrate nonahydrate ($Fe(NO_3)_3 \cdot 9H_2O$)

Each solution of X doped SnO_2(X=Zn,Mn,Cu,Fe) was agitated magnetically at 500 rpm for 1 hour 25 minutes at 25°C, then left to stand overnight for complete homogenization. Representative images after stirring process for Cu-, Fe-, and Mn-based solutions are shown in FigureII.16.

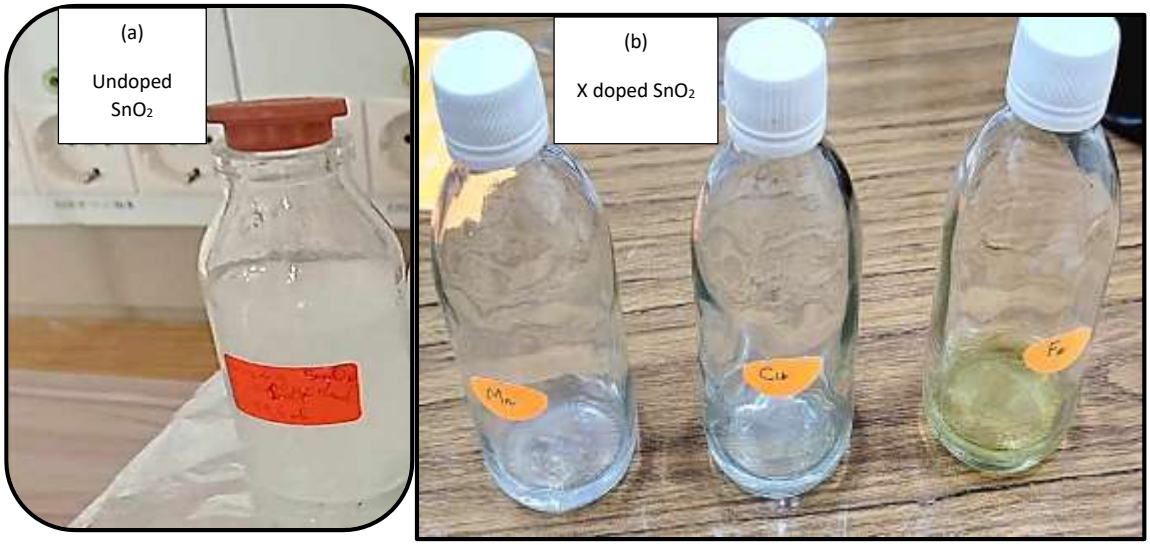


Figure II.16. Appearance of spray solutions after magnetic stirring (a) undoped SnO_2,(b)X-doped SnO_2, witch X=Mn, Cu, and Fe

II.6.3.4. Thin film deposition process

After preparing the initial solutions of the materials to be deposited and cleaning the substrates, we start the deposition process by following simply steps:

- Place the substrate on top of the electric heater and let it heat up from room temperature to the required temperature (450°C) to avoid thermal shock to the glass substrates.
- After heating the substrate to the required temperature, we start spraying very fine drops of 5ml solution on the surface of the heated substrate, this allows the chemical reaction between the components of the solution to be activated, the solution evaporates and a thin layer of oxide is formed.
- After the deposition process is complete, we close the electric heater and leave the substrate on it until its temperature drops to room temperature to avoid breakage and complete the oxidation process of the prepared layer.
- We repeat the process each time by changing the type of solution and the same volume until we obtain homogeneous films

II.6.3.5. experimental Conditions

The experimental conditions used to prepare thin films of oxides (undoped SnO_2, Zn, Mn, Cu, Fe doped SnO_2) are summarized in Table II-2:

Table II-2. Déposition Conditions (Concentration, Temperature, etc.)

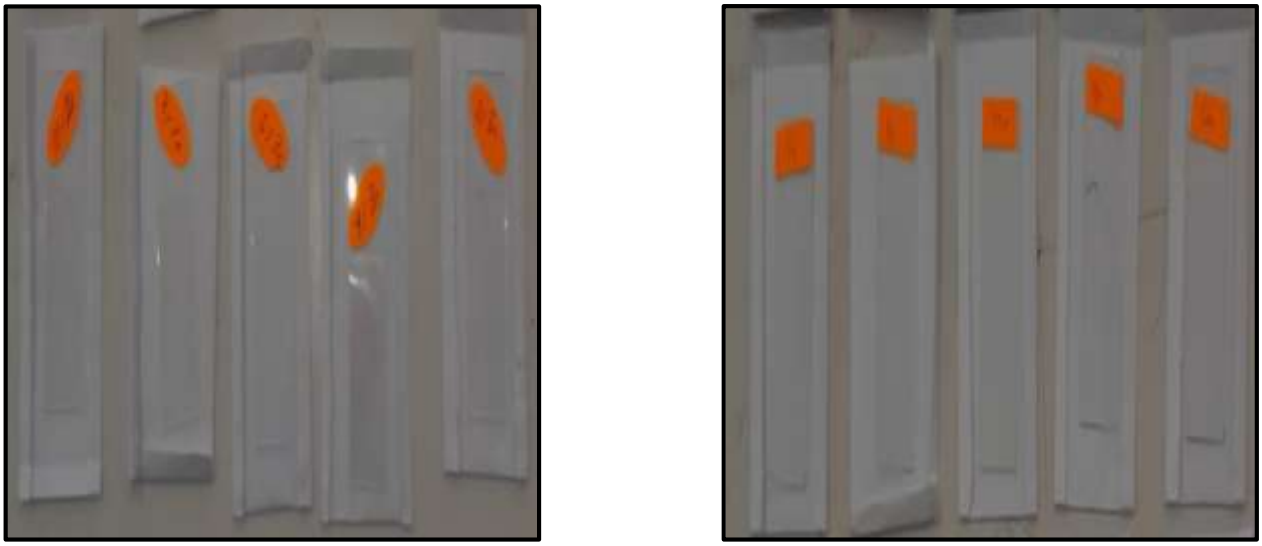
Parameter	Zn-doped Samples (0-8%)	Mn/Cu/Fe-doped Samples (6% each one)
Preheating Duration	10 minute	10 minutes
Cooling Method	Passive (25°C ambiant)	Gradual temperature lowering
Precursor Solution	0.1 M $SnCl_2 \cdot 2H_2O$ + Zn acetate	0.1 M $SnCl_2 \cdot 2H_2O$ + Mn/Cu/Fe salts
Doping Concentrations	0%, 2%, 4%, 6%, 8%.	6% (each dopant)
Substrate Temp.	450°C	450°C
Nozzle-substrate Distance	25 cm	25 cm
Spray Method	Manual bursts via fine-mist glass bottle	Intermittent pulses with 5-second intervals
Spray Volume	5 mL per sample	5 mL per sample
Stirring Duration	1.5 hours at 500 rpm	1 hour and 25minutes at 500 rpm

Ambient Atmosphere	Normal laboratory air	Normal laboratory air
Reference Area	Created using perpendicular glass at substrate edge	Created using perpendicular glass at substrate edge
Deposition Monitoring	Visual inspection for uniform coverage	Visual inspection for uniform coverage

Finally, we obtained two sets of samples as shown in the figureII.17:

The first set contains 05 samples grafted with different concentrations of zinc, namely: 0%, 2%, 4%, 6% and 8%(FigureII.17a)

As for the second group, tin oxide is doped with different materials but with the same concentration 6%,, namely: Fe ,Cu ,Mn, Zn(FigureII.17b)



(a) First group **(b) second group**

Figure II.17. Prepared samples

II.7. UV-Visible Spectroscopy Characterization

The optical characterization of the doped SnO_2 thin films was carried out using UV-Visible spectroscopy, a non-destructive method that probes electronic transitions by measuring light absorption across ultraviolet and visible wavelengths **[109], [111].** The measurements were performed using a JASCO V-730 double-beam spectrophotometer (FigureII.18), equipped with a deuterium lamp for the ultraviolet region (190–400 nm) and a tungsten-halogen lamp for the visible region (340–800 nm), providing a working range from 190 to 1,100 nm with a fixed spectral bandwidth of 1 nm and stray light below 0.02% **[109].**



Figure11.18. spectrophotometer used for measurements.

Wavelength selection was achieved through a motorized monochromatic. The selected light was then directed through an optical system (FigureII.19) that splits it into two beams using a half-mirror: one beam passes through a reference cuvette (containing the blank substrate), while the other passes through the doped SnO_2 thin film. These beams are then detected and compared by photomultiplier detectors, allowing for the acquisition of transmittance spectra in the 300–900 nm range **[110].**

All measurements and data acquisition were controlled using Spectra Manager™ II software **[109].** From the recorded spectra, it is possible to estimate the thickness of the film and determine its optical characteristics: the optical absorption threshold, the absorption coefficient, the band gap width, the Urbach energy, and the refractive index **[111].**

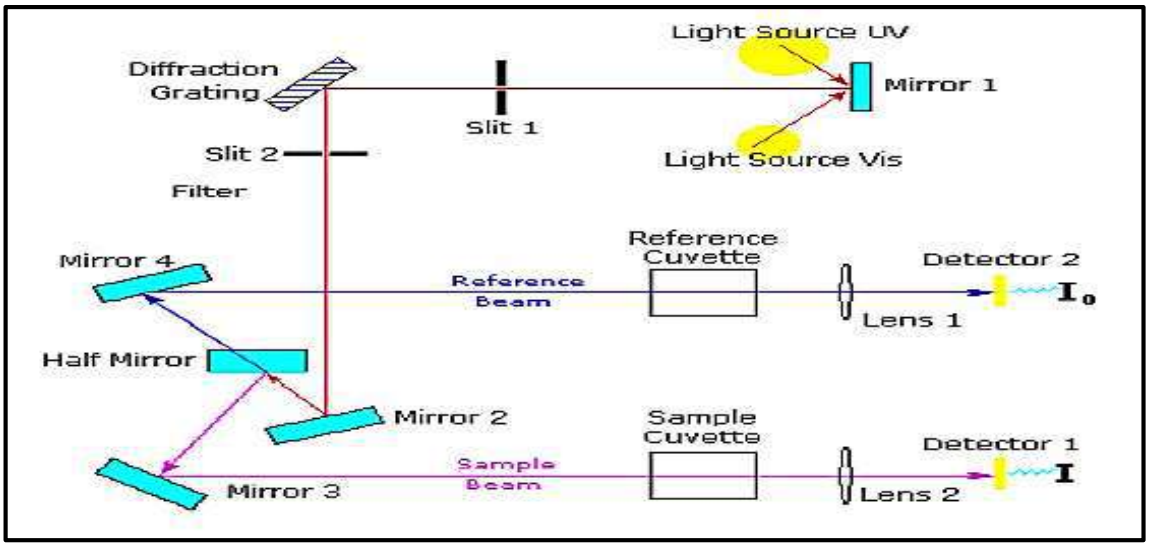


Figure II.19. Schematic diagram of the working principle of the UV-VIS spectrometer

II.8 Optical parameter Studied.

Analytical techniques are an essential tool for characterizing materials and revealing many of their physical constants. The study of the optical properties of thin films is critical to understanding the behavior of thin films and assessing their physical quality, which allows determining the most suitable experimental conditions for their preparation in an effective way that ensures high quality. There are several analytical methods that depend on the spectral domain used. Most notably, the UV-Vis spectroscopy technique, used in this work, is harmless to the surface of the samples and is widely used to study the optical properties of thin films and determine their thickness.

In this work we have calculated some of the parameter, related to the optical properties of the SnO_2 thin films, such as: transparency, gap energy, Urbach energy, (E_g, E_U, K), by exploiting the values of the transparency changes in terms of wavelength **[112].**

II.8.1.Absorption Coefficients

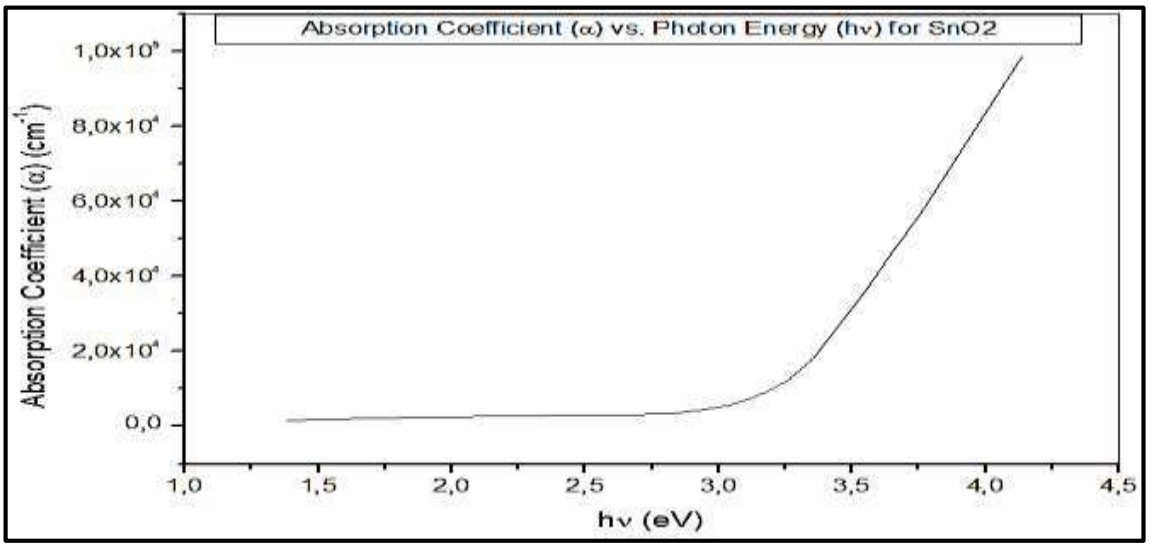
The optical absorption behavior of the thin films can be analyzed using the transmittance spectra (FigureII.20). By applying Beer's law, which expresses the relation**[112]**:

$$T = e^{-\alpha d} \dots\dots\dots\dots\dots\dots\dots\dots\dots\dots\dots\dots\dots\dots\dots\dots\dots (II.1)$$

Where T is the transmittance and d is the film thickness, one can derive the absorption coefficient α **[112]**.When the transmittance is provided in percentage, the formula becomes:

$$\alpha = \frac{1}{d}\ln\left(\frac{100}{T}\right) \dots\dots\dots\dots\dots\dots\dots\dots\dots\dots\dots\dots\dots\dots\dots\dots\dots (II.2)$$

This expression is widely used for estimating absorption, although it generally overlooks the portion of light lost due to reflection at different interfaces such as air/film and film/substrate, which becomes more relevant in thinner films/



FigureII.20. Absorption coefficient (α) as a function of photon energy (hν) for Undoped SnO_2 thin films.

II.8.2. Extinction Coefficients

The extinction coefficient k, which accounts for the damping of the electromagnetic wave inside the material, is derived from the absorption coefficient using the relationship:

$$K = \frac{\alpha\lambda}{4\pi} \dots\dots\dots\dots\dots\dots\dots\dots\dots\dots\dots\dots\dots\dots\dots\dots\dots\dots (II.3)$$

Both coefficients α and k are essential for understanding the film's optical density and light interaction behavior **[113].**

II.8.3. Optical Band Gap (Eg)

The energy band gap Eg can be estimated using the Tauc method, which involves analyzing the absorption coefficient in the region of strong absorption (FigureII.20). The method is based on the following general form:

$$(\alpha hv)^{\frac{1}{n}} = A(hv - Eg) \dots\dots\dots\dots\dots\dots\dots\dots\dots\dots\dots (II.4)$$

Here, hv is the photon energy, A is a constant, and n is an exponent that reflects the type of electronic transition **[114].** For materials with a direct allowed transition, such as SnO_2, the value of n is taken as 1/2 **[117, 114].** So for studying SnO_2 thin films the relation in the simplified expression coming:

$$(\alpha hv)^2 = A(hv - Eg) \dots\dots\dots\dots\dots\dots\dots\dots\dots\dots\dots (II.5)$$

By plotting $(\alpha hv)^2$ against hν , the linear portion of the curve can be extrapolated to intersect the energy axis (FigureII.21). The intercept gives an estimate of the band gap energy Eg **[71], [111], [117].**

An example of obtained value for undoped SnO_2 (Eg ≈ 3.72 eV) is consistent with previously reported results, which indicate Eg values typically ranging between 3.72 and 4.03 eV depending on deposition temperature and treatment conditions **[115].**

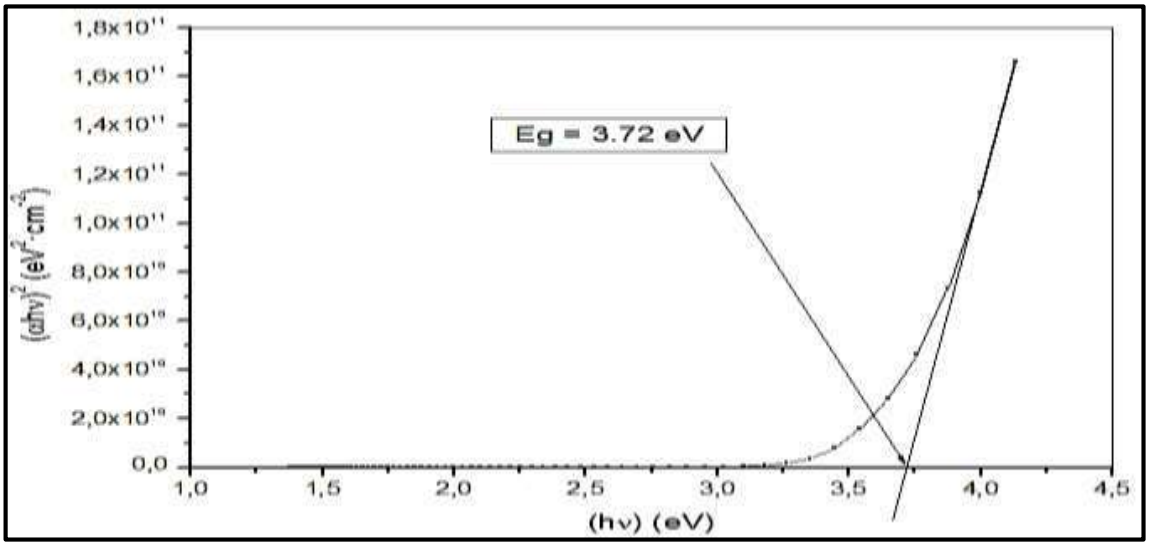


Figure II.21. The direct band gap (Eg = 3.72 eV) for Undoped SnO_2 thin films was determined by extrapolating the linear region Tauc plot (By plotting $(\alpha h\nu)^2$ against hν).

II.8.4. Urbach Energy (E_u)

The Urbach energy E_u reflects the extent of disorder and localized states in the material. It is related to the exponential of the absorption edge and can be described using the following empirical relation:

$$\alpha = \alpha_0 e^{\frac{h\nu}{E_U}} \dots\dots\dots\dots\dots\dots\dots\dots\dots\dots\dots\dots\dots\dots (II.6)$$

Taking the natural logarithm of this expression gives:

$$\ln(\alpha) = \ln(\alpha_0) + \frac{h\nu}{E_U} \dots\dots\dots\dots\dots\dots\dots\dots\dots\dots (II.7)$$

by plotting α against hν, the slope of the linear region yields $\frac{1}{E_U}$, and thus the Urbach energy can be obtained as the inverse of this slope **[71], [117].** This parameter is especially useful in quantifying the degree of structural disorder and the presence of defects in the thin film.

An example show in figure II.22 of calculated value of Eu (≈ 0.26 eV) falls within the general range observed for SnO_2 thin films in literature , where Eu is commonly reported to lie between ~0.28 and ~0.32 eV for both doped and undoped samples **[116].**

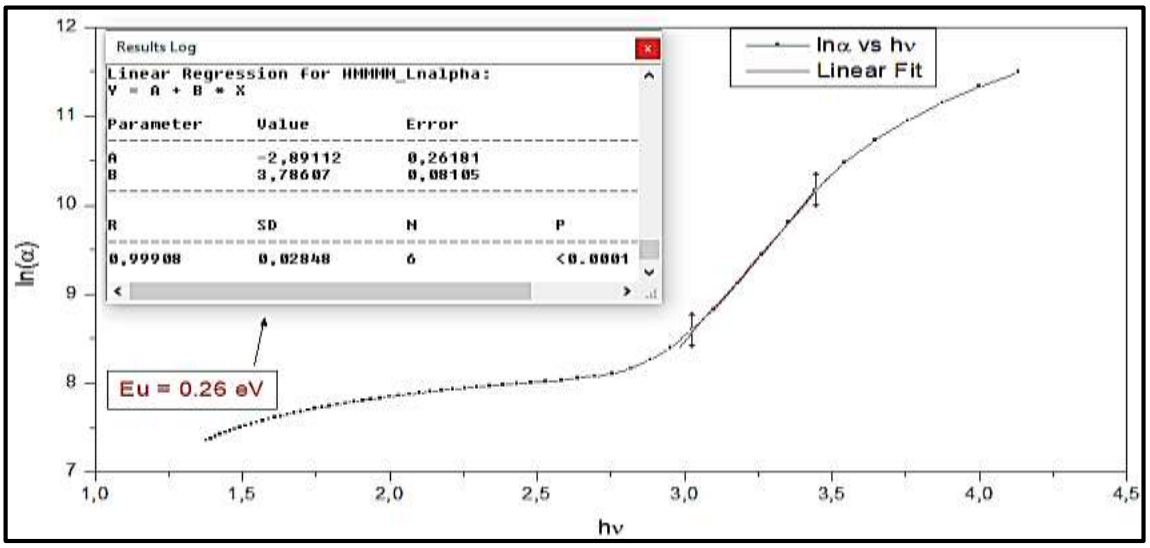


Figure II.22. Urbach extremity plot (ln(α) vs. hν) for SnO_2 thin films. The Urbach energy (Eu = 0.26 eV) was calculated from the slope of the linear region.

II.9. Conclusion

In this chapter, we talked in detail about how to prepare samples and how to extract their optical properties

Chapter III
Results and discussion

III.1. Introduction

In this chapter, the obtained results starting from the transparency curves of the studied samples will be explained, by dividing it into two sections:

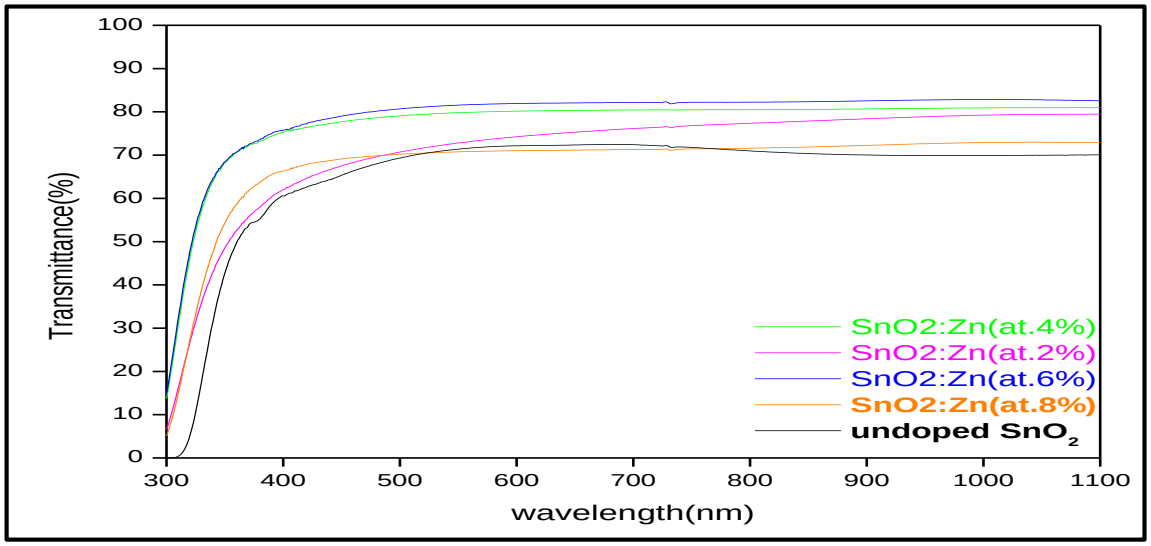
The first section studying the optical properties of undoped tin dioxide and doped tin dioxide with zinc at different concentrations, namely 2%, 4%, 6%, and 8%, to see how changing the doping concentration affects the optical properties of tin dioxide.

In the second section, choosing the concentration that gives good results in the first section of the study and choose three different materials, namely manganese (Mn), copper (Cu) and iron (Fe), and doped them to tin dioxide, so that we have four sample, and the aim of this study is to know the extent to which the type of restaurant affects the optical properties of tin dioxide

III.2.First section: Effect of Zn concentration on optical Properties of SnO_2 thin films

III.2.1. Transmittance

We use the UV-Vis spectrometer to study the optical properties of undoped SnO_2 and Zn doped SnO_2 (SnO_2:Zn), we were able to obtain spectra representing the variation of optical transmittance according to the wavelength recorded in the range of 300nm-1100nm with the precise experimental condition (Ts=450°C, d=25cm,P=1atm, $V_{solution}$=5ml) us indicate in figure III.1



FigureIII.1.Optical transmittance spectra of SnO_2 at different percentage of Zn

We can see from this figure that the transmittance spectrum of undoped SnO_2 and SnO_2:Zn changes with wavelength in the same way, being low at very low wavelengths and then increasing sharply in the region of the primary absorption edge λ=380nm, this indicates that the prepared thin films are all semiconductors with a wide energy band gap whose value varies as the Zn concentration changes **[1]**.

As well as the emergence of two regions in the UV spectrum for all samples**:** **At short wavelengths**, the decrease in transmittance is due to the high absorption in the ultraviolet range, because the energy of the emitted photons is close to the absorption edge (the value of the oxide energy gap).

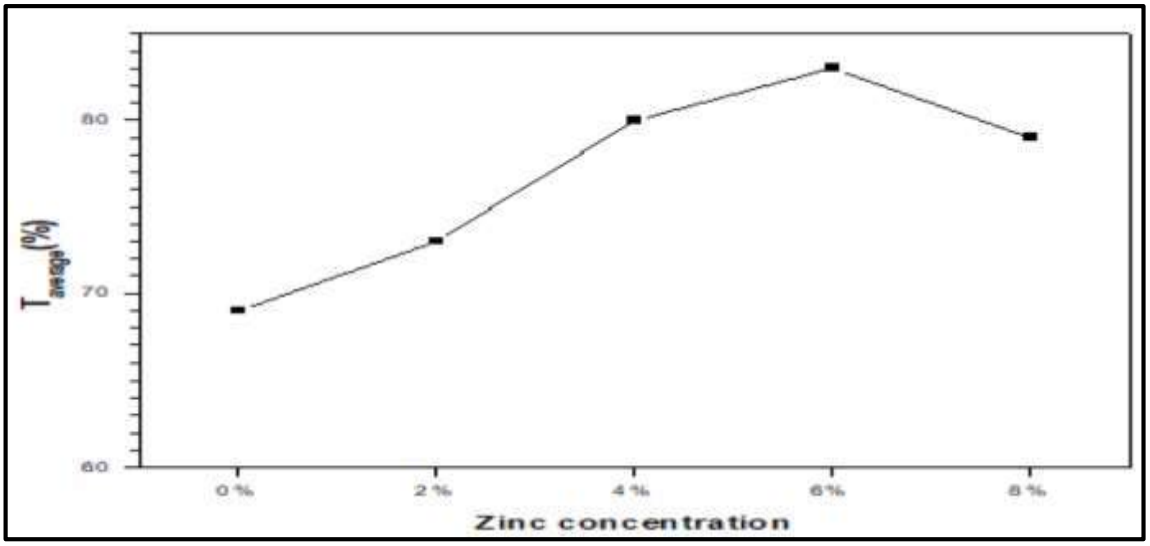
At longer wavelengths, the latter is transparent, which means a decrease in the number of electronic transitions between the transport and valence bands, as the optical energy is lower than the absorption edge, resulting in an increase in transmittance **[119]**.

We also note that the transmittance of the prepared tin dioxide's varies from one sample to another depending only on the concentration of zinc used for doping as shown in the figure III.2, as we obtained the lowest value of transparency in the thin film prepared from undoped tin dioxide 69% (when the zinc concentration is 0%), while the value varied between 73% and 83% in the visible region, according to the 2% and 6% of zinc concentration respectively, This shows similar optical behavior as in the transparent conductive oxide group, indicating that the prepared films are suitable for solar cell applications because the effective spectral region is located in the transparent region **[120], [121], [122]**. Almost the same results were obtained when tin dioxide was doped onto the nickel studied in Ref **[123]**. In this range of concentration; the transmittance was found to increase gradually when the zinc concentration increased. This increase might be attributed to the decrease in the both cluster size and surface roughness of the films **[124]**.

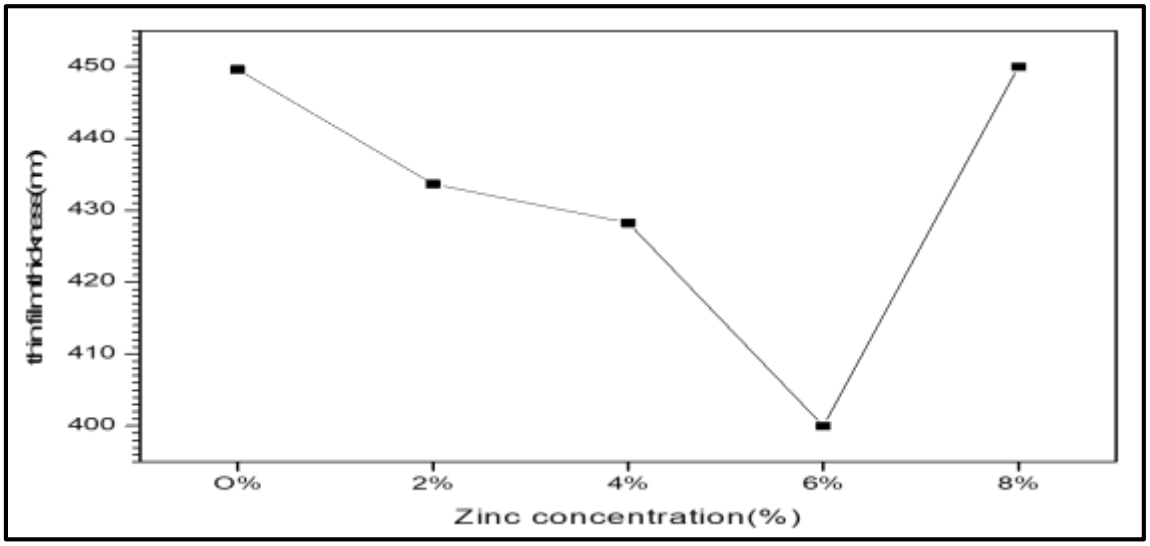
The decrease in the transmittance value of the sample associated with a zinc concentration of 8% may be due to an increase in absorption as a result of an increase in the thickness of the sample **[125]** as shown in figure III.3. As we showing that the prepared thin films demonstrated a thickness ranging from 400nm to 449,99nm, where the highest thickness value is at the doping ratio of 8 at% compared to the other ratios, and these magnitudes are also confirmed by the transmittance spectra.

In addition, it is worth noting the absence of interference fringes in the

region of high transparency. These fringes are generally attributed to the multiple reflections that occur at the film/substrate and film/air interfaces. The absence of such fringes reflects the fact that our films are thin.



FigureIII.2.Variation of Average Optical Transmittance of Zinc doped SnO_2 as function of concentration

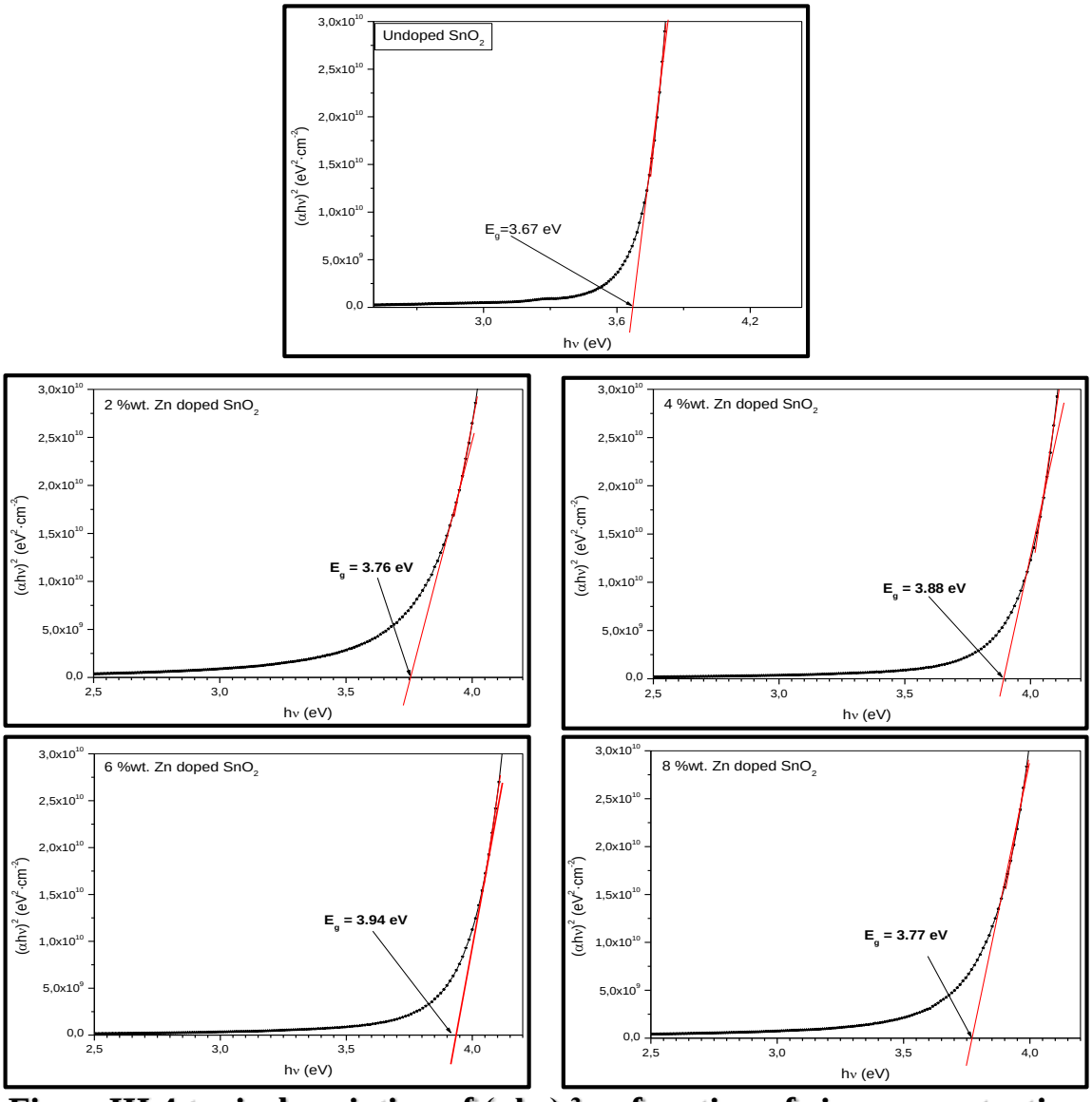


FigureIII.3.Variation of thickness of Zinc doped SnO_2 as function of concentration

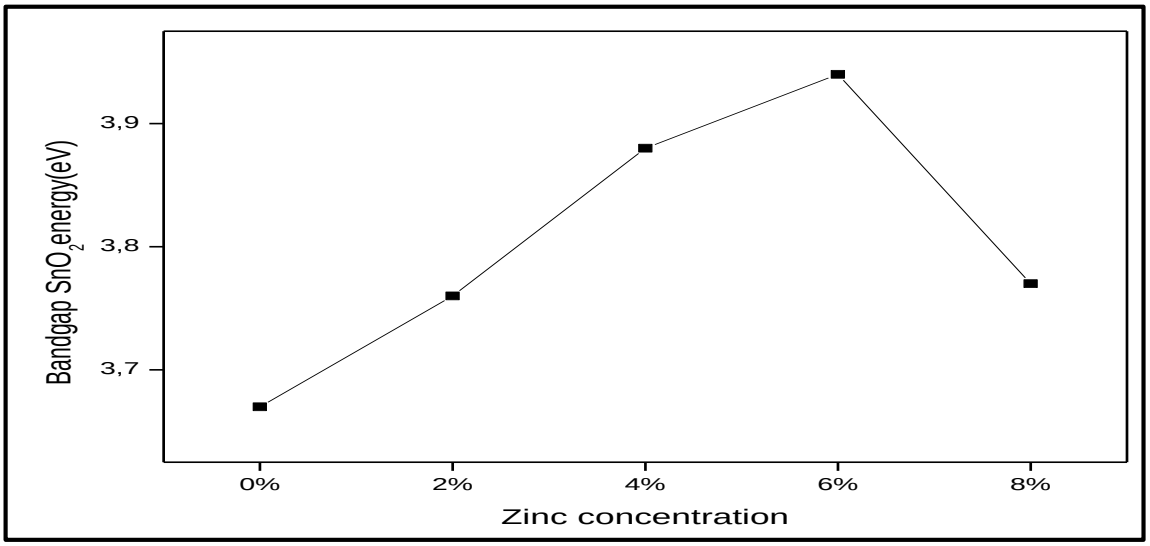
III.2.2. band gap energy

Tin dioxide is a direct-gap semiconductor. So its optical band gap energy (E_g) of the films was evaluated by conventional method by extrapolating the straight line portion of the $(\alpha h\nu)^2$ Vs. hν curve to α=0. The band gap energy deduced from Figure III.4 was plotted in figure III.4 as function of Zn concentration.

We found that the energy band gap of all sample is in the range of theoretical SnO_2 band gape (3.6eV-4.2eV) **[126]** which confirm that all the prepared samples are of good quality.



FigureIII.4.typical variation of $(\alpha h\nu)^2$ as function of zinc concentration



FigureIII.5.Optical band gap energy of SnO2 thin film at different Zinc concentration

From the figureIII-5, it was observed that the lowest value of the energy gap is carried by the sample containing a thin film of undoped tin dioxide (0% of zinc), and the zinc doping process at concentrations of 6%, 4% and 2% led to an increase in the values of the optical energy gap, this means that the doping led to a shift of the absorption edge towards higher energies, which can be described as the Burstein-Moss Shift because the energy levels near the conduction band are filled with electrons, so the electrons need more energy to move, and the energy gap appears to increase**[127].**

We also observe that the values of the band gap for all doped SnO_2 thin films are higher than the band gap of the undoped tin dioxide thin film, which can be explained by the fact that the thickness of the zinc-doped tin dioxide thin films is greater than that of the undoped tin dioxide thin film.

The reduction in the energy band gap in the case of the sample contain doped SnO_2 at 8% concentration, is can be due to the presence of Zinc in the SnO_2 structure which induces the formation of new recombination centers with lower emission energies

The smaller band gap energy value possessed by the thin film, the easier it will be for electrons to move from the valence band to the conduction band **[128, 129].** This results in the quality of a film being better used as a semiconductor material **[130, 131, 132]**

Also its may be due to increasing in the number of particles in the crystal structure, leads to this particles cannot be placed into proper lattice positions resulting a crystal defects who due to the enhancement in photon scattering because the lattice strain **[96].**

III.2.3. Urbach energy

We determined the value of Urbach energy, or the width of the localized states allowed within the energy gap and related to the absorption spectrum, by plotting the curve of variations (lnα) in terms of photon energy (hν) whose equation is shown in Chapter II.2, where the reciprocal of the slope of the resulting curve represents the values of Urbach energy

The variation of Urbach energy according the concentration of Zinc are shown in the figure III.6, It was observed that the value of Urbach energy decreases as the Zinc concentration increase in the sample due to the decrease in the width of the localized level bands because the number of energy levels in the optical energy gap decreases, resulting an increase in the value of the band gap energy, which means that the optical behavior of the Urbach energy value is opposite to the optical behavior so the relationship between them is inverse as shown in figureIII.7, where Urbach energy is the tail of the width of the transport and valence bands and the optical band gap is the energy difference between the tails of the bands **[133].**

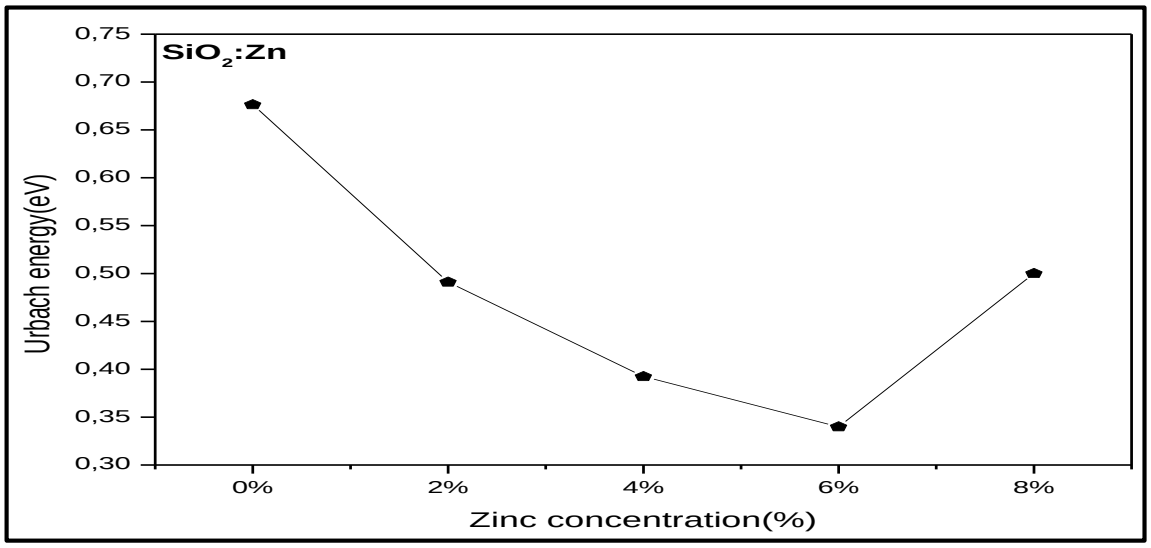
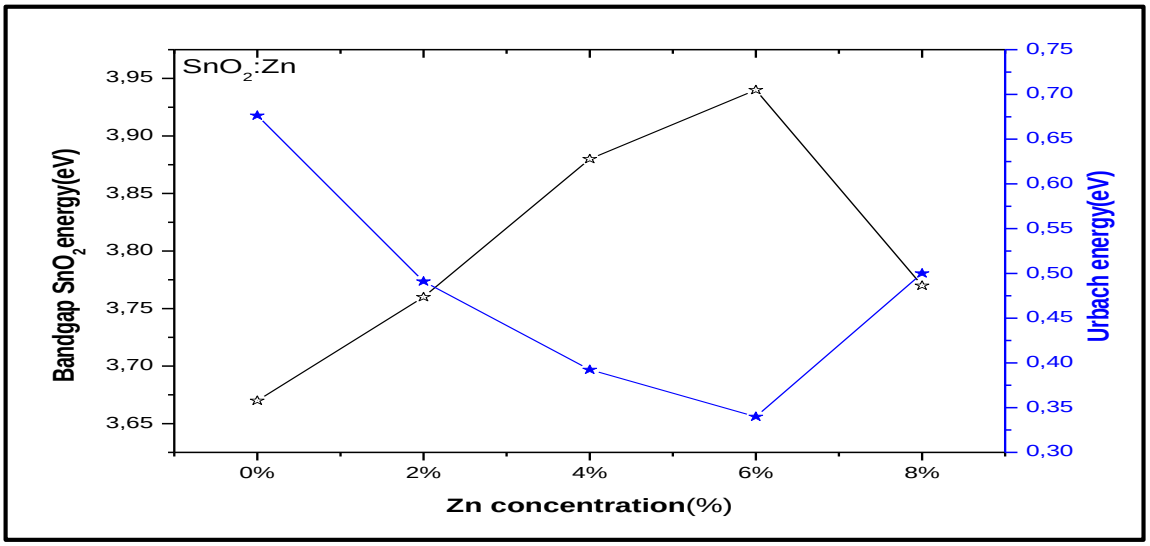


Figure III.6. Urbach energy of SnO_2 thin film Vs Zinc concentration



FigureIII.7. The inverse relationship E_g and E_U of SnO_2: Zn doping concentration

III.3.Second section: Effect of doping type on optical Properties of SnO_2 thin films

A number of studies have been performed dealing with various properties on SnO2 thin films, furthermore, previous studies suggested that doping on tin dioxide thin films with transition metals enhance their activity by change in band structure of tin dioxide **[134,135]**

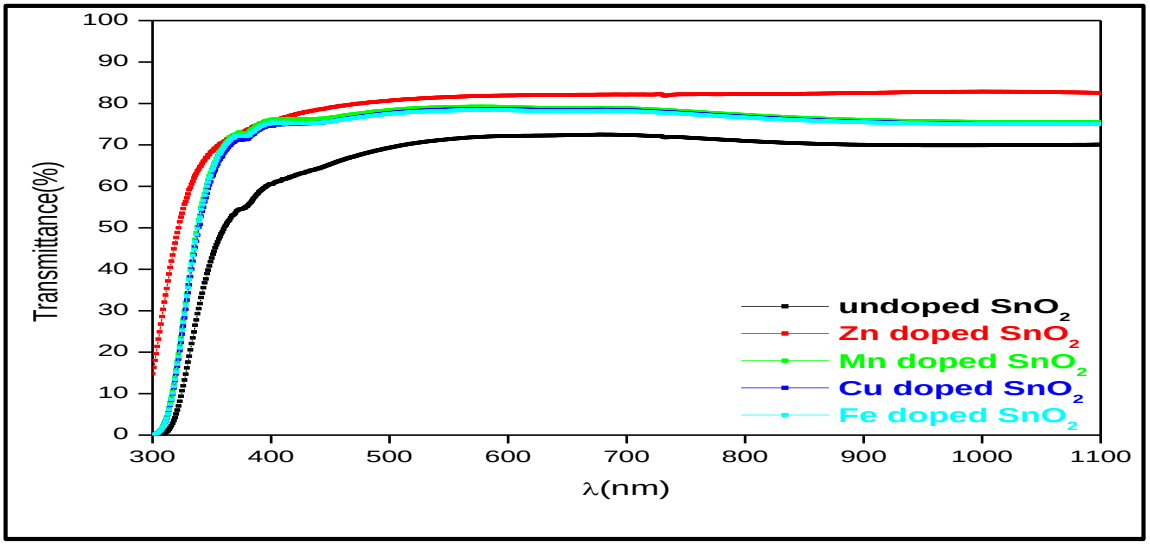
That's why we will study in this part, the optical properties of undoped tin dioxide doped with four types of transition metals: zinc, manganese, copper and iron to see how these properties are affected by the type of doping.

III.3.1.Effect of doping on the optical transmittance of SnO_2 thin films

The figure III.8 represents the change in the transmittance value of undoped tin dioxide and tin dioxide doped with three types of doping in terms of the change in wavelength in the range of 300 to 1100 nm. We can see from this figure that the transmittance spectrum of undoped SnO_2 and SnO_2:X while X: Zn, Mn, Cu, Fe, changes with wavelength by the same mode, being low in the ultraviolet region of the spectrum in the range (nm. 300 - 400) and then a gradually increase with increasing wavelength values in the visible region (nm. 700 - 400) and we observe that the transmittance values are almost constant in the near infrared region this indicates that the prepared thin films are all semiconductors with a wide energy band

gap **[136]**.

The absence of interference fringes in the high transparency region shows that our films are thin.



FigureIII.8.Optical transmittance spectra of undoped SnO_2, SnO2:Zn, SnO2:Mn, SnO2:Cu and SnO2:Fe

The maximum transparency value for all samples is in the visible range of the transmittance spectrum, confirming that all samples are suitable for solar cell applications. **[137], [138], [139].**

We obtained the lowest value of transparency in the thin film prepared from undoped tin dioxide 69% (undoped SnO_2) while the value varied between 75% and 83% in the visible region, according to SnO_2: Fe and SnO_2: Zn respectively. The difference in transparency value as we change the type of dopant indicate the effect of the nature of the dopant on the transmittance of tin dioxide.

The reason for the increase in transparency value in the doped samples is due to the fact that the doping process helps to generate a number of vacancies within tin dioxide, which decreases the number of free electrons and this may lead to a decrease in the value of its absorption of visible light energy and increase its transparency **[140].**

Of course, the number of holes generated will vary depending on the type and nature of the doped material. Looking at the transmittance curves (figureIII.8), zinc as a dopant helps to increase the number of holes within tin dioxide compared to

manganese, copper and iron and thus improves the optical properties of tin dioxide.

The close proximity of the transmittance value of the Cu-doped SnO_2 and Fe-doped SnO_2 samples can be explained by the convergence of the thickness of these samples.

III.3.2.Effect of doping on the thickness of SnO_2 thin films

The figure III.9 shows the thickness of thin films of undoped tin dioxide and doped tin dioxide with different materials.

It is clear that the process of doping tin dioxide with various doped materials contributed to the reduction of its thickness, proving the effect of the doping process on its properties.

The lowest value of the thickness of the samples was obtained when we doped tin dioxide with 6% zinc, where its value was 400 nm compared to the undoped tin dioxide film (449,61nm), which indicates that the presence of zinc inside the tin dioxide network affected the nature of the surface and grain size, where surface regularity and grain size increased

The convergence of the value of the thickness for SnO_2: Mn, SnO_2:Cu and SnO_2:Fe shows that they have almost identical film properties.

We conclude that the doping process by adding zinc, manganese, copper and iron impurities increased the crystallinity and homogeneity of the crystal structure of tin dioxide and reduce its thickness so that its transparency to light is increased, as shown in the previous title.

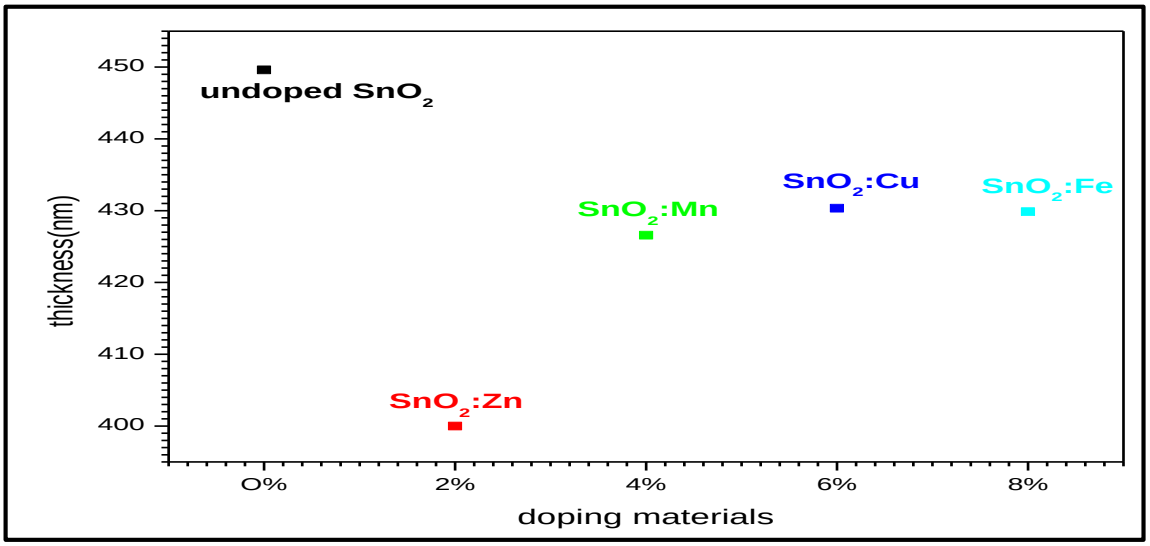


Figure III.9.thickness of undoped SnO_2, SnO2:Zn, SnO2:Mn, SnO2:Cu and SnO2:Fe

III.3.3.Effect of doping on the band gap of SnO_2 thin films

Figure III.10 shows the changes in the values of the band gap energy values of the prepared tin dioxide films with respect to the change in the doped material.

The increase of E_g in Zn-doped films is consistent with the Burstein–Moss effect in degenerately doped oxides. As carrier concentration rises, the Fermi level shifts into the conduction band, requiring more energy for optical transitions (the "band-filling" effect). In practice, Zn^{2+} substituting Sn^{4+} (and associated oxygen vacancies) donates extra electrons, widening the apparent gap. This explains why 6% Zn give the largest gaps (3.94 eV) compared to 3.67 eV for undoped SnO_2.

By contrast, the dopants Mn^{2+}, Cu^{2+}, and Fe^{3+} do not supply as many free carriers (and in some cases introduce more localized d states), so their films show only modest E_g shifts (3.74eV, 3.75eV and 3.77 eV) respectively as show in figure III.9. First-principles studies and experiments likewise report only slight band-gap shifts in Fe- or Mn-doped SnO_2. In short, Zn doping effectively raises E_g (via carrier injection and possible lattice contraction), whereas Mn/Cu/Fe doping produces relatively unchanged gap energies, reflecting lower dopant activation and spin–orbit interactions that do not strongly fill the conduction band.

In summary, No substantive red shifts of the edge are seen in any doped film –

any band-gap modulation is consistent with defect- and carrier-driven blue-shifts reported for SnO_2 **[141], [142].** The blue shift in E_g at SnO_2:x was possibly due to excess oxygen and may also be affected by sudden increases in crystallite size.

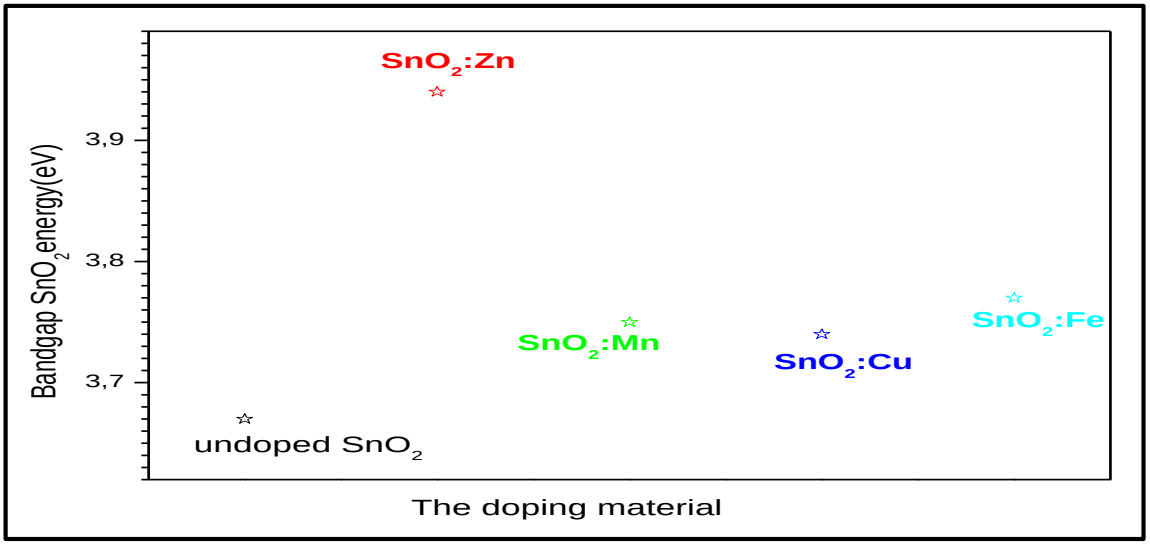


Figure III.10.band gap of undoped SnO_2, Zn, Mn, Cu, Fe- doped SnO_2 thin films

III.3.4.Effect of doping on the Urbach energy of SnO_2 thin films

The figure III.11 shows the inverse relationship between the Urbach energy and the energy gap for each sample. The undoped SnO_2 has $E_g \approx 3.67$ eV and $E_U \approx 740$ meV. Notably, Zn-doped films exhibit significantly higher Eg (~3.94 eV) whereas Mn-, Cu-, or Fe-doped films show only modest E_g shifts (3.75eV, 74eV and 3.77 eV) respectively relative to undoped SnO_2. Conversely, the Urbach energy is much lower in Zn-doped films ($E_U \approx 310$ meV) than in the undoped film, indicating a broad absorption tail, while Mn- , Cu- , and Fe-doped films maintain lower E_U than undoped SnO_2,with only slight decreases in the range(680 meV–640 meV)

As conclude that Zn doping pushes the optical gap into the deep UV, and preserves a sharp absorption edge, whereas Mn, Cu and Fe doping yields only small gap changes but at the cost of pronounced disorder. Mn-,Cu-, and Fe- doped films in our study exhibit E_U (680–640 meV) comparable to or even slightly below undoped SnO_2(740mev), indicating fewer localized states and a sharper edge. Indeed, Seghi et al. **[141]** observed that moderate Fe-doping of SnO_2 actually reduced E_U (down to ~0.30 eV at 2–4 wt% Fe) while marginally increasing E_g. This suggests that Zn dopant either substitute cleanly or relieve strain, improving crystallinity.

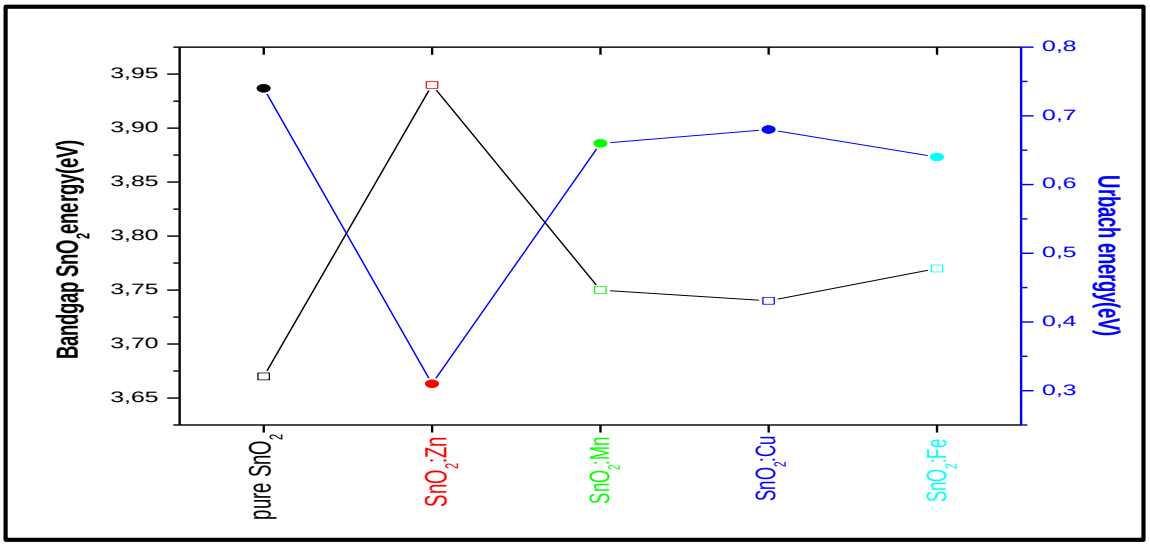


Figure III.11.band gap Vs Urbach energy of undoped SnO_2, Zn, Mn, Cu, Fe- doped SnO_2 thin films

III.4.Influence of Methanol Solvent

The use of methanol as the spray precursor solvent is a key factor in these results. Methanol is a strong reducing agent, so its incorporation promotes oxygen-deficient growth conditions **[143].** As Elangovan et al. explain, adding methanol prevents full oxidation of Sn^{2+}, yielding SnO_2 with abundant oxygen vacancies (donors) **[143]**. These extra vacancies will raise carrier density (enhancing the Burstein– Moss shift and broadening E_U) and also limit crystal growth. Indeed, reducing atmospheres often yield smaller grain/crystallite sizes. Smaller Nano crystals enhance band gap via quantum-size effects: for example, 2–3 nm SnO_2 quantum dots have E_g near 4.00 eV (blue-shifted from the 3.6 eV bulk value) **[144].** Although our films have larger grains than quantum dots, the general trend holds that finer grains widen E_g. Thus, methanol likely contributes to both (a) raising E_g (through vacancy- induced carriers and size reduction) and (b) increasing E_U (through the accompanying disorder). The concurrent influence on dopants is also important: a reducing environment can make dopants more soluble and electrically active. In summary, the alcohol solvent amplifies the Zn-doping effect (wide E_g) by creating vacancies and hindering coarsening, which together broaden the optical gap **[143]**.

III.5.Implications for UV Detection and TCO Applications

The observed E_g and E_U trends have direct implications for applications. For UV photo detectors and transparent conducting oxides (TCOs), a wide band gap is desirable to ensure high UV sensitivity and visible transparency, but a low Urbach tail is also crucial to minimize sub-gap absorption. SnO_2 is a well-known TCO material used in solar cells and smart windows **[143].** In TCOs, low E_U (sharp bsorption edge) correlates with high transparency and figure-of-merit **[145].**

In our case, zinc-doped films offer greater E_g (deep cut in the UV), which can increase UV sensitivity, while maintaining low E_U. These samples thus combine a fairly wide gap with minimal tail absorption, making them optically "cleaner". In contrast, films doped with magnesium, copper and iron maintain $E_g \approx 3.74\text{-}3.77$ eV (still in the UV range) but their high E_U means many anomalies that reduce optical clarity.

For TCOs use the Mn,Cu and Fe-doped SnO_2 may thus provide a better compromise of transparency and conductivity (via some doping) than the heavily Zn-doped films

III.6.Conclusion

In this chapter, we studied the effect of different concentrations of an doped material as well as the effect of a particular concentration of several dopants on the optical properties of tin dioxide and found that the activation process has a significant effect on the latter, significantly changing its transparency, band and Urbach energy, making its applications different depending on the type of doped materials.



General Conclusion



General Conclusion

In this work, we studied the effect of doping with different types of transition materials on the optical properties of SnO_2 thin films. We prepared all the samples by thermal chemical spraying method at 450 °C and under atmospheric pressure, we prepared two sets of samples: (0%, 2%, 4%, 6% and 8%), while the second set of samples were prepared by varying the concentration of zinc impregnated with tin oxide (SnO_2:Zn) with different elements: SnO_2:Mn, SnO_2:Zn, SnO_2:Fe, SnO_2:Cu
We studied the optical properties of all samples using UV-Vis spectroscopy, and by analyzing the transmittance curves in terms of wavelength change in the range [300-1100nm] we concluded the following:

✓ All the thin films prepared in the two groups are transparent conducting oxides because the active zone is located in the visible region.

✓ The high percentage of transparency in all doped SnO_2 samples than undoped SnO_2 sample indicates that the doping process has improved the optical properties of tin oxide.

✓ In terms of the thickness, the doping process in the thin films of all doped samples, whether in the first or second group, led to a significant decrease from 61,449 nm in the pure tin oxide to 400 nm in the doped tin oxide thin films at a concentration of 6%, which indicates that the presence of impurities within the tin oxide network affected the nature of the surface and grain size as the surface regularity and grain size increased, especially for the SnO2:Zn sample.

✓ As for the energy gap, we found that the doping process increased its width, as it was 3.69eV in pure tin oxide and increased in the range of 3.74eV-3.94eV in copper-doped and zinc-doped samples, respectively, indicating the presence of the Burstein–Moss effect, but in different proportions, and the reason for this is due to possibly due to excess oxygen, which is also affected by sudden increases in crystal size.

✓ We also studied the Urbach energy and found that the inverse relationship between it and the energy gap is true. We found that the Urbach energy is lower in all doped SnO_2 thin films (down to $E_U \approx 310$ meV) than in undoped SnO_2 film (Eu ≈ 740 meV), indicating that the doping process Displaced the optical gap into the deep UV, but with varying values.

✓ From all of the above, we conclude that our work has allowed us to realize that the process of doping with zinc, manganese, copper or iron has a significant effect on the optical properties of tin oxide but differently depending on the type of doped material



List of references



List of references

[1] M.R. DAS, A. Mukherjee, P. Mitra. (2017) "Structural, optical and electrical characterization of CBD synthesized CdO thin films: influence of deposition time", Materials Science-Poland, 35 470-478.
[2] K. Usharani, A.R.Balu, V.S.Nagarethinam, M.Suganya. (2015) "Characteristic analysis on the physical properties of nanostructured Mg-doped CdO thin films—Doping concentration effect", Progress in Natural Science: Materials International 25 251–257.
[3] Renu Kumari, Vipin Kumar. (2019) "Impact of zinc doping on structural, optical, and electrical properties of CdO films prepared by sol–gel screen printing mechanism", Journal of Sol-Gel Science and Technology.
[4] B G Jeyaprakash, K Kesavan, R Ashok Kumar, S Mohan and A Amalarani. (2011) "Temperature dependent grain-size and microstrain of CdO thin films prepared by spray pyrolysis method", Bull. Mater. Sci., 34 601–605.
[5] Campos-Gonzalez E., Guillén-Cervantes A., Santoyo-Salazar J., Zelaya-Angel O. (2015) "Growth of CdO films from CdO_2 films by chemical bath deposition: Influence of the concentration of cadmium precursor", Superficies y Vacío 28 25-29
[6] M. Anitha, V. Tamilnayagam, N. Anitha, Tamiloli Devendhiran, Keerthika Kumarasamy, Vasudevan Thangaraj, Kannagi Devendhiran and L. Amalraj. (2018) "Influence of Carrier Gas Pressure on the Physical Properties of CdO Thin Films", Z. Phys. Chem.
[7] Z. Y. Banyamin et al., "Electrical and Optical Properties of Fluorine Doped Tin Oxide Thin Films Prepared by Magnetron Sputtering", Coatings, vol. 4, no. 4, pp. 732–753, 2014.
[8]ح. خنفر، "دراسة الخواص الضوئية لأغشية رقيقة من أكسيد الزنك النقي المحضرة بتقنية رذاذ الانحلال الحراري"، جامعة قاصدي مرباح ورقلة، ورقلة، الجزائر، 2020.
[9] N. Mancer, "Influence du co-dopage sur les propriétés des couches minces à base de ZnO", Université Mohamed Khider de Biskra, Biskra, Algeria, 2023-2024.
[10] C. Habis, J. Zaraket, and M. Aillerie, “Transparent Conductive Oxides. Part I. General Review of Structural, Electrical and Optical Properties of TCOs Related to the Growth Techniques", Materials and Dopants,” Defect and Diffusion Forum, vol. 417, pp. 243–256, Jun. 2022, doi: 10.4028/p-207xgk.
[11] R. Barir, "Caractérisation Spectroscopique des Couches minces d’oxyde de Nikel (NiO) Elaborées par Spray", Ph.D. dissertation, Dept. Phys., Faculté des Mathématiques et des Sciences de la Matière, Université Kasdi Merbah Ouargla, Ouargla, Algeria, May 2018.
[12] L. Bergerot, "Étude de l'élaboration d'oxyde transparent conducteur de type-p en couches minces pour des applications à l’électronique transparente ou au photovoltaïque", Ph.D. dissertation, Univ. Grenoble Alpes, Grenoble, France, Jan. 2015.

[13] R. A. Afre, N. Sharma, M. Sharon, and M. Sharon, "Transparent conducting oxide films for various applications" A review, Rev. Adv. Mater. Sci., vol. 53, pp. 79–89, 2018
[14] A. Stadler, "Transparent conducting oxides—An up-to-date overview", Materials, vol. 5, no. 4, pp. 661–683, Apr. 2012.
[15] M. Khechba, "Elaboration et étude des couches minces d'oxyde d'étain" , Ph.D. dissertation, Dept. Phys., Fac. Sci. Exactes, Univ. Frères Mentouri Constantine 1, Constantine, Algeria, 2018.
[16] A. A. Bensekhria, "Élaboration de couches minces de ZnO:V transparentes conductrices à basse pression et à pression atmosphérique pour applications photovoltaïques", M.S. thesis, Énergie Matériaux et Télécommunications Ctr., INRS, Univ. du Québec, 2020.
[18] S. Berrezoug, "L'effet des couches de TCO et BSF sur les Paramètres Electriques de la Cellule Photovoltaïque Cu In1-x Gax Se". Master's thesis, Fac. Sci., Dept. Phys., Université Abou-Bekr Belkaid, Tlemcen, Algeria, 2021.
[19] S. C. Dixon, D. O. Scanlon, C. J. Carmalt, and I. P. Parkin, "N-type doped transparent conducting binary oxides" An overview, J. Mater. Chem. C, vol. 4, no. 29, pp. 6946–6961, 2016, doi: 10.1039/C6TC01881E.
[20] N. Boubrik, "Comparaison des effets antireflets du SnO_2 et ZnO utilisés comme couches antireflet sur les propriétés de la cellule solaire à homo-jonction", Magister's thesis, Dept. Electron., Fac. Génie Electrique et Informatique, Univ. Mouloud Mammeri, Tizi-Ouzou, Algeria, 2013.
[21] M. Allaham, R. Dallaev, D. Burda, D. Sobola, A. Nebojsa, A. Knápek, M. Mousa, and V. Kolarik, "Energy gap measurements based on enhanced absorption coefficient calculation from transmittance and reflectance raw data," Phys. Scr., vol. 99, no. 2, Feb. 2024, Art. no. 025002, doi: 10.1088/1402-4896/ad1cb8.
[22]ي. لطرش و ف. ز. س. عثمان، "دراسة تأثير سمك الطبقات الرقيقة لأكسيد النيكل على بعض الخصائص الفيزيائية"، مذكرة ماجستير، قسم علوم المواد، كلية العلوم الدقيقة وعلوم الطبيعة والحياة، جامعة محمد خيضر، بسكرة، الجزائر، 2022.
[23] W. Aouina, "Étude des propriétés structurales, optiques et électriques des couches minces de ZnO:Al", Master's thesis, Mohamed Boudiaf University of M'Sila, Algeria, 2017.
[24] : F. Z. Bedia, "Caractérisations et optimisations des dépôts des couches minces d'oxyde de zinc (ZnO) en vue d'applications dans les énergies renouvelables", Thèse de doctorat, Faculté des Sciences, Université Abou Bekr Belkaïd – Tlemcen, Algérie, 2015.
[25] A. Bounegab, "Study, realization and characterization of thin films based on TCO for micro-technology applications," Doctoral dissertation, Dept. of Electronics and Communications, Faculty of New Information and Communication Technologies. Univ. Kasdi Merbah, Ouargla, Algeria, 2024.

[26] D. S. Y. Jayathilake and T. A. N. Peiris, “Overview on Transparent Conducting Oxides and State of the Art of Low-cost Doped ZnO Systems,” SF Journal of Material and Chemical Engineering, vol. 1, no. 1, Art. no. 1004, Jan. 26, 2018.
[27] K. Kettafa and H. Douibi, "Les oxydes transparents conducteurs : Propriétés et Applications", Licence thesis, Département Sciences de la Matière, Faculté des Sciences et de la Technologie, Université Mohamed Elbachir Elibrahimi – Bordj Bou Arreridj, Algeria, Jun. 17, 2014.
[28] M. Salah, J. Yoon, M. M. El-Desoky, Z. Hussain, H. Ju, and S.-K. Mo, "Electronic structure of p-type transparent conducting oxide $CuAlO_2$", Current Applied Physics, vol. 39, pp. 107–112, 2022.
[29] F. Z. Issaad and N. E. H. Touidjine, "Élaboration et caractérisation de couches minces à base de SnO_2 par la méthode sol–gel, et leur application en photodétection UV", Master’s thesis, Dept. of Material Sciences, Faculty of Exact Sciences and Natural and Life Sciences, University Larbi Ben M’Hidi – Oum El Bouaghi, Algeria, Jul. 6, 2022.
[30] G. T. Chavan et al., "A Brief Review of Transparent Conducting Oxides (TCO): The Influence of Different Deposition Techniques on the Efficiency of Solar Cells," Nanomaterials, vol. 13, no. 7, p. 1226, 2023, doi: 10.3390/nano13071226.
[31] K. H. L. Zhang, K. Xi, M. G. Blamire, and R. G. Egdell, "P-type transparent conducting oxides", J. Phys.: Condens. Matter, vol. 28, no. 38, Art. no. 383002, Sep. 2016, doi:10.1088/0953-8984/28/38/383002.
[32] J. Patel, R. K. Sharme, M. A. Quijada, and M. M. Rana, "A review of transparent conducting films (TCFs): Prospective ITO and AZO deposition methods and applications," Nanomaterials, vol. 14, no. 24, p. 2013, 2024, doi: 10.3390/nano14242013.
[32] A. Allag, "Optimisation des conditions d’élaboration des couches minces d’oxyde d’étain SnO2 par spray", Ph.D. dissertation, Dept. Phys. Mater., Univ. Mohamed Khider - Biskra, Biskra, Algeria.
[33] D. Yeboah, E. G. Asenso, and P. B. Fosuah, "Comprehensive evaluation of transparent electrode materials: A hybrid methodology of AHP, FOM, and cost-efficiency metrics," Next Res., vol. 2, no. 1, p. 100157, 2025, doi: 10.1016/j.nexres.2025.100157.
[34] National Center for Biotechnology Information, "PubChem compound summary for CID 29011, Tin(IV) oxide," 2025. Available: https://pubchem.ncbi.nlm.nih.gov/compound/Tin_IV_-oxide.
[35] G. K. Dalapati et al., "Tin oxide for optoelectronic, photovoltaic and energy storage devices: a review," J. Mater. Chem. A, vol. 9, no. 31, pp. 16621-16684, 2021, doi: 10.1039/D1TA01291F.
[36] N. Houaidji, "Synthèse et caractérisation des couches minces du SnO2: (F, Co) destinées à des applications photovoltaïques", Ph.D. dissertation, Dept. Phys., Badji Mokhtar Univ., Annaba, Algeria, 2019/2020.

[37] S. Yahiaoui, "L'effet de la molarité des différentes sources d'étain sur les propriétés des couches minces d'oxyde d'étain SnO_2 élaborées par Spray Ultrasonique", Magister thesis, Univ. Mohamed Khider, Biskra, Algérie, 2014.
[38]ل. سقني، "تحديد خصائص أكسيد القصدير المطعَّم بالحديد "، مذكرة ماجستير، قسم الفيزياء، جامعة الشهيد حمه لخضر – الوادي، الوادي، الجزائر، 2016.
[39]م. حنكة، "تحديد الخصائص البصرية لطبقات رقيقة لأكسيد القصدير المطعَّم بالفلور المحضرة بطريقة الرش الفوق صوتي"، مذكرة ماجستير، قسم علوم المواد، كلية الرياضيات وعلوم المادة، جامعة قاصدي مرباح ورقلة، ورقلة، الجزائر، 2014.
[40] A. Ben Haoua, "Caractérisation des couches minces de SnO2 élaborées par spray ultrasonique utilisées dans les cellules solaires", Ph.D. dissertation, Dept. Phys., Kasdi Merbah Univ., Ouargla, Algeria, Oct. 9, 2016.
[17] S. Benyahia and K. Aoumeur, "Synthèse et caractérisation des couches minces d'oxyde d'étain (SnO_2) dopé fluor (F) par procédé Sol-Gel", Mémoire de Master en Physique, Spécialité : Technologie et Physique des Couches Minces Nano Structurées, Université Ibn Khaldoun – Tiaret, 03 juin 2015.
[41] S. J. Ikhmayies and R. N. Ahmad-Bitar, "Effect of processing on the electrical properties of spray-deposited SnO_2:F thin films", *Am. J. Appl. Sci.*, vol. 5, no. 6, pp. 672–677, 2008.
[42]م. محمودي، "التحديد الطيفي للخصائص الكهروضوئية لشرائح أكسيد القصدير المضاعفة التطعيم والموضوعة بطريقة الرش الحراري بواسطة فوهة تتحرك"، أطروحة دكتوراه، قسم الفيزياء، جامعة قاصدي مرباح ورقلة، ورقلة، الجزائر، 2021.
[43] I. Chadou, "Etude des Propriétés Electriques des Couches Minces de SnO2 Obtenues par Sol-Gel", M.S. thesis, Dept. Phys., Ferhat Abbas Univ., Sétif, Algeria, Sept. 5, 2007.
[44] F. Azzouz, "Investigation théorique des propriétés structurales, électroniques et thermoélectriques des composés binaires à base cadmium", M.S. thesis, Dept. Phys., Ibn Khaldoun Univ., Tiaret, Algeria, Jul. 6, 2021.
[45] N. Hadjadj, "Etude microstructurale et optique des films minces nanostructurés du SnO2 dopé azote par spray pyrolyse ultrasonique", M.S. thesis, Dept. Phys., Ibn Khaldoun Univ., Tiaret, Algeria, Jun. 10, 2018.
[46] J. Jeong, S. P. Choi, K. J. Hong, H. J. Song, and J. S. Park, "Structural and optical properties of SnO_2 thin films deposited by using CVD techniques," J. Korean Phys. Soc., vol. 48, no. 5, pp. 960-963, May 2006.
[47] M. T. Rahman, Z. Ahmed, Y. Ahmed, M. Rahman, and F. T. Z. Toma, "Investigating the effect of annealing temperatures on SnO_2 nanostructural thin films and their properties," J. Mater. Sci. Res., vol. 13, pp. 1-12, 2022.
[48] S. J. Ikhmayies, "Thickness dependence of the optical parameters of spray-deposited SnO_2:F thin films," in TMS 2015 144th Annual Meeting & Exhibition, Cham, Switzerland, 2016, pp. 593-600. doi: 10.1007/978-3-319-48127-2_74.
[49] M. N. A. Bitu, N. I. Tanvir, S. Islam, and S. F. U. Farhad, "Effect of substrate surface on the wide bandgap SnO_2 thin films grown by spin coating,", Sep. 2022.

[50] S. Gürakar and T. Serin, "Effect of Co doping on optical parameters of SnO_2 thin films," Opt. Mater., vol. 111, p. 110579, Jan. 2021, doi: 10.1016/j.optmat.2020.110579.
[51] N. Boufaa, "Elaboration and characterization of tin oxide (SnO_2) nanopowders," M.S. thesis, Dept. Phys., Univ. Mentouri Constantine, Constantine, Algeria, May 24, 2012.
[52] K. Bennaceur, "Elaboration and characterization of SnO_2:In thin films deposited by spray pyrolysis technique," Ph.D. dissertation, Dept. Mater. Sci., Univ. Mohamed Khider, Biskra, Algeria, 2020.
[53] H. Mezenner, B. Nouicer, "Synthèse et caractérisation des couches minces SnO_2 dopées Sb pour des applications opto-électriques", Mémoire de fin d'études, Université Mohammed Seddik Benyahia – Jijel, Faculté des Sciences et de la Technologie, Département Génie des Procédés, 2019.
[54] N. Chaabia, "Conception et caractérisation d'oxydes TiO_2, SnO_2 et mixtes et investigation de leurs performances photocatalytiques vis-à-vis de polluants organiques", Thèse de Doctorat en Sciences, Université Ferhat Abbas - Sétif 1, Faculté de Technologie, Département de Génie des Procédés, s.d.
[55] B. J. Jeon, C. Hudaya, and J. K. Lee, "Pilot-scale electron cyclotron resonance-metal organic chemical vapor deposition system for the preparation of large-area fluorine-doped SnO_2 thin films," J. Vac. Sci. Technol. A, vol. 34, no. 3, p. 031501, May 2016, doi: 10.1116/1.4943389.
[56] J. I. Scott, R. F. Martinez-Gazoni, M. W. Allen, and R. J. Reeves, "Optical and electronic properties of high quality Sb-doped SnO2 thin films grown by mist chemical vapor deposition," J. Appl. Phys., vol. 126, no. 13, 2019, doi: 10.1063/1.5116719.
[57] A. H. Pinto et al., "Doped tin dioxide (d-SnO_2) and its nanostructures: Review of the theoretical aspects, photocatalytic and biomedical applications," Solids, vol. 3, no. 2, pp. 327–360, 2022. doi: 10.3390/solids3020024.
[58] J. Garnier, "Elaboration de couches minces d'oxydes transparents et conducteurs par spray CVD assisté par radiation infrarouge pour applications photovoltaïques", École Nationale Supérieure d'Arts et Métiers, Thèse, 2009.
[59] K. Khaoula and H. Douibi, "Les oxydes transparents conducteurs : Propriétés et Applications", Mém. de fin d'études, Université Mohamed Elbachir Elibrahimi – Bordj Bou Arreridj, Faculté de Sciences et de la Technologie, Département Sciences de la Matière, June 17, 2014.
[60] D. Lalam, "Étude et Optimisation des Cellules Solaires en Couches Minces CdTe/CdS", Mémoire de Master Académique, Université Mouloud Mammeri de Tizi-Ouzou, Faculté de Génie Electrique et Informatique, Département d'Electronique, 2016.
[61] A. Khadidja, "Simulation Des Propriétés Structurales Et Électroniques Des Oxydes Transparents Conducteurs Dopés", Mém. de Master, Centre Universitaire de

Tissemsilt, 2019/2020.
[62] R. D. Shannon, "Revised effective ionic radii and systematic studies of interatomic distances in halides and chalcogenides," Acta Cryst. A, vol. 32, no. 5, pp. 751–767, 1976.
[63] B. Xu, X.-G. Ren, G.-R. Gu, L.-L. Lan, and B.-J. Wu, "Structural and optical properties of Zn-doped SnO_2 films prepared by DC and RF magnetron co-sputtering," Superlattices Microstruct., vol. 89, pp. 34–42, Jan. 2016.
[64] M.-M. Bagheri-Mohagheghi, N. Shahtahmasebi, M. R. Alinejad, A. Youssefi, and M. Shokooh-Saremi, "Fe-doped SnO_2 transparent semi-conducting thin films deposited by spray pyrolysis technique: Thermoelectric and p-type conductivity properties", Solid State Sciences, vol. 11, no. 1, pp. 233–239, 2009. doi: 10.1016/j.solidstatesciences.2008.05.005.
[65] Y. Fu, N. Sun, L. Feng, S. Wen, Y. An, and J. Liu, "Local structure and magnetic properties of Fe-doped SnO_2 films, Journal of Alloys and Compounds", vol. 698, pp. 863–867, 2017. doi: 10.1016/j.jallcom.2016.12.297.
[66] K. Gopinadhan, S. C. Kashyap, D. K. Pandya, and S. Chaudhary, "High temperature ferromagnetism in Mn-doped SnO_2 nanocrystalline thin films", J. Appl. Phys., vol. 102, no. 11, p. 113513, Dec. 2007. doi: 10.1063/1.2817825.
[67] K. Vadivel, V. Arivazhagan, and S. Rajesh, "Mn doped SnO_2 semiconducting magnetic thin films prepared by spray pyrolysis method", Int. J. Sci. Eng. Res., vol. 2, no. 4, pp. 1-5, Apr. 2011.
[68] S. S. Roy and J. Podder, "Synthesis and optical characterization of pure and Cu doped SnO_2 thin films deposited by spray pyrolysis", J. Optoelectron. Adv. Mater., vol. 12, no. 7, pp. 1479-1484, Jul. 2010.
[69] S. Benzitouni, M. Zaabat, A. Khial, D. Rechem, A. Benaboud, D. Bouras, A. Mahdjoub, M. Toubane, and R. Coste, "High Sensitivity of Porous Cu-Doped SnO_2 Thin Films to Methanol", Adv. Nanopart., vol. 5, pp. 140-148, May 2016, doi: 10.4236/anp.2016.52016.
[70] A. Hafdallah, "Étude du Dopage des Couches Minces de ZnO Élaborées par Spray Ultrasonique", Mémoire de Magister, Université Mentouri - Constantine, Faculté des Sciences Exactes, Département de Physique, Spécialité : Sciences des Matériaux, Option : Semi-Conducteurs, 2007.
[71]د. رحموني، "تأثير تغير التركيز المولاري لنترات النيكل على الخواص البصرية لأغشية أكسيد النيكل الرقيقة"، مذكرة ماجستير، قسم علوم المواد، جامعة العربي التبسي – تبسة، الجزائر، 2023.
[72] L. Liljeholm, "Reactive Sputter Deposition of Functional Thin Films", Ph.D. dissertation, Acta Universitatis Upsaliensis, Uppsala Univ., Uppsala, Sweden, 2012. ISBN: 978-91-554-8403-3.

[73]و. ح. فيحان، "الأغشية الرقيقة"، مشروع تخرج، قسم الفيزياء، كلية التربية للعلوم الصرفة، جامعة بابل، العراق، 2023.

[74] : S. K. Shrivastava, "Deposition Techniques for High-Tc Superconducting YBCO Thin Films", International Journal of Engineering & Scientific Research, vol. 5, no. 6, Jun. 2017.
[75] A. Mennad, "Les techniques de dépôt de couches minces et leurs applications," Revue des Energies Renouvelables, vol. 18, no. 4, pp. 713-719, 2015.
[76] N. Khennafi-Benghalem, M. Hamidouche, and N. Derouiche, "Caractérisation des propriétés optiques de couches minces obtenues par évaporation sous vide et par sputtering sur du verre," Verres, Céramiques & Composites, vol. 5, no. 1, pp. 12-20, 2016.
[77] D. A. Jameel, "Thin Film Deposition Processes", Int. J. Mod. Phys. Appl., vol. 1, no. 4, pp. 193–199, 2015.
[78] : VAC AERO, "Five Main Reasons for Using Vacuum," Vacaero, Jun. 5, 2018. Available: https://vacaero.com/information-resources/vacuum-pump-technology-education-and-training/153727-five-main-reasons-for-using-vacuum.html
[79] N. A. Shepelin, Z. P. Tehrani, N. Ohannessian, C. W. Schneider, D. Pergolesi, and T. Lippert, "A Practical Guide to Pulsed Laser Deposition," Lib4RI, 2023. Available: https://www.dora.lib4ri.ch/psi/islandora/object/psi%3A51839/datastream/PDF/Shepelin-2023-A_practical_guide_to_pulsed-%28published_version%29.pdf.
[80] A. Jilani, M. S. Abdel-wahab, and A. H. Hammad, "Advance Deposition Techniques for Thin Film and Coating," in Modern Technologies for Creating the Thin-film Systems and Coatings, InTech, Mar. 8, 2017. Available: https://doi.org/10.5772/65702
[81] M. C. Rao, "Pulsed laser deposition — ablation mechanism and applications," Int. J. Mod. Phys. Conf. Ser., vol. 22, pp. 355–360, Jan. 2013. Available: https://doi.org/10.1142/S2010194513010362
[82] C. Khelifi, "Tin Dioxide SnO_2 Thin Films Deposited by Ultrasonic Spray Technique: Properties and Applications", Doctorate thesis, Univ. of Med Khider Biskra, Algeria, 2018.
[83] H. Slimi, "Élaboration et caractérisation de couches minces co-dopées In, Co, préparées par la pulvérisation cathodique, applications aux cellules photovoltaïques", Thèse de doctorat, Univ. du Littoral Côte d'Opale; Univ. de Sfax, 2019.
[84] A. A. Kamil, N. A. Bakr, T. H. Mubarak, and J. Al-Zanganawee, "Effect of Au and Ag nanoparticles addition on the morphological, structural and optical properties of ZnO thin films deposited by sol-gel method", Journal of Ovonic Research, vol. 18, no. 3, pp. 431–442, May–Jun. 2022.
[85] S. Obregón and V. Rodríguez-González, "Photocatalytic TiO_2 thin films and coatings prepared by sol-gel processing : A brief review," J. Sol-Gel Sci. Technol., vol. 102, pp. 125–141, Apr. 2022, doi: 10.1007/s10971-021-05628-5.
[86] N. U. Saidin, K. K. Ying, and N. I. Khuan, "Electrodeposition: Principles, Applications and Methods," presented at the Nuclear Technical Convention 2011

(NTC 2011), Bangi, Malaysia, Sep. 13–15, 2011.
[87] S. F. U. Farhad, M. M. Hossain, N. I. Tanvir, and S. Islam, "Texture and bandgap tuning of phase pure Cu_2O thin films grown by a simple potentiostatic electrodeposition technique," ECS Meeting Abstracts, vol. MA2020-01, no. 19, pp. 1212, May 2020, doi: 10.1149/MA2020-01191212mtgabs.
[88] M. Boussafeur, "Elaboration par Spray Pyrolyse et caractérisations structurales de couches minces d'oxyde de zinc", M. Sc. thesis, Département Sciences de la Matière, Université Larbi Ben M′Hidi, Oum El Bouaghi, Algeria, 2012.
[89] S. Haffas and M. Berak, "Caractérisation des couches minces Co_3O_4 : Cu élaborée par la technique spray pneumatique", M.Sc. thesis, Département des Sciences de la Matière, Université Mohamed Khider de Biskra, Biskra, Algeria, Sept. 20, 2020.
[90] L. Filipovic, "Modeling and Simulation of Novel Semiconductor Devices," Ph.D. dissertation, Institute for Microelectronics, TU Wien, Vienna, Austria, 2013.
[91] S. Boulmelh, "Élaboration et caractérisation d'un dépôt de couches minces d'oxyde de zinc par spray pyrolyse", Magister thesis, Département d'Electronique, Faculté des Sciences de la Technologie, Université de Frères Mentouri Constantine, Constantine, Algeria, Nov. 12, 2015.
[92] A. Elkali, "Étude de l'effet du Fluor sur les propriétés optoélectroniques des couches minces de SnO_2 déposées par spray pyrolyse", M.Sc. thesis, Département Electronique, Faculté de Technologie, Université Mohamed Boudiaf - M'Sila, M'Sila, Algeria, 2021-2022.
[93] F. Hijazi, "Étude des propriétés physiques et de transport dans des films d'ITO et de ZnO (dopé ou non) pour dispositifs optoélectroniques organiques", Ph.D. thesis, Ecole Doctorale Science – Technologie – Santé, Faculté des Sciences et Techniques de Limoges, Université de Limoges, Limoges, France, Oct. 21, 2010.
[94] Y. Doumbia, "Elaboration et caractérisation des couches minces pérovskites hybrides organiques-inorganiques pour les cellules solaires photovoltaïques", Ph.D. thesis, Departamento de Física Aplicada-IDF, Universitat Politècnica de València, Spain, Jan. 18, 2024. Supervisors: Prof. Dr. B. Marí Soucase and Dr. D. Soro Donafologo.
[95] Z. Oulad Elhmaidi, "Élaboration de couches minces de Cu_2ZnSnS_4 par ablation laser pulsée et leur intégration en cellules solaires à haut rendement de photoconversion", Ph.D. thesis, Institut National de la Recherche Scientifique, Centre Énergie Matériaux Télécommunications, Université du Québec, Montréal, Canada, Aug. 2020.
[96] R. Benmerad, "Effect of Cr doping on optical and electrical properties of ZnO thin films deposited by spray pyrolysis technique", Master's thesis, Dept. Matter Sci., Univ. Larbi Tebessi, Tebessa, Algeria, 2022/2023.
[97] L. Herissi, L. Hadjeris, N. Attaf, M. S. Aida, A. Hafdallah, and W. Darenfad, "Influence des conditions de dépôt sur les propriétés optiques des couches minces

d'oxyde de zinc élaborées par spray pyrolyse", 2008. Available: https://doi.org/10.13140/RG.2.2.32745.93283
[98] L. Herissi, L. Hadjeris, M. S. Aida, F. Serradj, and A. Hafdallah, "Étude de la dépendance avec les conditions de dépôt des propriétés de couches minces d'oxyde de zinc préparées par spray pyrolyse", 2008, DOI: 10.13140/RG.2.2.15151.89763.
[99] L. Herissi, "Élaboration par pulvérisation pyrolytique et caractérisation de couches minces semiconductrices et transparentes d'oxyde de zinc : Perfectionnement du système de dépôt," Magister thesis, Dept. Phys., Univ. Larbi Ben M'Hidi, Oum El Bouaghi, Algeria, 2008. Available: https://doi.org/10.13140/RG.2.2.22422.70728
[100] L. Herissi, L. Hadjeris, N. Attaf, M. S. Aida, A. Hafdallah, and W. Darenfad, "Réalisation et étude de couches minces de ZnO transparentes et conductrices," Algerian Journal of Advanced Materials, vol. 4, pp. 415–418, 2008.
[101] B. Fleischmann, "Influences du procédé d'atomisation et du matériau précurseur sur les mécanismes de compaction et les propriétés métallurgiques de pièces élaborées par CIC," Ph.D. dissertation, Univ. Bourgogne Franche-Comté, Belfort-Montbéliard, France, 2022.
[102] V. K. Singh, "Thin film deposition by spray pyrolysis techniques," J. Emerg. Technol. Innov. Res., vol. 4, no. 11, pp. 910–915, Nov. 2017.
[103] Y. Munikrishna Reddy and M. Nagendra Vara Prasad, "Properties of CdS chemically deposited thin films on the effect of ammonia concentration," IOSR J. Appl. Phys., vol. 4, no. 4, pp. 1-7, Sep.-Oct. 2013.
[104] S. Tian, Y. Feng, Z. Zheng, and Z. He, "TiO_2-Based Photocatalytic Coatings on Glass Substrates for Environmental Applications," Coatings, vol. 13, no. 8, p. 1472, 2023, doi: 10.3390/coatings13081472.
[105] A. Mammana, M. Hamanaka, T. Santos, D. Engelsen, and C. Mammana, "Stress behavior of thin SnO_2 films on various substrates at high temperature", 2012.
[106] M. Khalfallah, "Élaboration et caractérisation de l'effet du dopage des couches minces de SnO_2 déposées par spray pyrolyse pour l'application optoélectronique", Ph.D. dissertation, Dept. Electron., Univ. Mohamed Boudiaf - M'sila, M'sila, Algeria, 2022.
[107] Valley Design, "Soda Lime Glass (Borosilicate, Fused Silica, Quartz)", 2023. Available: https://valleydesign.com/soda-limepic/.
[108] T. Mahdaoui, N. Bouaouadja, M. Hamidouche, J. Simons, and F. Petit, "Study of SnO_2 thin film deposited on soda-lime glass using the spray pyrolysis coating method," International Review of Mechanical Engineering (I.RE.M.E.), vol. 1, no. 3, pp. 1–5, May 2007.
[109] Jasco, Brochure. Available: https://www.norlab.fi/library/brochure/10886.
[110] M. Khechba, "Elaboration et étude des couches minces d'oxyde d'étain", Doctorat en Sciences, Université des Frères Mentouri Constantine 1, Faculté des Sciences Exactes, Département de Physique, 2018.

[111] A. Hafdallah, "Dépôt et caractérisation des électrodes en couches minces transparentes et conductrices", Ph.D. dissertation, Dept. of Physics, Univ. des Frères Mentouri Constantine, Algeria, 11 Jul. 2016.
[112] F. Hanini, "Etude des propriétés physiques de couches minces TiO_2 élaborées par différentes techniques," Ph.D. dissertation, Dept. Phys., Univ. Constantine 1, Constantine, Algeria, 2014.
[113] M. K. Agarwal, M. Saxena, and S. Gupta, "A study on optical parameters of Ge-Se-Te thin film for optical storage devices," Int. J. Comput. Sci. Eng., vol. 6, no. 12, Dec. 2018.
[114] B. D. Viezbicke, S. Patel, B. E. Davis, and D. P. Birnie III, "Evaluation of the Tauc method for optical absorption edge determination: ZnO thin films as a model system", Phys. Status Solidi B, vol. 252, no. 8, pp. 1700–1710, 2015, doi: 10.1002/pssb.201552007.
[115] A. A. Bamfo-Asante, I. Nkrumah, M. Paal, and K. Singh, "Effect of deposition and annealing temperatures on optical band gap of SnO_2 thin films deposited on glass substrate by chemical vapour deposition (CVD) method", Int. J. Adv. Res. Eng. Technol. (IJARET), vol. 6, no. 4, pp. 09–16, Apr. 2015.
[116] H. Habieb and N. Hamdadou, "Preparation and characterization of undoped and antimony doped tin oxide thin films synthesized by spray pyrolysis", Mater. Phys. Mech., vol. 48, no. 3, pp. 367–378, 2022, doi: 10.18149/MPM.4832022_7.
[117] F. Z. Hadj Ben Fetima, "Étude des propriétés structurales et optiques des couches minces de SnO_2 dopé Ni", Master's thesis, Dept. Phys., Univ. Saad Dahlab Blida 1, Blida, Algeria, 2023.
[118] S. Hariech, "Elaboration Et Caractérisation Des Couches Minces De Suleure De Cadmium(Cds) Préparées Par Bain Chimique (Cbd)", Mémoire De Magister, Universite Constantine, (2009).
[119] W. Daranfed, M.S. Aida, A. Hafdallah, H. Lekiket, Thin Solid Films 518 (2009) 1082-1084
[120] H. L, Royg, "Atmospheric presure chemical vapor deposition transparent conducting film of fluorine doped zinc oxide and their application to amorphous siilicon solar cells" J.MaterSci, 42,6388-6399(2007).
[121] Hassan Abass "Van der Pauw Measurements Of The Hall Effect In. A.] S Nanoparticulate Silicon Layers" Diploma at AIMS, University of Cape Town; South Africa, (2008).
[122]م. فرج الله، "تحضير ودراسة تأثير تطعيم أكسيد القصدير على بعض الخصائص الفيزيائية"، مذكرة ماجستير، جامعة محمد خيضر، بسكرة، الجزائر، 2023.
[123] M. Khechba, A. Bouabellou, F. Hanini, and S. Touati, "Effect of Al doping on the structural and optical properties of SnO_2 thin films elaborated by sol-gel technique", J. New Technol. Mater., vol. 7, no. 2, pp. 72–75, 2017.
[124] N. Guermat et al., "Effects of zinc doping on structural, morphological, optical and electrical properties of SnO_2 thin films", Eur. Phys. J. Appl. Phys., vol. 97, no.

14, 2022, doi:10.1051/epjap/2022210218
[125]س. يحياوي و ز. غولي، "الدراسة البنيوية والكهربائية والضوئية لأكسيد القصدير المطعَّم بالحديد "، مذكرة ماجستير، قسم الفيزياء، كلية الرياضيات وعلوم المادة، جامعة قاصدي مرباح ورقلة، الجزائر، 2020.
[126] A. Doyan, Susilawati, L. Muliyadi, S. Hakim, H. Munandar, and M. Taufik, "The effect of dopant material to optical properties: energy band gap Tin Oxide thin film", in J. Phys.: Conf. Ser., vol. 1816, no. 1, p. 012114, 2021, doi: 10.1088/1742-6596/1816/1/012114.
[127]ن. م. ع. الكرخي، "دراسة الخصائص التركيبية والبصرية لأغشية المحضرة بطريقة التحلل الكيميائي الحراري"، رسالة ماجستير، كلية العلوم، جامعة ديالى، العراق، 2011.
[128] A. Doyan, Susilawati, S. Hakim, L. Muliyadi, and M. Taufik, "The effect of annealing temperature thin films indium doped SnO_2 to optics properties and material composition", J. Phys.: Conf. Ser., vol. 1572, p. 012072, 2020, doi: 10.1088/1742-6596/1572/1/012072.
[129] Susilawati, A. Doyan, L. Muliyadi, S. Hakim, and M. Taufik, "The thickness effect to optical properties of SnO_2 thin film with doping fluorine", J. Phys.: Conf. Ser., vol. 1572, p. 012085, 2020, doi: 10.1088/1742-6596/1572/1/012085.
[130] A. Doyan, Susilawati, A. Harjono, S. Azzahra, and M. Taufik, "Characterization of tin oxide doping antimony thin layer with sol-gel spin coating method for electronic device", Mater. Sci. Forum, vol. 966, pp. 30–34, 2019.
[131] A. Doyan, Susilawati, S. A. Fitri, and S. Ahzan, "Crystal structure characterization of thin layer zinc oxide", Mater. Sci. Eng., vol. 196, pp. 1–6, 2017.
[132] A. Doyan, Susilawati, M. Taufik, S. Hakim, and L. Muliyadi, "The optical properties of thin films tin oxide with triple doping (aluminum, indium, and fluorine) for electronic device", Solid State Phenom., vol. 317, pp. 477–482, 2021.
[133] B. Benhaoua, A. Rahal, and S. Benramache, "The structural, optical and electrical properties of nanocrystalline ZnO:Al thin films", Superlattices Microstruct. Available: www.elsevier.com/locate/superlattices.
[134] Y. Feng et al., "The magnetic and optical properties of 3d transition metal doped SnO_2 nanosheets", RSC Adv., vol. 5, pp. 24306–24312, 2015, doi:10.1039/C5RA00788G. Available: https://doi.org/10.1039/C5RA00788G.
[135] J. Mhalla et al., "Investigation of the impact of transition metals (TM = Fe, Co, Ni) doping on the optoelectronic properties of tin dioxide SnO_2: first-principles analysis", Digest J. Nanomater. Biostruct., vol. 19, no. 4, pp. 1677–1691, 2024, doi:10.15251/djnb.2024.194.1677. Available: https://doi.org/10.15251/DJNB.2024.194.1677.
[136] K. von Rottkay and M. Rubin, "Optical indices of pyrolytic tin-oxide glass", Mater. Res. Soc. Symp. Proc., vol. 426, p. 449, 1996.
[137] P. Lisnic, L. Hrostea, L. Leontie, and M. Girtan, "Fluorine-Doped SnO_2 Thin Films in Solar Cell Applications. Morphological, Optical and Electrical Properties", Arch. Metall. Mater., vol. 68, no. 2, pp. 483–490, 2023, doi:10.24425/amm.2023.142426

[138] O. S. Elsherif et al., "Structural, optical and electrical properties of SnO_2:F thin films deposited by spray pyrolysis for application in thin film solar cells", J. Mater. Sci.: Mater. Electron., vol. 27, pp. 12280–12286, 2016, doi:10.1007/s10854-016-5206-x.
[139] K.-T. Park et al., "Undoped tin dioxide transparent electrodes for efficient and cost-effective indoor organic photovoltaics," NPG Asia Mater., vol. 13, Art. 43, 2021, doi:10.1038/s41427-021-00310-2.
[140] L. Xiong et al., "Performance enhancement of high temperature SnO_2-based planar perovskite solar cells: electrical characterization and understanding of the mechanism", J. Mater. Chem. A, vol. 4, pp. 8374–8383, 2016, doi:10.1039/C6TA01839D.
[141] L. Segueni, A. Rahal, B. Benhaoua, N. Allag, A. Benhaoua, and M. S. Aida, "Iron doping SnO_2 thin films prepared by spray with moving nozzle: Structural, morphological, optical, and type conductivities", Dig. J. Nanomater. Biostruct., vol. 14, no. 4, pp. 923-934, Oct.-Dec. 2019.
[142] A. V. Babu, S. Murugan, and D. C. B. Victoria, "Fabrication of Zn doped SnO_2 thin films and its tuning effects", Int. J. Adv. Res. Eng. Technol., vol. 11, no. 11, pp. 1490-1498, Nov. 2020, doi: 10.34218/IJARET.11.11.2020.136.
[143] E. Elamurugu and K. Ramamurthi, "Studies on optical properties of polycrystalline SnO_2:Sb thin films prepared using $SnCl_2$ precursor", Cryst. Res. Technol., vol. 38, pp. 779-784, 2003, doi: 10.1002/crat.200310095.
[144] A. Das, V. Bonu, A. K. Prasad, D. Panda, S. Dhara, and A. K. Tyagi, "The role of SnO_2 quantum dots in improved CH_4 sensing at low temperature", J. Mater. Chem. C, vol. 2, no. 1, pp. 164-171, 2014, doi: 10.1039/C3TC31728E.
[145] M. Mezyen, G. El Fidha, N. Bitri, F. Harrathi, I. Ly, and E. Llobet, "Visible light activated SnO_2:Dy thin films for the photocatalytic degradation of methylene blue", RSC Adv., vol. 13, no. 44, pp. 31151-31166, Oct. 2023, doi: 10.1039/d3ra05424a.



Abstract



Abstract

The pure SnO_2 thin film and X-doped SnO_2 thin films while X is: Zn, Mn, Cu and Fe are synthesized by using spray pyrolysis technique at 450°C and under atmospheric pressure. The optical properties of all samples was investigated by the transmittance curves analyzing in terms of wavelength change in the range [300-1100nm], and it has shown that pure tin oxide and doped tin oxide with different concentrations of zinc or doped with different transition materials are transparent conducting oxides. We found that the doping process reduced the thickness and increased the band-gap energy (E_g) while reducing the Urbach energy (E_U) of tin oxide thin films and is therefore very important for improving its photovoltaic properties.

Keywords: SnO_2: X، X=Mn ،Cu ،Fe، Zn, SnO_2, Thin films, Transparent conducting oxide, Spray pyrolysis, optical ban gap, Transmittance, Urbach energy, thickness.

Résumé

Résumé

Le film mince de SnO_2 pur et les films minces de SnO_2 dopés par X, X étant : Zn, Mn, Cu et Fe sont synthétisés en utilisant la technique de spray pyrolyse à 450°C et sous pression atmosphérique. Les propriétés optiques de tous les échantillons ont été étudiées par l'analyse des courbes de transmittance en termes de changement de longueur d'onde dans la gamme [300-1100nm],et a montré que l'oxyde d'étain pur et l'oxyde d'étain dopé avec différentes concentrations de zinc ou dopé avec différents matériaux de transition sont des oxydes conducteurs transparents. Nous avons constaté que le processus de dopage réduisait l'épaisseur et augmentait l'énergie de la bande interdite (E_g) tout en réduisant l'énergie d'Urbach (E_U) des films minces d'oxyde d'étain et qu'il était donc très important pour améliorer ses propriétés photovoltaïques.

Mots-clés : SnO_2: X‹ X=Mn ‹Cu ‹Fe‹ Zn, SnO_2, Couches minces, Oxyde conducteur transparent, Spray Pyrolyse, gap optique, Transmittance, Energie d'Urbach, Epaisseur



ملخص



ملخص

الأغشية الرقيقة SnO2 النقية والأغشية الرقيقة SnO_2 المطعمة بـX ، حيث X هي الزنك والمنغنيز والنحاس والحديد، تم تحضيرها باستخدام تقنية االرش بالانحلال الحراري عند درجة حرارة 450 درجة مئوية وتحت الضغط الجوي .تمت دراسة الخواص الضوئية لجميع العينات من خلال تحليل منحنيات النفاذية بتغيير الطول الموجي في النطاق [300-1100 نانومتر]، وأظهرت أن أكسيد القصدير النقي وأكسيد القصدير المشوب بتراكيز مختلفة من الزنك أو المطعم بمواد انتقالية مختلفة هي أكاسيد موصلة شفافة .لقد وجدنا أن عملية التطعيم قللت من السمك وزادت من فجوة الطاقة (E_g) مع تخفيض طاقة الأورباخ (E_u) للأغشية الرقيقة لأكسيد القصدير، وبالتالي كانت مهمة جدًا لتحسين خصائصها الكهروضوئية.

الكلمات المفتاحية: SnO_2: X، X=Mn ، Cu، Fe، Zn ، الأغشية الرقيقة، أكسيد ناقل شفاف، الرش بالانحلال الحراري ، عرض عصابة الطاقة، النفاذية، طاقة الأورباخ، السمك



THESIS of MASTER of
Riad BOUKHALFA

